MINERALOGICAL AND GEOCHEMICAL EFFECTS OF BASALTIC DIKE INTRUSION INTO EVAPORITE SEQUENCES NEAR CARLSBAD, NEW MEXICO

by

Cynthia A. Loehr

Submitted in partial fulfillment
of the Requirements for the Degree of
Master of Science in Geology

New Mexico Institute of Mining and Technology

Socorro, New Mexico

May 1979

ABSTRACT

The alteration sequence imposed upon clay minerals associated with potash-rich evaporites surrounding Tertiary lamprophyre dikes in the Kerr McGee mine near Carlsbad, New Mexico is characterized by a $1M_d$ phlogopitic clay ± saponite ± irregular saponite-rich chlorite/saponite mixed-layer ± talc silicate assemblage within 1.5m of the intrusions. This assemblage changes to irregular chlorite/saponite mixed-layer + illite + chlorite + talc between 1.5 and 7.4m. At a distance greater than 7-8m from the dikes, the assemblage returns to normal: partially ordered corrensite + illite + talc + chlorite. It is suggested that clay seams, best developed near the dikes, played a major role in providing an open-system aqueous environment for altering these clay and associated non-clay mineral assemblages. Intense alteration of the water-soluble fraction takes the form of sulfate development and leaching of sylvite; the latter mechanism occurred throughout the altered profile.

The dikes display strong chemical, mineralogical, and textural effects of assimilation of host materials; the major reaction involved increased orthoclase/plagioclase ratios. Dike contribution of heat to the host rocks caused melting of the salts up to 15.2cm from dike margins.

CONTENTS

INTRODUCTION

A subparallel series of relatively thin (<5m) basaltic dikes intrude Ochoan evaporites in southeastern New Mexico along a 130km N50°E linear trend from the western margin of the Delaware Basin south of White City into the potash enclave northeast of Carlsbad within the basin (Fig. 1). The uniqueness of the several evaporite lithologies and their included silicate (clay) fractions provide an excellent opportunity to evaluate contact metasomatism and accompanying thermal metamorphic phenomena. Contact metamorphic phenomena in marine evaporite successions have only rarely been described, e.g. Sokolv and others (1975) document the recrystallization of evaporite clays to a talc-serpentine-tremolite-epidote assemblage accompanying dolerite intrusion into a potassium-deficient halite-anhydrite succession on the Siberian Platform. In this report the effects of basaltic intrusion on both a bedded gypsum lithology and a sylvite-halite potash ore assemblage is described.

The Delaware Basin is tectonically bounded by the Diablo and Central Basin Platforms to the west and east, respectively, and by the Northwestern Shelf Area (Fig. 2). During the Permian the basin was continually subsiding relative to the platform and shelf areas. The evolution was such that reef buildup on the platforms in Guadalupian time culminated in the development of a restricted basin with ensuing hypersaline conditions resulting in deposition of basin-filling evaporites throughout most of the Ochoan. (King, 1942; Adams, 1969).

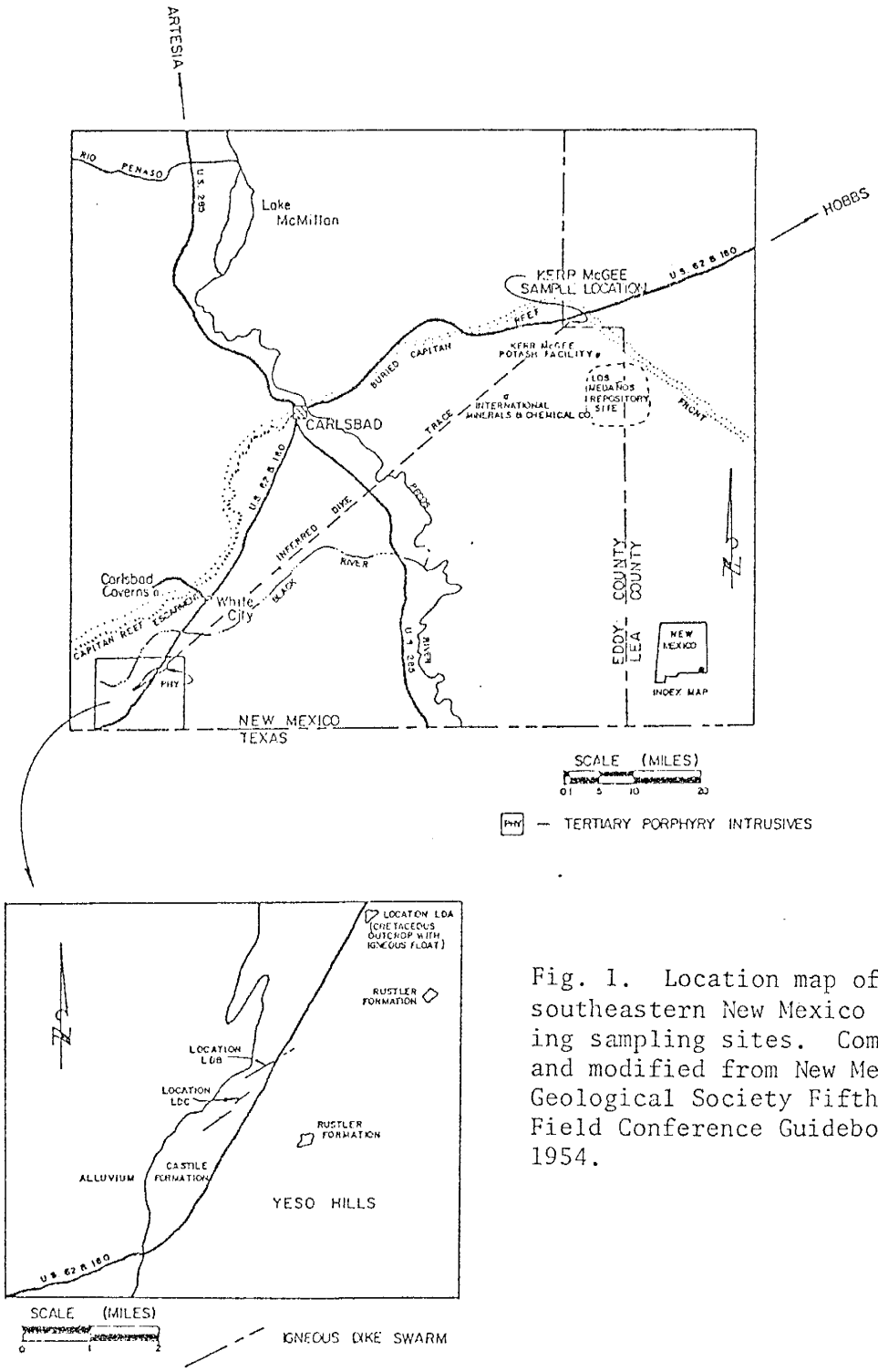

Fig. 1. Location map of southeastern New Mexico showing sampling sites. Compiled and modified from New Mexico Geological Society Fifth Field Conference Guidebook, 1954.

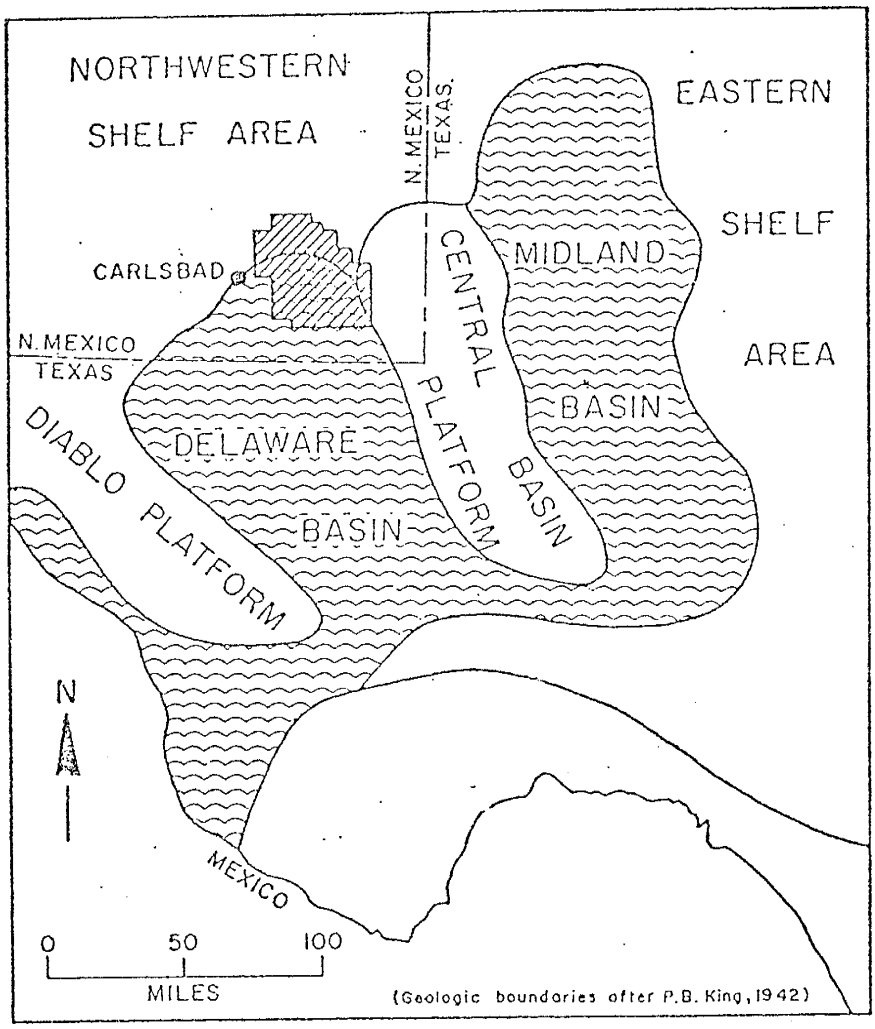

Figure 2

LOCATION MAP OF SEDIMENTARY PROVINCES OF THE PERMIAN BASIN OF SOUTHEAST NEW MEXICO, WEST TEXAS, AND THE CARLSBAD POTASH DISTRICT

(from Linn and Adams, 1966)

The stratigraphy reflects the structural provinces and depositional environments during the Permian. Wolfcampian and Early Leonardian sediments include basinal shales with limestones on the adjacent shelf and platforms. Late Leonardian sediments consist of evaporites and red beds which predominate on the shelf, accompanying limestone and shale deposition in the basin; platform limestones interfingered with these sediments. A major regression is recorded in Early Guadalupian time, followed by a transgression and reef development at the basin margins with evaporite deposition moving southward from the Northwest Shelf through Late Guadalupian. During Ochoan time the basin itself received marine evaporites with deposition of the Castile, Salado, Rustler, and Dewey Lake Formations which collectively comprise a thickness in excess of 1220m of evaporites and associated clastics (Fig. 3)(Adams and others, 1939; Jones, 1954).

The dike complex has been dated as Tertiary in age (Urry, 1936; Calzia and Hiss, 1978). It has been reported as occurring in mines, numerous drill holes and in outcrop along its trend and appears to be distributed as a swarm of closely emplaced dikes and sills (Darton, 1928; Lang, 1947; Pratt, 1954; Jones and Madsen, 1959; Kelley, 1971; Jones, 1973; unpub. rept., Elliot Geophysical Co., Tucson, Ariz., 1976; and Calzia and Hiss, 1978).

South of White City the dike complex is exposed on the surface and has been examined petrographically by several workers who identify it variously as an alkali trachyte, a soda trachyte, an andesite or microdiorite, and basaltic andesite. Pratt (1954) lists the components of the alkali trachyte as principally oligoclase, ilmenite, and apatite with minor orthoclase, titaniferous magnetite and epidote. Vesicles

System	Series	Formation		Lithology	Thickness Feet (Meters)
Quaternary	Holocene			Alluvium and Eolian Sand	0-3 (0-1)
	Pleistocene	Gatuna Formation		Sandstone and Caliche	0-105 (0-32)
UNCONFORMITY					
Triassic	Upper	Dockum Group	Santa Rosa Sandstone	Sandstone; Minor Siltstone and Conglomerate	872-1423 (266-434)
UNCONFORMITY					
Permian	Upper	Ochoan	Dewey Lake Formation	Siltstone and Sandstone	0-40 (0-12)
			Rustler Formation	Anhydrite, Dolomite, Halite, Sandstone	0-124 (0-38)
			Salado Formation	Halite; minor Anhydrite and Polyhalite and Potash ores	0-2300 (0-700)
			Castile Formation	Halite; Anhydrite and Anhydrite interlayered with Limestone	0-1840 (0-560)

Fig. 3. Stratigraphic relationships in the Carlsbad district (compiled from Jones 1954, 1972).

are filled with gypsum and lined with pyrite. The rock labeled a soda trachyte contains, in order of decreasing abundance, anorthoclase, albite, chloritic material, ilmenite, magnetite, with calcite and gypsum lining vesicles (Pratt, 1954). Resorbed intermediate plagioclase phenocrysts, bleached biotite altering to chlorite, abundant apatite and opaques, and augite make up the andesite or microdiorite (personal communication, Robert Blakestad, 1976). Plagioclase (An47-54), ferromagnesium minerals altered to chlorite, magnetite, biotite, and apatite in decreasing order of abundance constitute the basaltic andesite; secondary minerals include carbonates, zeolites, anhydrite, and chalcedony (Calzia and Hiss, 1978). Studies by these workers of the dike at Lang's (1947) Cretaceous outcrop where dike rock is present only as float found the mineral sanidine to be an additional component in some instances; names of biotite trachyte, altered olivine trachyandesite, and biotite trachyandesite have been applied to the rock. The rock is vesicular at this location and thought to have cooled close to the surface.

The physical and mineralogic characteristics of the dike in the International Minerals Corporation mine have been documented by Jones and Madsen (1959). This alkaline basalt is composed of andesine phenocrysts with siderite and antigorite pseudomorphous after pyroxene and a groundmass of orthoclase, and biotite altered to vermiculite; minor ilmenite, apatite, anatase, and pyrite are also present. Numerous accessory minerals, both silicates and evaporite salts, are contained in scattered amygdules (Jones, 1973; personal communication, Joseph Taggart, 1978).

Calzia and Hiss (1978) term the igneous rock at the Kerr McGee

Potash Facility a biotite basalt or basaltic andesite. In order of decreasing abundance, they list the mineral composition as plagioclase (andesine-labradorite), ferromagnesium minerals with biotite, magnetite, and chlorite reaction rims, magnetite, biotite, apatite, and the secondary minerals carbonates, zeolites, chalcedony, anhydrite, halite, gypsum, and pyrite.

The two localities selected for this study are 1) potash bearing evaporites in the workings of the Kerr McGee Potash Facility and 2) gypsum of the Castile Formation in the Yeso Hills (Fig. 1).

SAMPLING SITES

Kerr McGee

In the SW ¼ of the NE ¼ of Sec 31, T20S, R32E east of Carlsbad, New Mexico, two dikes (5 and 1.4m thick) intrude the 10th McNutt potash ore zone of the Salado Formation. The dikes strike N45°E and are nearly vertical. Recrystallized and bleached halite constitutes a halo of relatively intense alteration which interrupts bedding features 2.5-15.2cm from the dike-salt contact. The 9.7m interval between the dikes exhibits evaporite strata severely depleted in potash. Inclusions of recrystallized evaporite minerals and sulfides are contained within the dike as blebs, pods, and lenses. Chilled dike margins are brecciated into 1-2cm thick laths which are parallel to the contacts in an evaporite matrix. A small, apparently discontinuous, subparallel 7.6-10.2cm wide polyhalite dike occurs in the evaporites within 0.3m of the northernmost lamprophyre contact.

At the Kerr McGee mine, the 1.0-1.5m thick lower member of the 10th ore zone is mined for the potassium-bearing chloride minerals sylvite

and carnallite and is stratigraphically bounded by a continuous clay seam above and a halite bed below (Jones, 1972). The upper 12.7-20.3cm thick unit of this member is clean sylvinite (sylvite and halite) rock, under which lies a 1.0m thick lower unit composed of argillaceous halite with accessory amounts of sylvite. The argillaceous content decreases downward to the basal clay seam.

Twenty-two samples were collected along a 30.5m N-S traverse at varying intervals from the dike. The collection extended as far as 13m from the dikes where ore grade is average for the mine (14.0-16.9% K_2O) (Fig. 4). Grab samples were also collected at points farther from the dike.

Yeso Hills

In gypsum of the Castile Formation 16.1km south of White City along U.S. Highway 62 in the Yeso Hills, the dikes crop out sporadically along a trend which averages N65°E in T26S, R24E. The intrusions occur as a series of closely spaced irregular dikes less than 3m wide which on any given traverse vary in number from one to five in zones up to 46m wide. The rock is highly altered and weathered, but in places displays recognizable chilled margins with calcitization of the contact gypsum. No other alteration is evident in the host rock; banding or "varving" within the gypsum remains constant - apparently undeformed - up to the contact. An extensive amount of slumping and surficial deformation of the gypsum and possibly of the dike itself pervades the entire area and precludes definitive determination of dike-host relations.

Twelve samples were collected from three locations; two suites with apparent control on distance from the dike (Fig. 5).

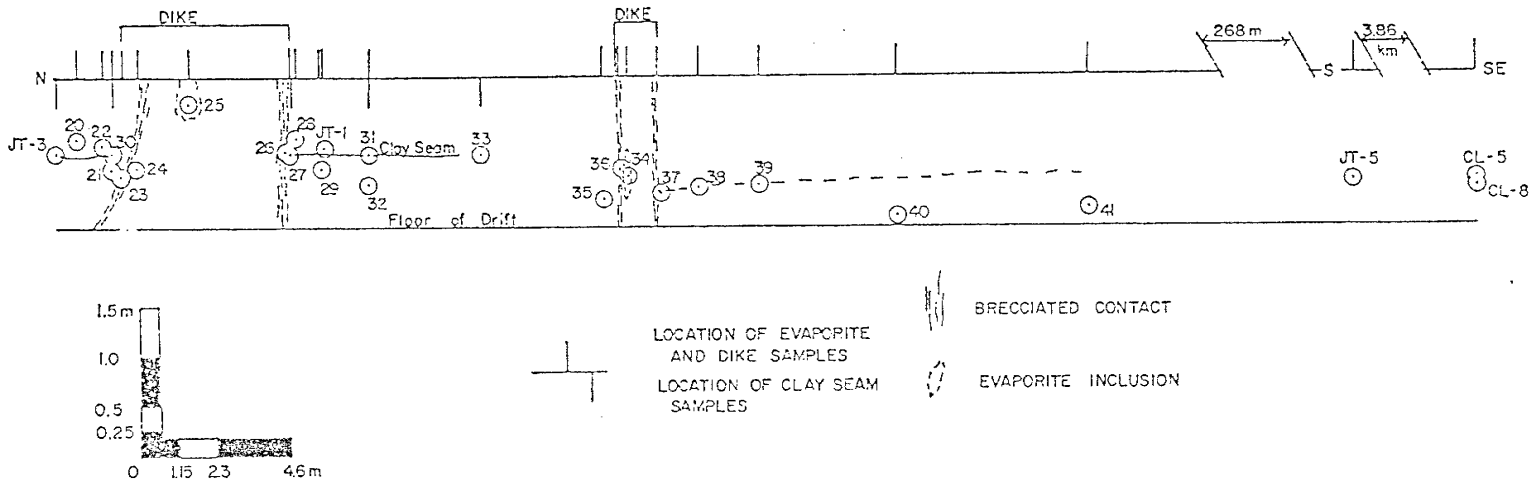

Fig. 4. Horizontal and vertical sample distribution at the Kerr McGee mine. Numbers standing alone represent those preceded by the label MB-76- in research records.

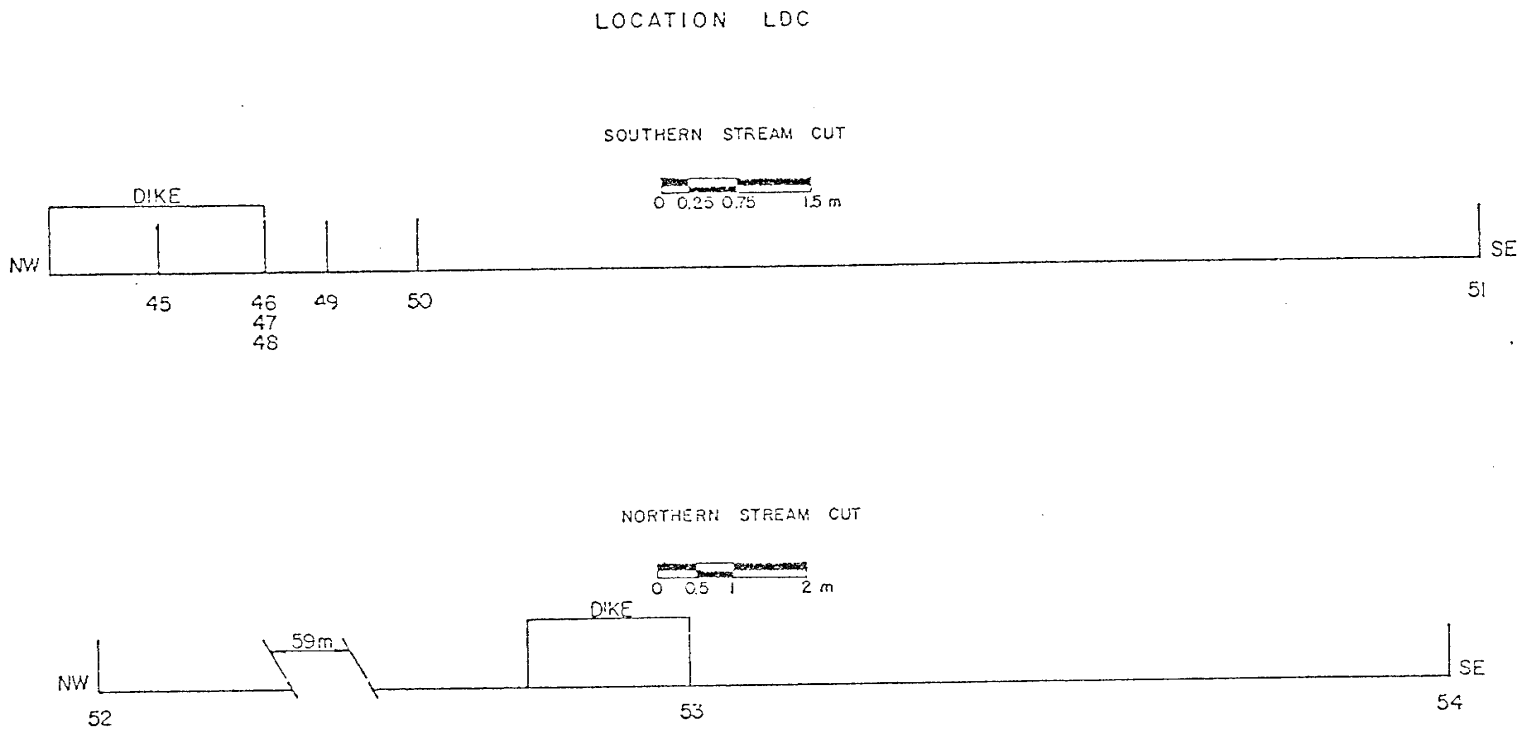

Fig. 5. Horizontal sample distribution of location LDC, Yeso Hills area.

SAMPLE PREPARATION AND ANALYTICAL PROCEDURES

Sample preparation

Whole rock samples were prepared for all rock types. Two additional fractions of the evaporites were prepared: a water-leach fraction from which the highly soluble chloride and sulfate salts were removed, and an acid-leach fraction which eliminated the carbonate minerals and the Ca-sulfate constituents. All fractions were dry ground to less than 200 mesh and pressed under 20 tons pressure into briquetts using bakelite or boric acid backing.

Preparation of the bulk dike rock involved grinding and washing of the samples. Bulk evaporites were pulverized and a fraction of this was retained as the whole rock sample. The remainder was used to obtain assemblage fractionation of the evaporites where distilled water served to dissolve the salts, and ethylenediaminetetraacetic acid (following Bodine and Fernalld, 1973) the carbonates and sulfates. Following each solution treatment, the respective insoluble residues were collected through repeated centrifugation, washing, redispersion, and finally, drying at 60°C.

For clay analysis, smear and/or <2μ sedimented slides of the silicate (acid-insoluble) fraction were prepared. The clay fraction was removed by gravity settling. Analytical treatments included solvation with ethylene glycol at 60°C and heating at 340°C (or 375°C) and 500°C. Selected Na and Mg saturations were made with 1M solutions of NaCl and $MgCl \cdot 6H_2O$, respectively.

Supplemental bromine analyses required two separations. Silicates were filtered from salts by washing with distilled water; thus, K and

Br contents solely of the salts could be compared. To distinguish bromine in the salts from bromine contained in fluid inclusions, an ether wash was applied to and filtered from the crushed salt fraction (personal communication, Joseph Taggart, 1978).

X-ray diffraction analysis

A conventional Norelco X-ray generator and diffractometer was used throughout this study. Normally a scanning speed of two degrees 2θ per minute with one inch per minute chart speed, and 1°-4°-1° slits were employed with Cu-radiation and a curved crystal monochrometer. A limited amount of powder camera work was done on selected samples.

X-ray fluorescence analysis

Analyses for SiO_2, TiO_2, Al_2O_3, total Fe as Fe_2O_3, MnO, MgO, CaO, Na_2O, K_2O, S as SO_4^{-2}, Cl, and Br were performed using a Norelco Universal Vacuum spectograph and Tennelec and Kicksort electronic accessories for identifying and recording appropriate energies for each element. The analyses achieved a 1% standard deviation in counting statistics.

Net counts of the sample per net counts of the drift pellet was the value correlated with concentration. The correlation curves for each element were derived from linear regression (least squares fit) calculations using U.S.G.S. and analyzed standards of known chemical composition. The fit of the standard data to the curve was acceptable for values better than 0.99. The coefficients of the regression were considered satisfactory when previously analyzed samples yielded fluorescence values within 3% of the known values, where these values were significant. Concentration of unknowns were then found from the regression coefficients.

Matrix effects (enhancement or depression of net counts for one

element by another) were corrected using a computer program modified by New Mexico Bureau of Mines and Mineral Resources staff (Marr III, 1976; personal communication, Joseph Taggart, 1978).

Chemical analysis

A minor amount of wet chemistry was performed by atomic absorption and colorimetric methods for Al_2O_3, Fe_2O_3, MgO, CaO, K_2O, and TiO_2 respective determinations. The procedures followed that of Brandvold (1974) for acid digestion of the samples and Maxwell (1968, p. 176-177) for the colorimetric preparation.

RESULTS

Kerr McGee mineralogy

The mineral assemblages which define the alteration sequence in the Kerr McGee mine fall into three general categories distributed spatially around the dikes. The zone of most intense alteration is located immediately adjacent to and included within the dikes. Moderate modification of the evaporites and their included silicates occurs around the dikes within distances of 1.5-7.4m. Apparently "normal" hypersaline assemblages are present in the sediments at greater distances. The figures of this section show the distribution and intensity of the minerals in various fractions of the rock and their chemical characteristics in spatial relation to the intrusions. Mineral proportions (intensities) are based on relative peak amplitudes of diffraction patterns and do not represent absolute percentages for each sample and chemical values are normalized. X-ray diffraction figures show patterns for the sample when air dried (AIR), solvated in ethylene glycol (E.G.), and heated at 340°C (or 375°C) and 500°C.

In the bulk rock evaporites of the Kerr McGee sample suite, halite, polyhalite, anhydrite, gypsum, magnesite, and sylvite have been identified by X-ray diffraction (Fig. 6). Large amounts of halite and minor polyhalite are ubiquitous in all samples. Magnesite is evident in trace amounts in the less altered samples and sylvite generally at larger distances from the dikes. Anhydrite is present in varying amounts in the highly altered rocks at dike margins and in dike contained evaporite inclusions. Evaporites and clay seams show essentially the same major bulk mineralogies, which have been noted by Schaller and Henderson (1932), Grim and others (1960), and Jones and Madsen (1968) in past studies of the Permian Basin.

Mica-clays, magnesite, talc, gypsum, anhydrite, quartz, chlorite, smectite, and mixed-layer clays, as well as pyrite identified by diffraction in water-insoluble fractions, show the mineralogical alteration sequence in greater detail (Fig. 7). This is true since the highly soluble salts and sulfates, which dominated bulk rock patterns, have been removed. In large abundance, mica is ubiquitous throughout the profile; magnesite is increased to an amount comparable to the mica, and quartz to a lesser extent, in moderately altered rocks. Except where argillaceous content is low, talc content in altered rocks is generally proportional to that of mixed-layer material; usually both are present in significant amounts. However, occasional inverse relationships between these minerals are recorded. In one salt sample adjacent to the smaller dike and in unaltered salt samples, talc intensities are greater than those of the mixed-layer; in essentially unaltered clay-rich samples, the reverse is true. Gypsum and/or anhydrite occur as described above where no clays or talc and only minor

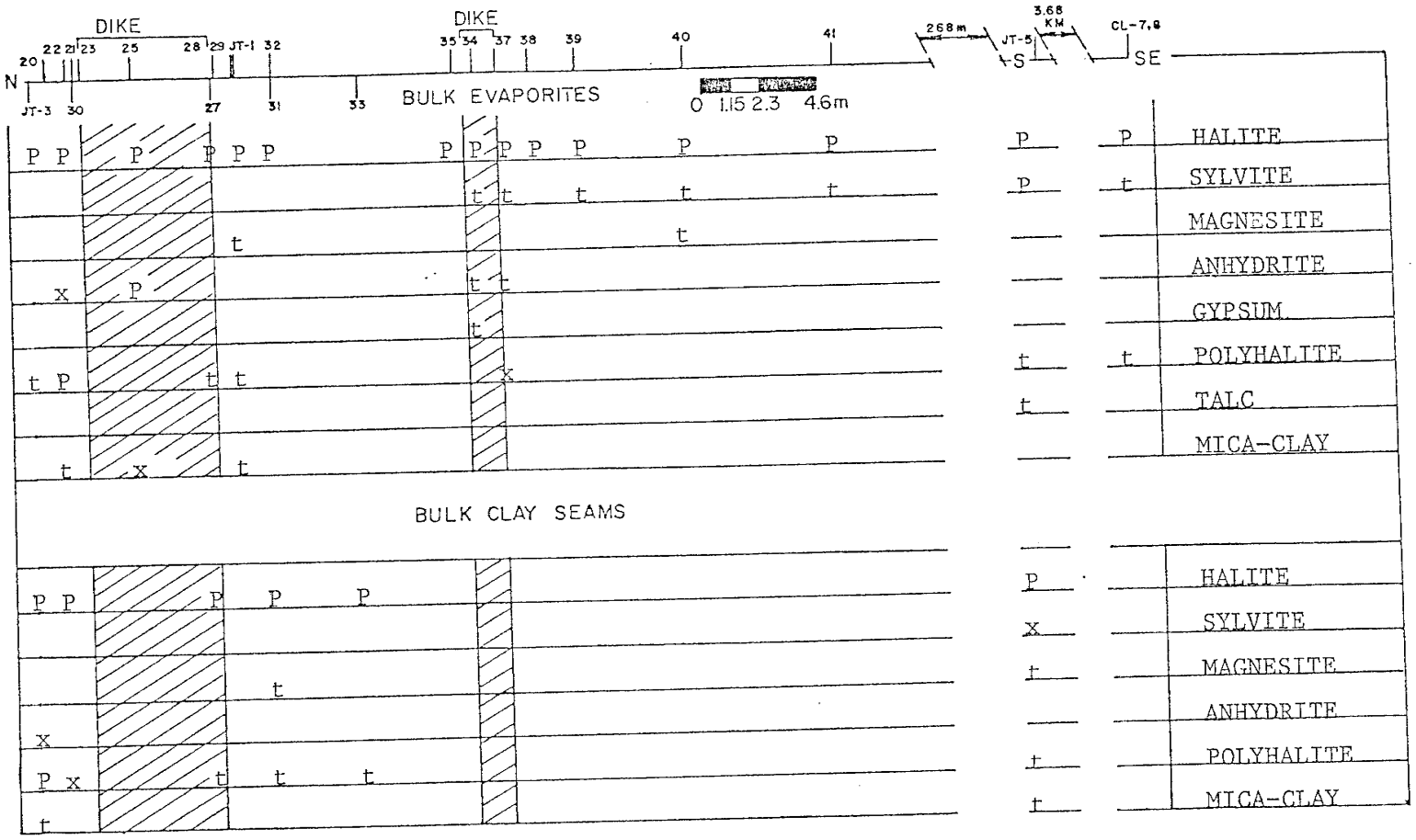

Fig. 6. Bulk evaporite and associated clay seam mineralogy of the Kerr McGee locality. Estimated mineral proportions are based on relative peak intensities of diffraction patterns for each sample.

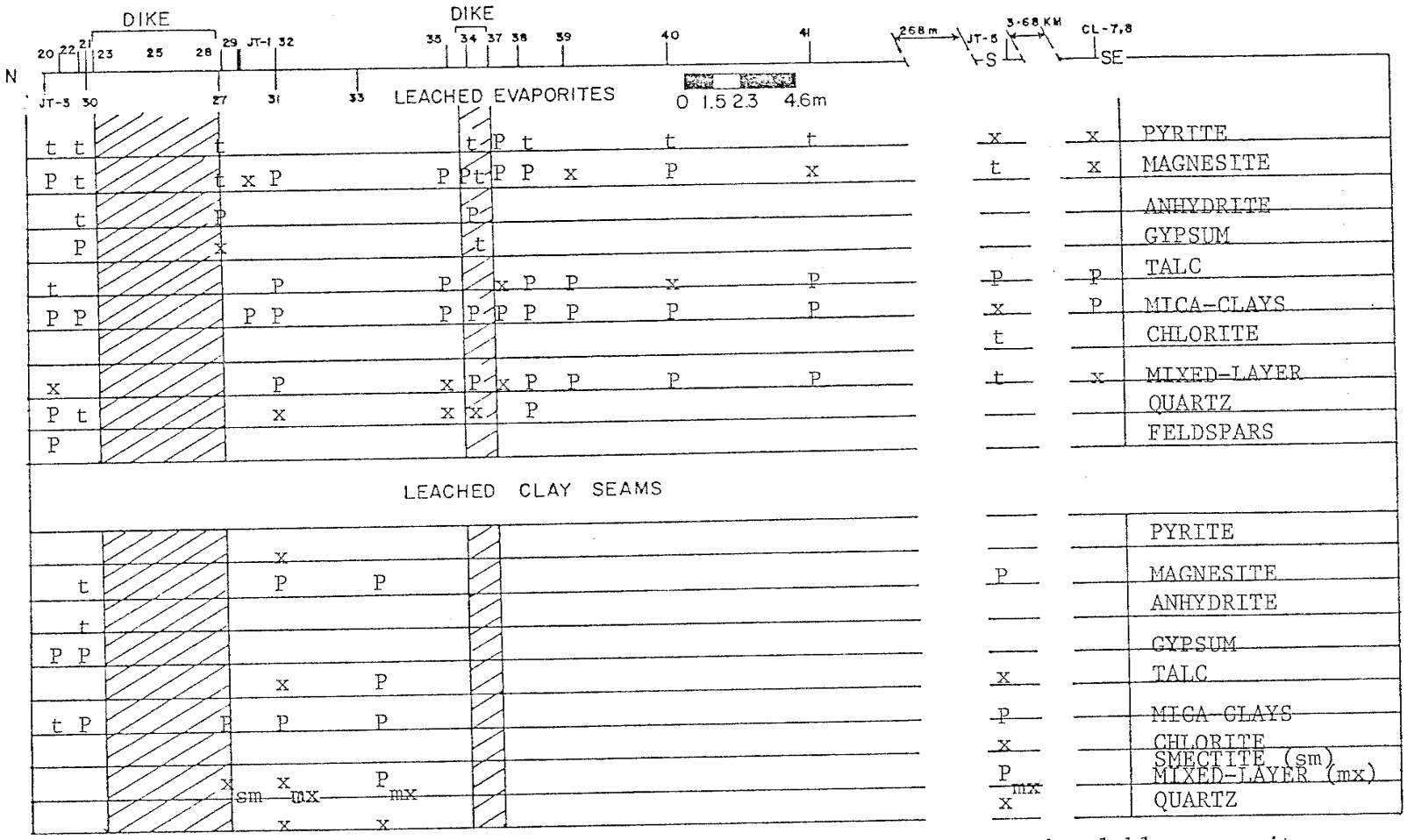

Fig. 7. Mineralogy of the water-insoluble evaporite and associated clay seam residues, Kerr McGee locality. Estimated mineral proportions are based on relative peak intensities of diffraction patterns for each sample.

mica-clay is apparent. In this fraction, chlorite is apparent in unaltered rocks. The distribution of pyrite exhibits a trend in evaporite horizons where it constitutes a larger proportion of the minerals in unaltered rocks.

In the silicate fraction subtleties of clay relationships become more apparent where, in addition to quartz and pyrite, eight types of clays can be distinguished by diffraction. These are: talc, partially ordered and disordered corrensite (interstratified chlorite/saponite), mixed-layer material distinct from disordered corrensite, discrete trioctahedral smectite (saponite), chlorite, illite, and phlogopitic-clay.

The presence of partially ordered interlayered chlorite/saponite was originally identified by Lippmann (1956) in the German Zechstein and later in the Permian Basin by Grim and others (1960) and Fournier (1961). Identification criterion are: the expansion of the (002) basal peak from 13.7Å to 15.4Å upon glycolation and the progressive collapse to a greatly broadened and smaller (with regard to intensity relative to (001) mica peak) 12.45Å peak at 500°C. The 9.6Å (003) peak is distinguishable where the mineral is not accompanied by a significant showing of the 9.4Å (001) talc peak. These and accessory peaks diagnostic of corrensite can be seen in Figure 8. The determining factors for the degree of ordering are the presence of the (003) in more regular material and the degree of development of the superlattice peak which expands from 29Å to 32Å upon glycolation. Partially ordered corrensite has a small asymmetrical peak at these low angles; irregular chlorite/saponite merely exhibits a shoulder on the pattern background (Fig. 9). Expansion of the (002) peak of the

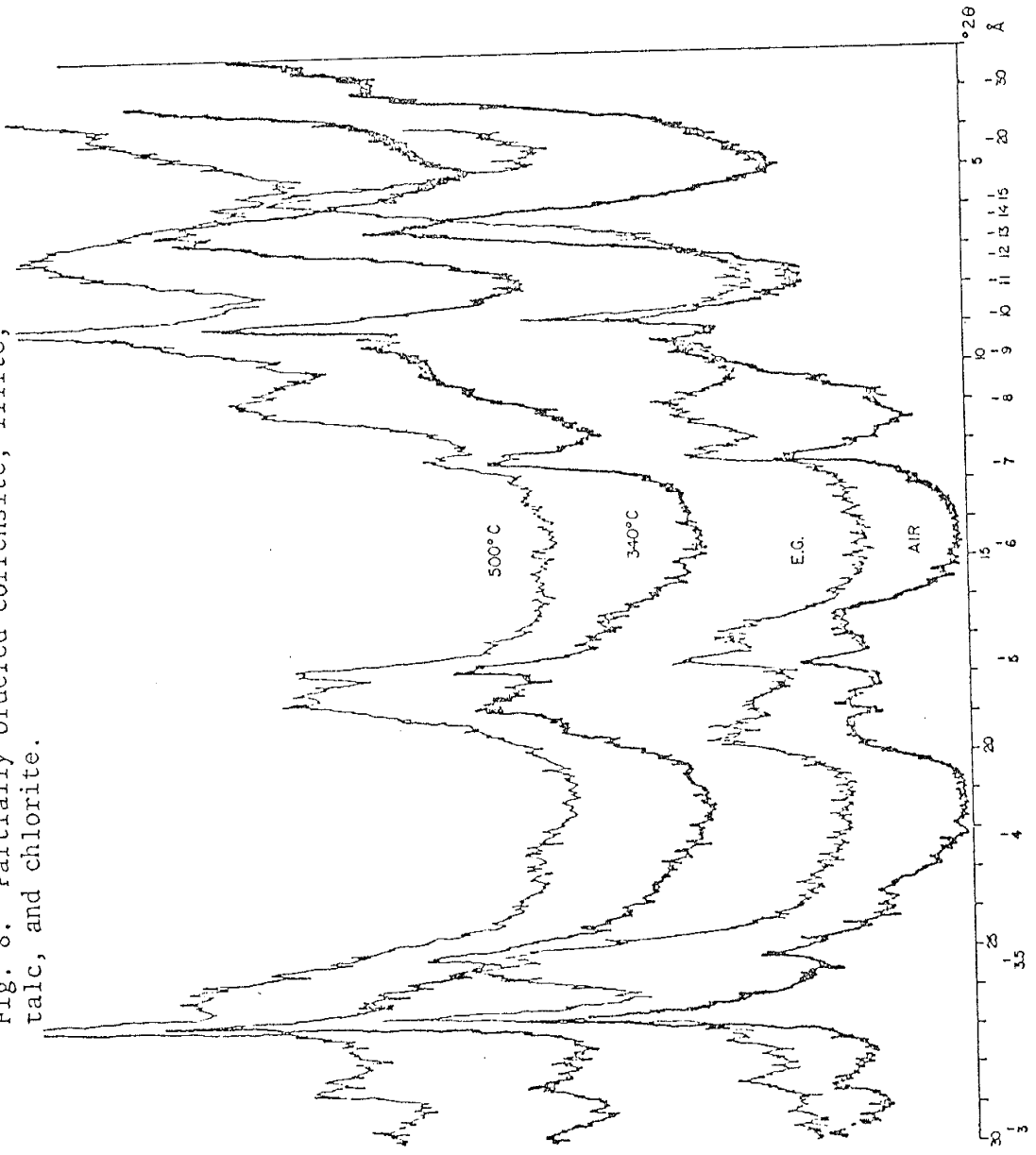

Fig. 8. Partially ordered corrensite, illite, talc, and chlorite.

irregular material is the same as for the more regular interstratified mineral, but collapse of the former at identical conditions is slightly smaller, e.g. to 13Å rather than 12.45Å; this is evidently controlled by a higher discrete chlorite/mixed-layer ratio.

Other, possibly related, irregular mixed-layer material exhibits a 12.3Å basal spacing which is smaller than that of corrensite; the mixed-layer normally expands to 12.99Å upon solvation with ethylene glycol and collapses totally to 10Å upon heating between 340°C and 500°C (Fig. 10). This material is interpreted here as being severely irregular corrensite with a larger amount of an interstratified smectite component as compared to the above description since it has smaller expandability, the d-spacing is smaller and the material collapses with greater ease. Figure 11 illustrates the opposite extreme, where the clay is characterized by increased regularity accompanied by high smectite component. Thus, it appears an entire spectrum of ordering is illustrated in the alteration profile.

The trioctahedral smectite (001) peak of saponite expands fully from 14.9Å to 16.67Å with glycolation and collapses to 10Å at 340°C (Fig. 12); the (060) peak is exhibited at 1.53Å.

The presence of chlorite is distinguished from other clay mineral basal spacings by the stationary nature of its (002) basal peak at 7.82Å upon glycolation and heating treatments (Figs. 8 & 9).

The mica-clays encountered in this study are characteristically non-expansive and show little, if any, collapse upon heating. The (001) and (003) basal peaks of illite are at 9.99Å and 3.33Å respectively (Figs. 8 & 9); for the phlogopitic mica-clay, these respective spacings are 10.12Å and 3.36Å (Figs. 10, 11, & 12). Detailed powder

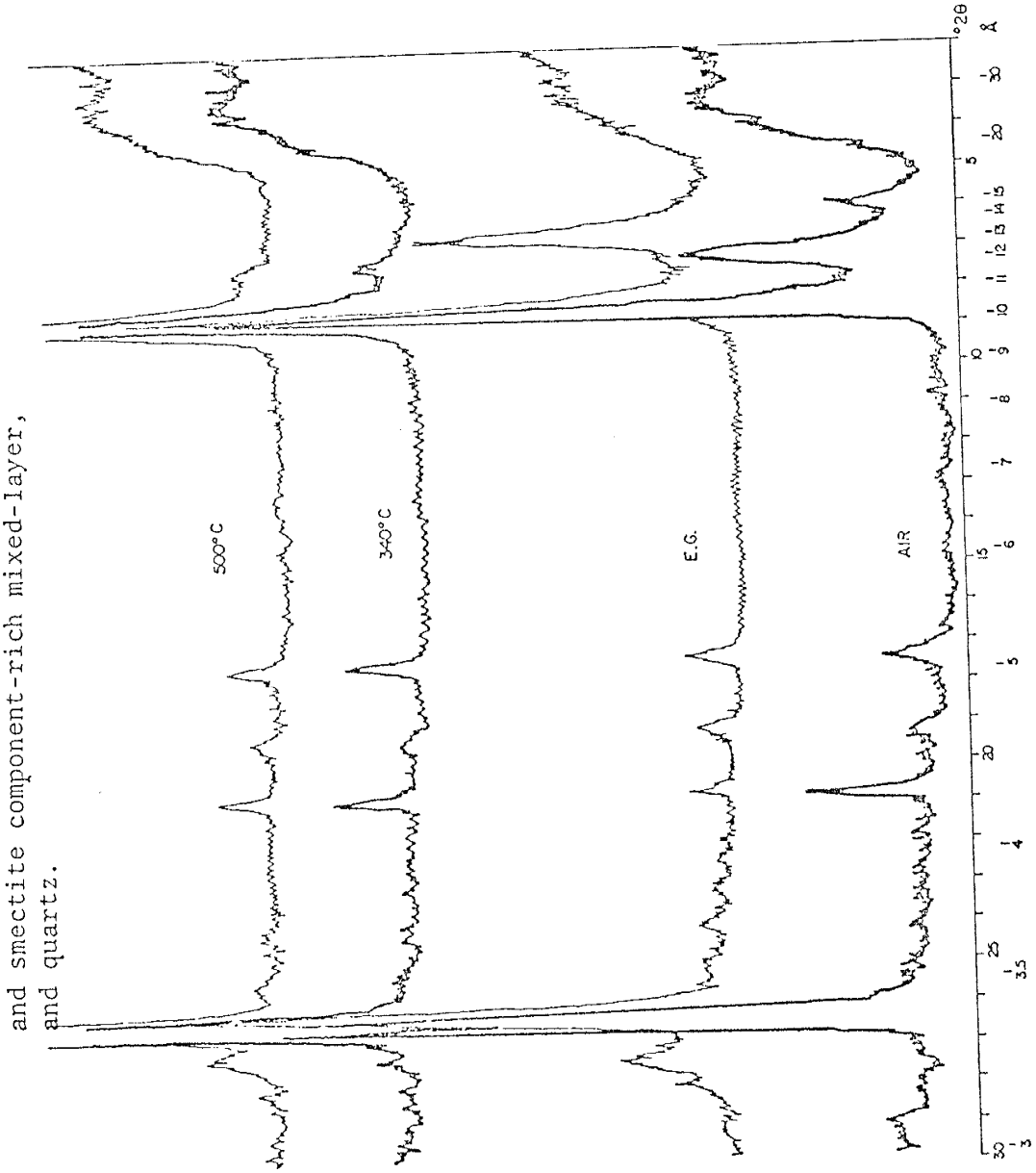

Fig. 10. Phlogopitic clay; highly irregular and smectite component-rich mixed-layer, and quartz.

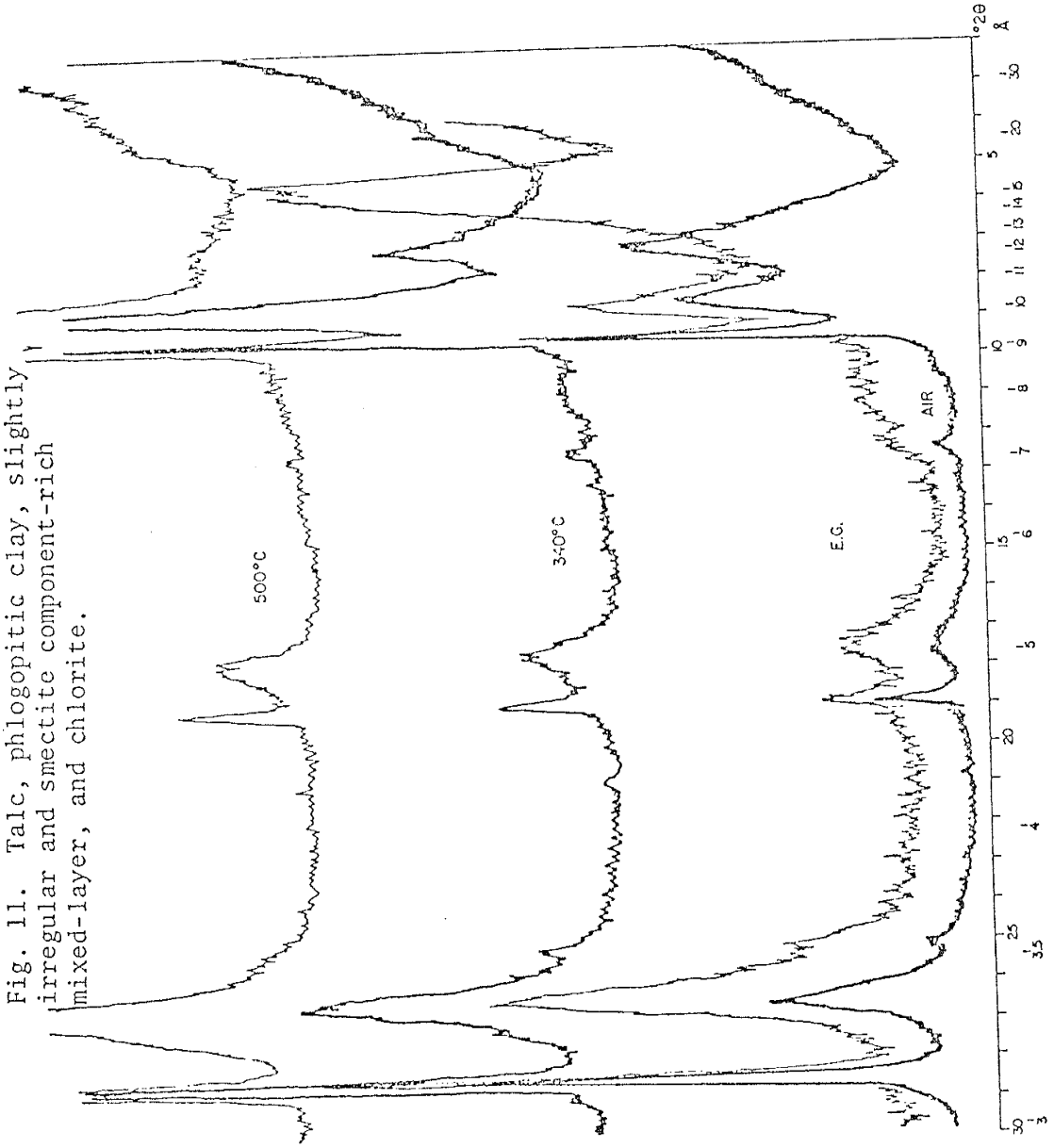

Fig. 11. Talc, phlogopitic clay, slightly irregular and smectite component-rich mixed-layer, and chlorite.

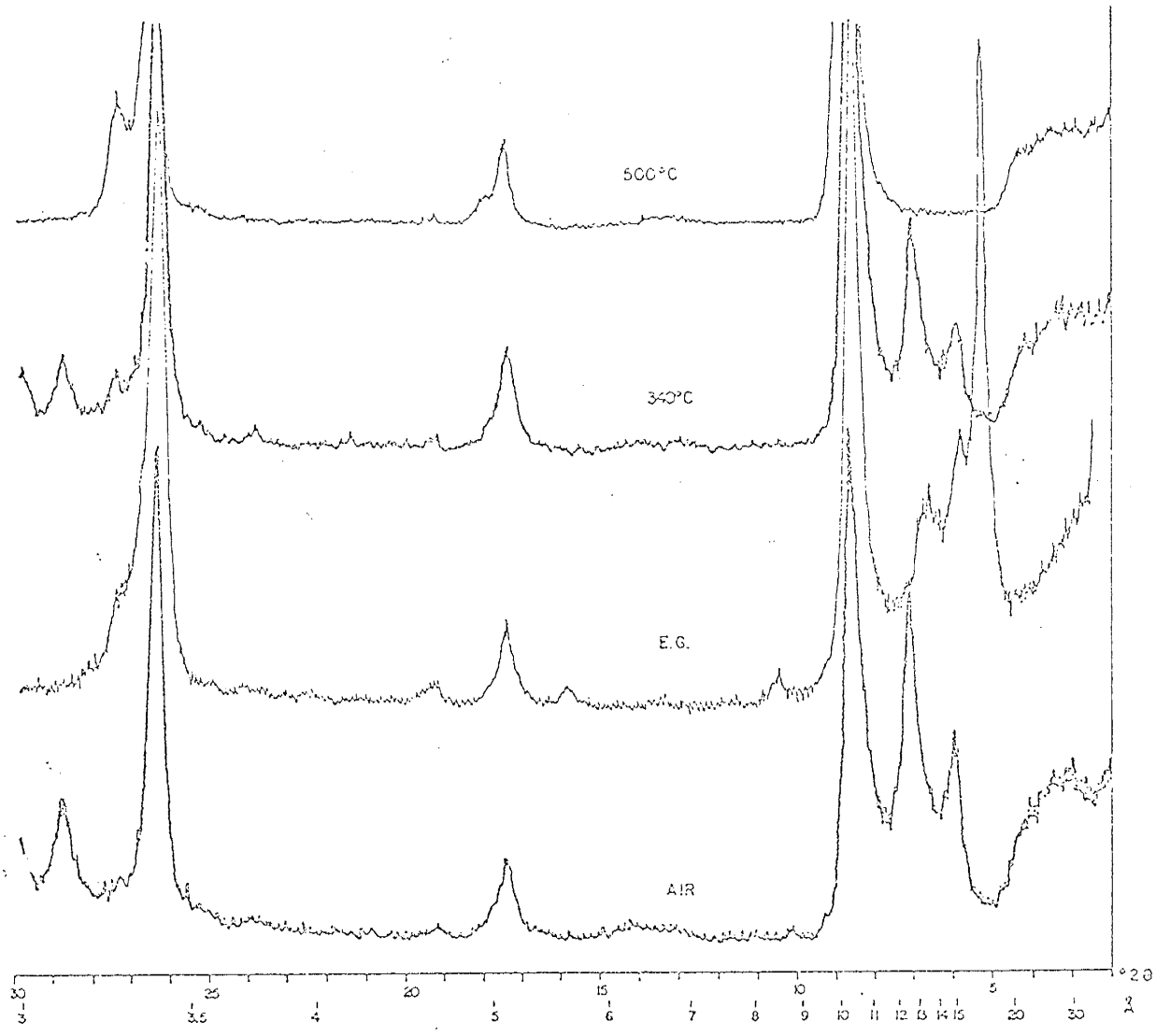

Fig. 12. Phlogopitic clay, smectite, and highly irregular and smectite component-rich mixed-layer.

camera investigation revealed that the phlogopite-clay is of the $1M_d$ type.

The distribution of these clay minerals and other silicates of the acid-insoluble fraction (Fig. 13) exemplify, clarify, and supplement the alteration profile outlined by the water-insoluble residues. The unaltered portion of the sequence is characterized by predominant partially ordered corrensite, dioctahedral illite, some talc, and lesser intensities of chlorite. As indicated in the leached fraction, pyrite occurrence suggests that it prevails in this unaltered portion of the sequence except in one instance, at the southern contact of the sub-dike where the sample contains small stringers of dike material.

Mineralogical changes from the normal assemblages become evident 1.5-7.4m from the intrusions where interlayered chlorite/saponite becomes more disordered, talc intensities increase slightly and chlorite persists as in the normal assemblages. Quartz, where present, exhibits significant intensities on diffraction patterns.

The most intensely altered zones within 1.5m of the dike margins exhibit assemblages distinct from those described above. The prominant change is that of the nature of the octahedral layer of the mica clay, e.g. the development of a trioctahedral phlogopitic clay. Saponite appears in this zone and/or in clay seam samples, generally with highly disordered mixed-layer material, a chlorite/saponite rich in its contained smectite component, evident only adjacent to dike margins. The discrete smectite is predominant in <2μ clay size fractions over the mixed-layer material. The phlogopitic-mica and smectite components of this zone appear to be fairly well crystallized. Other phenomena include the absence of chlorite and the lowest talc intensities recorded

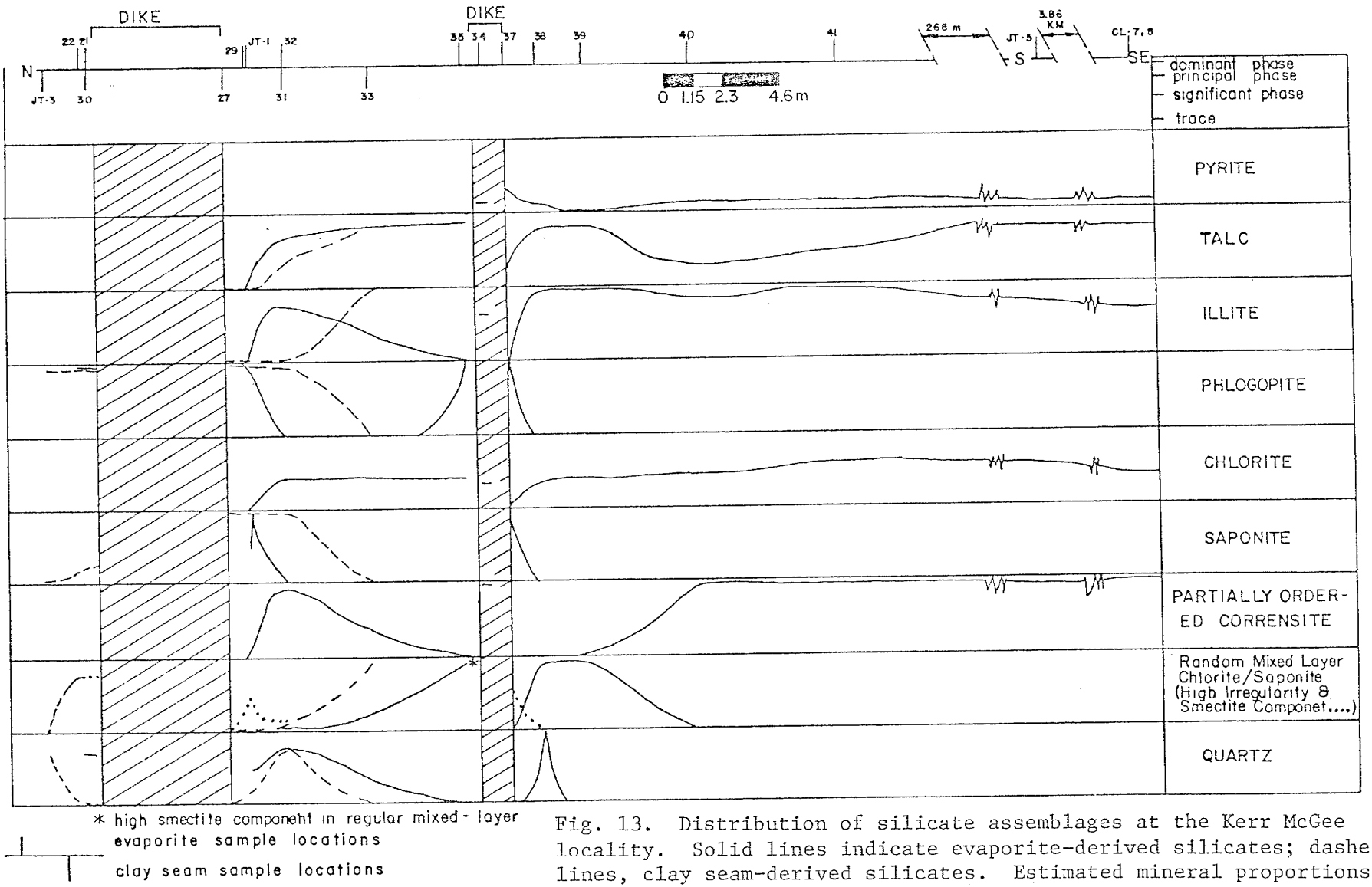

Fig. 13. Distribution of silicate assemblages at the Kerr McGee locality. Solid lines indicate evaporite-derived silicates; dashed lines, clay seam-derived silicates. Estimated mineral proportions are based on relative peak intensities of diffraction patterns

in the profile.

Naturally exceptions to the zones outlined here exist. One evaporite included within the thinner dike exhibits the mineral assemblage associated with unaltered rocks at large distances from the dikes. Also, between the two dikes and included within the zone of moderate alteration, two samples also show the same phenomenon to a lesser degree, suggesting that the spatial occurrence of this intermediate zone is somewhat variable.

Yeso Hills mineralogy

X-ray diffraction patterns of the whole rock samples of the Yeso Hills sample locality show major concentrations of gypsum and relatively minor to significant amounts of calcite (Table 1). The silicate fractions (Table 2) are dominated by quartz and feldspars, and somewhat variable trioctahedral illite/saponite (trioctahedral smectite) mixed-layer material relatively more abundant at dike margins. Trace showings of pyrite are evident in samples within 0.4m of the dike. A notable decrease in feldspar and accompanying increase in quartz intensities exists where the mixed-layer material is present in significant quantities. Only one sample, at 0.4m from the dike, does not record this occurrence, a sample with no detectable clay content.

The mixed-layer material (Fig. 14) expands from 12.3Å to 13.3Å upon ethylene glycol solvation and either collapses to 10.0Å when heated to 375°C or decreases in intensity at 375°C and collapses to 10.0Å between 375°C and 500°C. The partially ordered clay samples at dike contacts exhibit superlattice shoulders at high angstroms and a single, asymetrical to low Å side, peak at 12.3Å. Disordered, or irregular, mixed-layers show a broadened doublet between 10.0Å and 12.9Å.

Table 1. Bulk-rock mineralogy of Yeso Hills samples.

Sample	Calcite	Gypsum
47	t	XX
48	t	XX
49	t	XX
50	t	XX
51	t	XX
52	x	XX
53	t	XX
54	t	XX

XX - dominant phase
x - significant phase
t - trace

Table 2. Silicate residue mineralogy of Yeso Hills samples.

Sample	pyrite	discrete illite	illite/saponite mixed-layer	qtz	feldspar (plag)	
S stream cut						
- - - - dike						
47	t	t	x (p-d)	XX	X	✓
48	t	–	XX (p-d)	X	XX	✓
49	t	–		x	XX	✓
51	–	NG	x (d)	XX	X	✓
N stream cut						
52	–	t	t (d)	X	XX	✓
- - - - dike						
53	✓	–	XX (p)	XX	t	?
54	–	t	–	XX	XX(2) (2nd identity undefinable)	✓

XX - dominant phase
X - principal phase
x - significant phase
t - trace
p - partially ordered
d - disordered
p-d - partially to disordered
✓ - identified
— - not present (not detected)
NG - not glycolated, i.e. not tested for discrete illite but very minor if present

NOTE: presence of plagioclase (plag) only detectable where feldspar content high; presence of alkali feldspar only identifiable where quartz content low (not identifiable here)

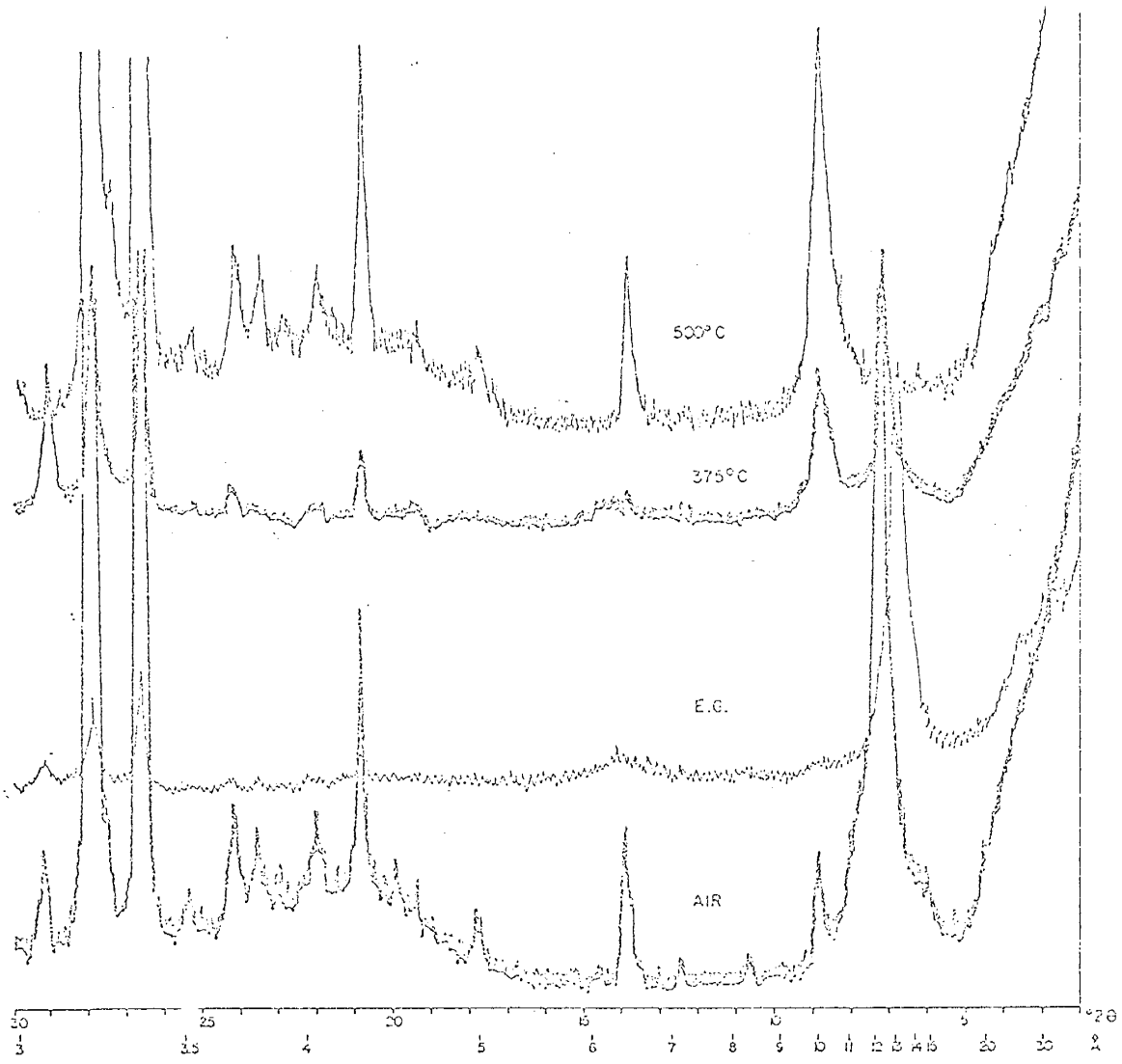

Fig. 14. Partially ordered trioctahedral illite/saponite mixed-layer, quartz, feldspar(s) (plagioclase ± orthoclase).

The trioctahedral nature of the smectite is defined by the 1.54Å spacing of the (060) peak. The illite component of the mixed-layer clay is trioctahedral since the 10.0Å (002)/4.95Å (004) ratio is greater than five. By comparison, the 10.0Å (001)/5.03Å (002) ratio for a dioctahedral 1M illite is one.

Dike rock mineralogy

Analysis by diffraction of the dike rock at the Kerr McGee occurrence shows, in decreasing order of predominance, feldspar, mica, chlorite, pyrite, ilmenite (sporadic in part due to the use of magnetic stirrers and thus the removal of ilmenite in sample preparation), and chlorite/smectite mixed-layers (Table 3). The alkali feldspar/plagioclase ratios appear to increase from interior to margin facies of the dike.

Through thin section work, the textural relationships of these minerals was examined and precision work on feldspars completed. The porphyritic nature of the rocks is exemplified by relatively sparse 10-6mm x 3.5-4.5mm subhedral plagioclase and 3mm x 3mm anhedral orthoclase phenocrysts; the groundmass is characterized by 60-70% plagioclase averaging An50, and lesser amounts of opaques (including magnetite grains with limonite centers, and trace amounts of pyrite), chlorite and biotite. The biotite is apparently titaniferous, and highly altered. In one slide there is a suggestion that a mafic mineral was originally present, possibly a pyroxene; however, this has been altered to chlorite and roughly outlined by magnetite. A trace of apatite is present. Occasional macroscopic vugs (1-3mm in size) disrupt the igneous textures described above and are lined with subrandomly oriented calcite crystals and other carbonate(s), show inward protruding anhydrite and

Table 3. Dike rock diffraction results

SAMPLE	PYRITE	ILMENITE	CALCITE	MICA	CHLORITE	OTHER CLAYS	FELDSPAR(S)
Kerr McGee Suite							
23*				X		t chl/sm mx-lyr	XX alk
36	x	x		XX	x	t chl/sm mx-lyr	XX plag>alk
24**	x	x		XX	x	t chl/sm mx-lyr	XX plag
Yeso Hills Suite							
southern stream cut-location LDC							
46*	t			x	x	x chl/sm mx-lyr	XX plag>alk
45D**	t		t	x		x sm	XX plag
45L†	t			t		x sm	XX plag
location LDB							
18A†	x					x sm	XX plag
18B†			t			x sm	XX alk, plag
19L†*			x				XX alk, plag
19D†	t			t	x	t chl/sm mx-lyr	XX plag
location LDA							
17			t	X	x	x chl/sm mx-lyr	XX alk, plag

XX - dominant phase
X - principal phase
x - significant phase
t - trace

* - marginal facies
** - interior facies
† - weathered

sm - smectite
chl/sm mx-lyr - chlorite/smectite mixed-layer
alk - alkali feldspar } distinguished by (201) peak
plag - plagioclase (excluding albite) }

carbonate (possibly magnesite) crystals, and have halite centers with occasional "floating" feldspar.

Thin section examination of one of the main dike margins in the Kerr McGee mine shows mineralogic alignment parallel to the vertical contact. The laths of dike rock, 2-4mm wide but also accompanied by smaller slivers, are nearly identical to the rock away from the margins, but are not as altered. The anorthite content of the groundmass plagioclase is slightly lower here (An44). Andesine phenocrysts are aligned subparallel to the dike laths and are even cut by adjacent 4-6mm laths of salt. Accessory carbonates and radiating aggregates of talc occur in selected portions of the halite and/or immediately adjacent to the dike rock. Calcite crystals are subrandomly oriented and do follow this distribution, but other carbonate appears to be concentrated in close proximity to and also radiating from the igenous material.

Diffraction work on the Yeso Hills dike rock indicates that its mineralogy closely parallels that of the dike from the Kerr McGee mine (Table 3), except a generally higher feldspar/mica ratio, and a smectite in interior facies rather than interlayered chlorite/saponite, which occurs only at the margin.

In thin section, the rock exhibits a coarser groundmass but the plagioclase phenocrysts are smaller (5-7mm in length) and more euhedral than at the Kerr McGee mine. The rock has two feldspars present - both as groundmass constituents and phenocrysts. Orthoclase is present only in small amounts in the groundmass; as 3mm x 2mm phenocrysts it exhibits a subhedral shape in contrast to the more euhedral nature of the plagioclase. As in the Kerr McGee, the groundmass contains approximately 60-70% plagioclase (An60), in places resorbed, and 30-40%

opaques (including extensive hematite, magnetite grains with limonite centers, and trace amounts of pyrite). Remnants of small augite (?) grains were tentatively identified, although the identification was hindered by abundant hematite staining, chlorite, and sericite throughout.

Hematite and limonite-bordered vugs are present in the rock and exhibit calcite ± talc filling. Often small amounts of dike material and anhydrite are included. Larger vugs (1-1.5mm) are oblong in cross section and relatively erratic and sparse in their distribution. Secondary spherical calcite vugs, comprising approximately 20% of the rock, and being less than 0.3mm in diameter, give the chilled margin of the dike a psuedo-porphyritic texture. Approaching the contact, these round vugs and also micro-fractures associated with the contact, are entirely hematite-filled.

The contact igneous material itself is composed of 40-50% andesine (An41), 30-45% opaques and 8-10% chlorite after augite (?). The rock is again highly altered. Porphyritic texture is not well developed; however, a significant percentage of plagioclase crystals are slightly larger than the majority of the groundmass. Pyrite, magnetite, hematite and limonite masses are present, but are not common. Ilmenite, however, is a prominant constituent (10-15%) in the finer portions of the rock, occurring in acicular aggregates and infiltrating the groundmass.

Kerr McGee chemistry

The chemical weight ratios shown in Table 4 reflect the major mineralogical distributions shown in Figure 6 but also indicate the presence of other mineral compositions masked by the great predominance of

Table 4. Chemical Ratios (wt.%) and Bromine (ppm) of Kerr McGee evaporites

Sample	Si/Cl	Fe/Cl	Mg/Cl	Ca/Cl	Na/Cl	K/Cl	S/Cl	Br(ppm)
20	0.0038	0.0001	0.0028	0.012	0.6210	0.013	0.00689	46
22	0.164	0.039	0.138	0.18	0.505	1.17	0.14	14
21	0.0041	0.0027	0.0021	0.0085	0.6221	0.015	0.0055	150
21S	0.00075	0.0008	0.001	0.010	0.6135	0.011	0.00537	58
30*	0.0403	0.0055	0.0287	0.0702	0.5379	0.110	0.145	132
23P	0.00	0.042	0.249	0.18	1.10	2.772	0.14	56
23S	0.0033	0.002	0.0095	0.183	0.6494	0.127	0.1194	47
27*	0.108	0.0076	0.0526	0.116	0.2964	0.178	0.0758	174
dike								
28W	0.0064	0.0003	0.0024	0.0038	0.5935	0.010	0.00	65
29*	0.1037	0.0057	0.0509	0.0032	0.4904	0.0760	0.00	248
JT-1	0.0340	0.0024	0.0366	0.0072	0.5415	0.0947	0.0020	203
31*	0.0645	0.0067	0.0455	0.0243	0.4119	0.113	0.0156	226
32	0.0112	0.0013	0.0053	0.0003	0.5655	0.0172	0.00	109
33*	0.0712	0.0087	0.0302	0.0298	0.5193	0.0696	0.0598	214
33S	0.0047	0.0004	0.0018	0.012	0.5938	0.0061	0.0019	52
35	0.0195	0.0030	0.0083	0.0089	0.5708	0.0296	0.0037	108
dike								
34	0.0037	0.0002	0.001	0.013	0.5882	0.0046	0.00091	50
34D	0.1500	0.0215	0.0624	0.001	0.3606	0.0643	0.00	334
37WDC	0.0146	0.0031	0.0070	0.0395	0.5581	0.0741	0.0262	110
37MDC	0.0381	0.0025	0.0180	0.0195	0.5400	0.0510	0.0119	114
38(*)	0.0226	0.0054	0.0068	0.0008	0.6228	0.011	0.00	108
39(*)	0.0879	0.0061	0.0300	0.002	0.5624	0.0286	0.00	168
40	0.0625	0.0074	0.0355	0.0063	0.5327	0.0428	0.0017	213
41	0.0726	0.0060	0.0372	0.013	0.4215	0.136	0.0126	284
JT-5	0.0416	0.0031	0.0299	0.0221	0.4943	0.120	0.0151	160
CL 7U	0.0048	0.0020	0.0027	0.0058	0.3082	0.2536	0.0020	122
CL 7L(*)	0.105	0.013	0.0672	0.00002	0.2417	0.2380	0.00	510
CL 8	0.0527	0.0049	0.0319	0.0031	0.4276	0.127	0.00	144

* Clay seam ; (*) clay-rich

halite. The analyses additionally illustrate distinct differences in composition between salt and clay seam samples, a phenomenon undetected by diffraction work on the bulk rock.

The rocks are apparently unaffected by the intrusions at distances greater than 7.4m where Si/Cl, Fe/Cl, and Mg/Cl ratios are characteristically and comparatively low on the profile except where the argillaceous content is high. Relatively high K/Cl ratios in all cases reflect the detection of the ore mineral sylvite (KCl) by diffraction. Iron oxide is commonly included in potash minerals, and also in polyhalite ($K_2Ca_2Mg(SO_4)_4 \cdot 2H_2O$), which occurs sporadically in the marine hypersaline sediments in minor amounts and which may accommodate K, Ca, and Mg ions where SO_4 is present. In the analyzed samples, Ca/Cl ratios are directly related to S/Cl values, suggesting that gypsum and/or anhydrite represent some fraction of sulfate minerals.

Partial alteration of the salts occurs within a 1.5-7.4m interval from dike contacts and between the dikes, and is evidenced by slightly higher Si/Cl and Na/Cl compared to unaltered salts. The K/Cl ratio is significantly decreased here. Other data parallels that for normal assemblages. These trends suggest a relative increase in silicates and halite and simultaneous decrease in potash ore minerals ± magnesite as the dike is approached.

Immediately adjacent to the dikes a more intensely altered zone is evident in non-argillaceous sediments by lower Si/Cl, Fe/Cl, Mg/Cl, and K/Cl values. The latter ratio is slightly higher where some clay and sulfate are chemically apparent by Si/Cl and S/Cl, respectively. Again, Ca values, relative to chlorine content, vary directly with the presence of sulfate, which is in general higher in this zone. Sodium

contents relative to chlorine are comparable to or higher than those in moderately altered rocks. Thus, K ± (Mg, Fe) - bearing chlorides are no longer present, but where these cations contribute to the minor presence of sulfates, the chloride anion has contributed to the domination of halite in this silicate-poor assemblage.

Clay-rich horizons in this extremely altered zone and in the moderately altered interval show inverse chemical relationships to the highly altered clean rock salts and a general enrichment in sulfates and Ca, accompanied by smaller Na/Cl values. Thus, it is apparent that within clay seams, Fe, Mg, K, and Ca contribute to the formation of a polyhalite, Ca-sulfate, and silicate rich assemblage which is relatively poor in halite. Virtually pure polyhalite samples (22, 23P) exhibit these relations (except silicate enrichment and definite Na depletion) most emphatically. In one case (23P), the Na/Cl ratio exceeds that required for total consumption of Na by Cl to form halite as a single chloride, suggesting that a feldspar, undetected by diffraction, is present. In clay seams surrounding the dikes, S/Cl ratios are higher than in unaltered rocks; this is especially apparent on the north side.

The two samples of inclusions within the smaller dike exhibit opposing characteristics. Sample 34 chemically resembles intensely altered salts but with an even more severe depression of K/Cl values and only minor occurrence of Ca-sulfate. Chemistry of the second sample (34D) closely parallels that of unaltered argillaceous rocks, the sole exception being a comparatively low - but not lowest - K/Cl ratio. The latter fact reflects the identification of trace amounts of the potash ore mineral sylvite at this location.

A K/Na vs. Br plot of total bulk rock samples (Fig. 15) shows, with few exceptions, increasing Br with increasing K/Na away from the dike. This suggests that a hydrothermally induced mechanism removing KBr was in operation and was most effective in non-argillaceous rocks. Selected treated samples were analyzed further (personal communication, Joseph Taggart, 1978) and revealed that Br content fluctuates in various fractions (Table 5). Sample 34D contains 44ppm in fluid inclusions, 88ppm in soluble salts, and 202ppm in the water-insoluble fraction (silicates and sulfates).

A survey of the data suggests that the most intense modification has occurred on the north side of the intrusions; e.g. relatively high S/Cl, K/Cl, Ca/Cl, Mg/Cl, Fe/Cl, and to a lesser extent, Na/Cl and Si/Cl values predominate in this area. This may be a function of a deviation from vertical dip of the dike at this position, which in turn may suggest development of a sill-like body at a lower level.

Where clay from dike material is included in the sample (37WDC), S/Cl, K/Cl, and Ca/Cl values are relatively high. Clay seams in general are best developed within a few meters of the dikes, and are relatively higher in Fe, Ca, S, K, and Mg to chlorine ratios compared to salt samples; the K/Cl and Mg/Cl values are highest in polyhalite samples. Relative to chlorine, Mg increases with increases in Si where sulfate content is relatively minor. Simultaneous increasing of Fe/Cl, Mg/Cl, and K/Cl are independent of sulfate content.

An inverse relationship exists throughout the profile between Na/Cl and K/Cl ratios in samples containing only minor sulfate (Fig. 16). The suggestion of this plot as to the extent of alteration in the form of leaching of potassium must be amended, however; Figure 17

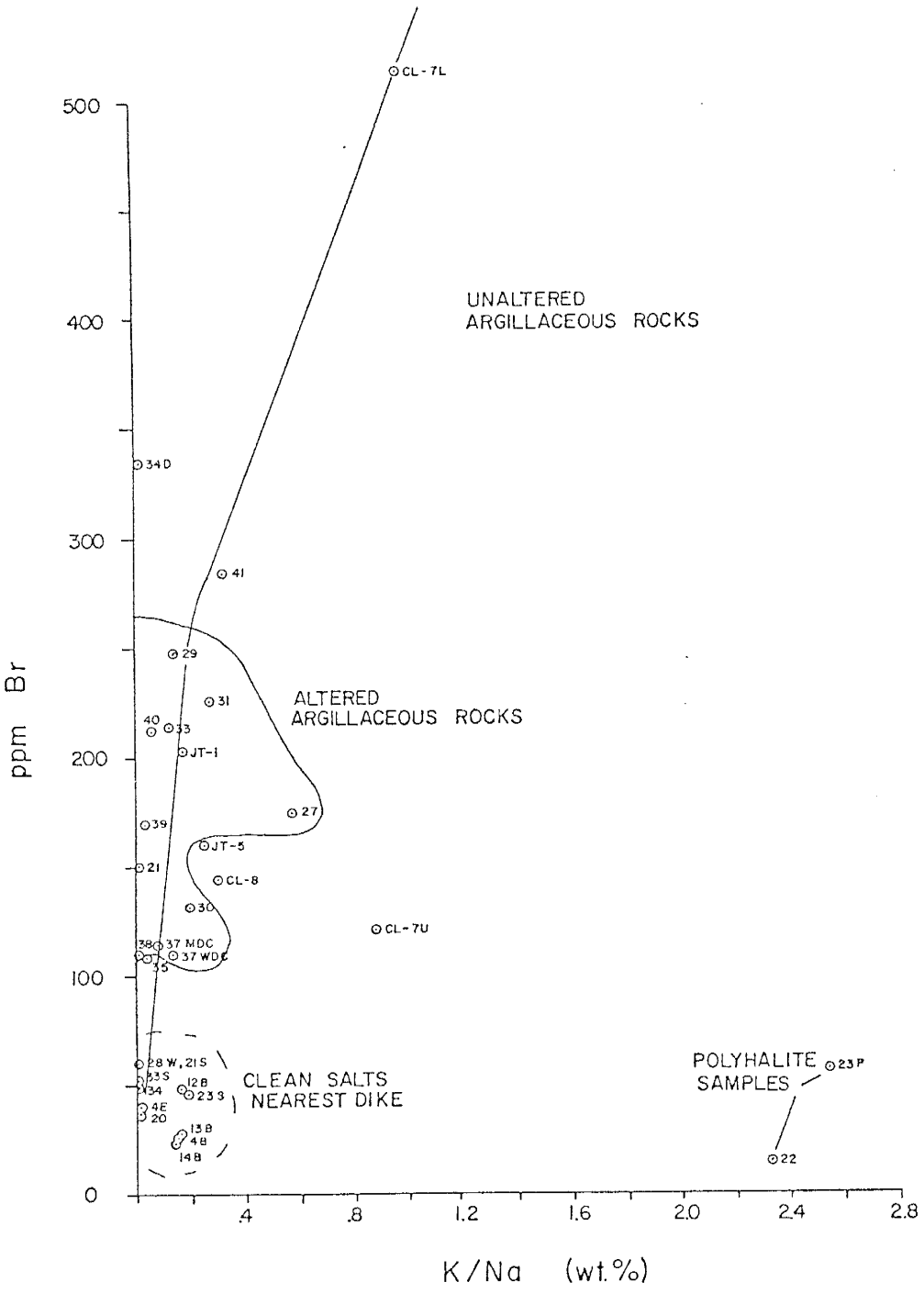

Fig. 15. K/Na vs. Br plot of bulk evaporite samples, Kerr McGee and International Minerals Corporation occurrences.

Table 5. Additional Bromine Data

JT -5	H_2O-soluble fraction	268ppm
34D	H_2O-soluble fraction	132ppm
	Salt minus fluid inclusions	88ppm
CL 7L	H_2O-soluble fraction	462ppm

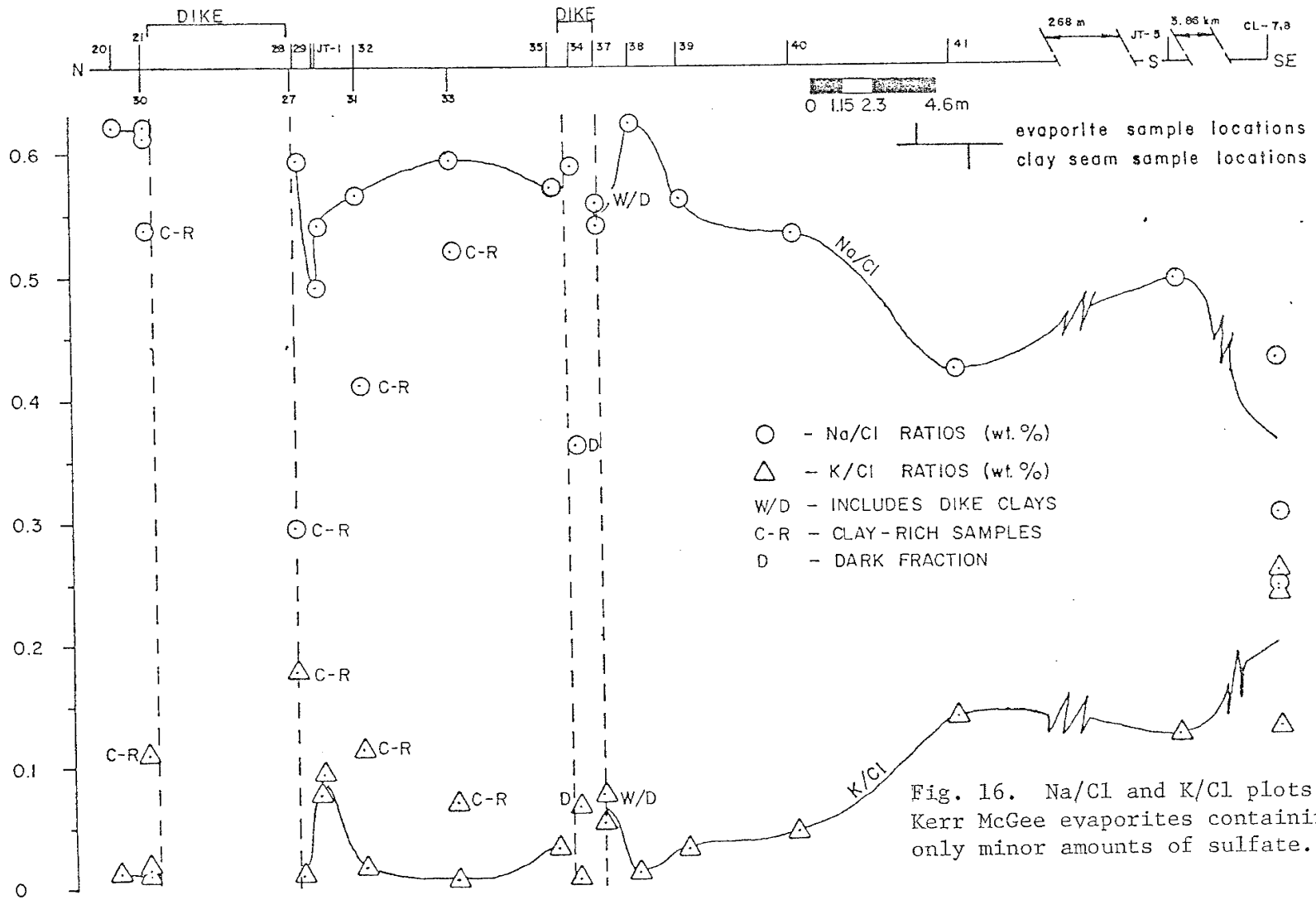

Fig. 16. Na/Cl and K/Cl plots of Kerr McGee evaporites containing only minor amounts of sulfate.

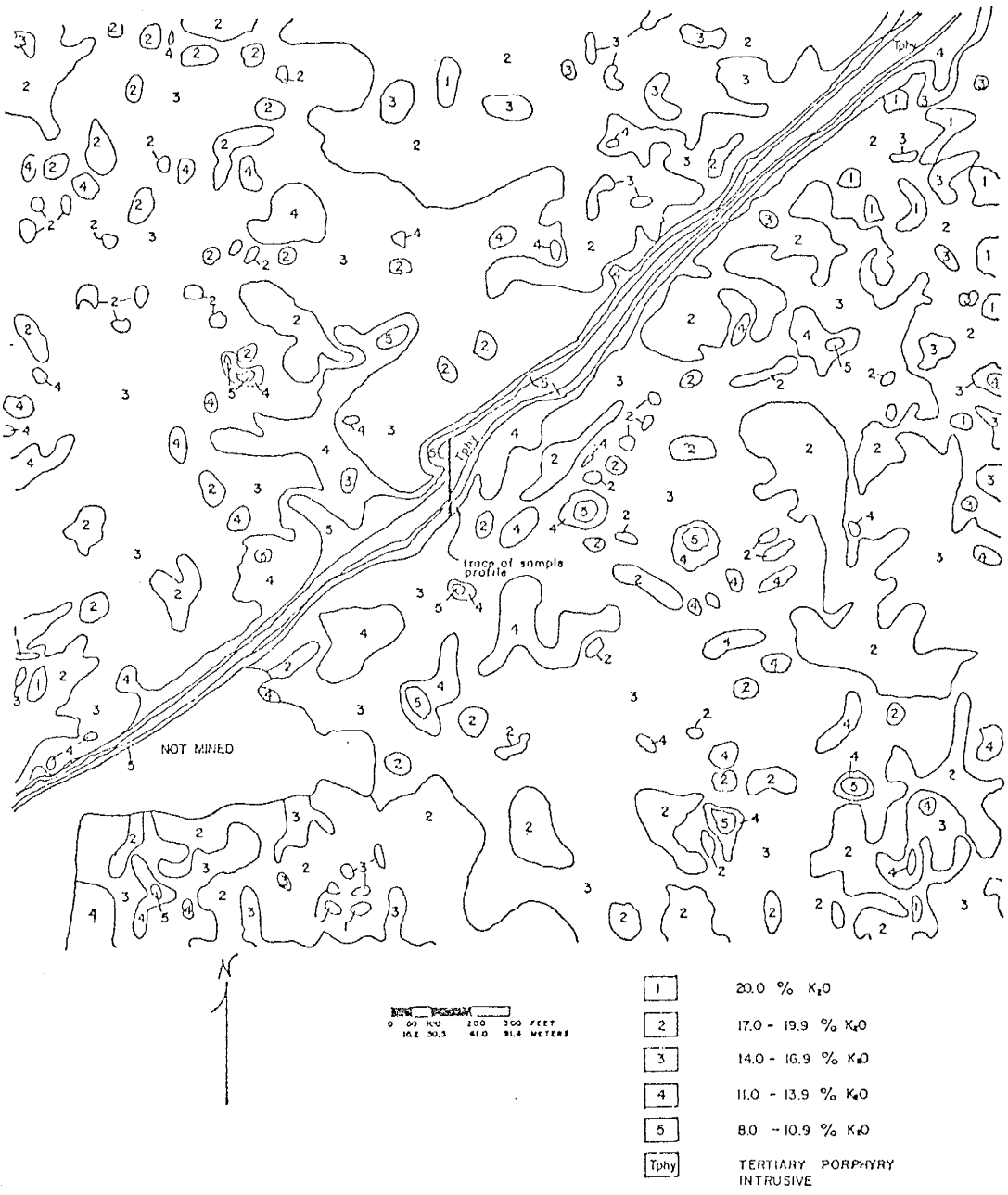

Fig. 17. Potash ore grade deliniations near Tertiary intrusions, Kerr McGee mine (modified from ore grade map, Kerr McGee Potash Facility).

indicates that this alteration is highly variable in a spatial sense, and can be much greater or more restricted than shown at the sample site.

The Si/Al ratios of silicate residues in the Kerr McGee mine (Fig. 18, Table 6) most readily reflect the clay content of the samples. Surrounding the principal dike, they are slightly lower due to the development of the relatively clean halite and sulfates. In contrast, the values surrounding the smaller intrusion are slightly higher than those for normal assemblages. In one sample (32) between the dikes, the value is high, and reflects free quartz recorded by diffraction. As described above, the salt inclusion reflects chemical characteristics of normal argillaceous K-rich evaporites.

Iron values are lowest in non-argillaceous salts; relatively high values compared to Al are present, with minor variability, away from the altered zones where normal assemblages are approached. This could reflect containment of iron oxide by potash minerals. The inclusion sample is even higher, reflecting pyrite contamination from the dike material.

Surrounding the larger intrusion, Mg/Al values are slightly depleted compared to values at larger distances from the dike. However, unnormalized (raw) MgO concentrations show the inverse relationship. An exception to this generalization is sample 32, which also exhibits excess SiO_2 amounts. By comparison, the smaller intrusion possesses higher than normal Mg/Al at its contacts. Talc follows the Mg/Cl distribution.

Calcium, in minor amounts, is distributed somewhat erratically throughout the profile, but all northerly located samples do have

Fig. 18. Distribution of chemical weight ratios of Kerr McGee silicate residues.

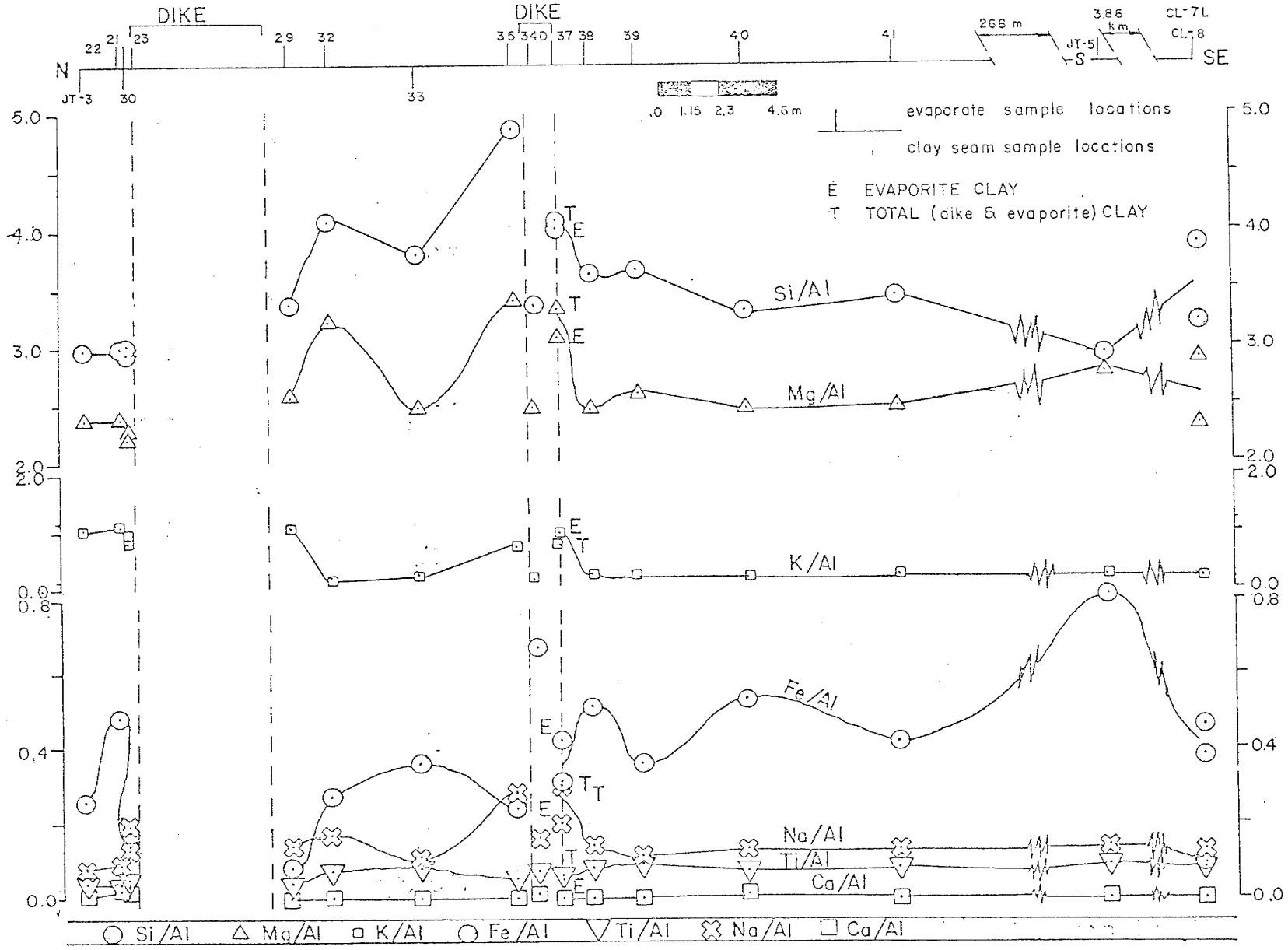

Table 6. Matrix corrected chemistry of Kerr McGee Silicates (wt %).

Sample	SiO_2	TiO_2	Al_2O_3	Fe_2O_3 (as total Fe)		MgO	CaO	Na_2O	K_2O	Total
JT-3	45.24	0.43	13.40	2.67		27.94	0.13	0.80	8.85	99.46
22	44.66	0.47	13.18	4.84		27.46	0.18	0.87	9.06	100.72
21	46.14	0.55	13.51	1.48		26.24	0.08	1.84	7.14	96.98
30*	45.46	0.60	13.63	1.84		27.25	0.09	1.24	7.89	98.00
					dike					
29*	46.21	0.41	12.14	0.70		27.29	0.00	1.22	8.03	96.00
32	44.63	0.57	9.68	1.95		27.41	0.00	1.14	1.32	86.70
33*	48.68	0.80	11.31	3.11		24.39	0.00	0.86	1.89	91.04
35	45.37	0.39	8.24	1.49		24.50	0.00	1.63	3.75	85.37
					dike					
34D	45.41	0.73	11.93	6.03		25.94	0.12	1.40	1.50	93.06
					dike					
37MXD	46.25	0.51	10.02	2.34		29.17	0.00	2.13	4.90	95.32
37MDC	46.79	0.44	10.27	3.25		27.73	0.003	1.45	6.31	96.24
38	47.48	0.77	11.57	4.45		24.98	0.03	1.13	1.74	92.15
39	46.14	0.88	11.13	3.07		25.40	0.00	0.87	1.39	88.88
40	45.42	0.75	12.08	4.81		26.19	0.07	1.15	1.60	92.07
41	46.53	0.86	11.96	3.77		25.98	0.02	1.09	1.66	91.87
JT-5	46.15	0.85	10.34	6.37		25.16	0.03	1.02	1.45	91.37
CL-77-7L(*)	45.99	0.92	12.66	3.63		25.86	0.02	0.83	1.56	91.47
CL-77-8	45.83	0.75	10.42	3.64		26.38	0.00	0.94	1.29	89.25

* clay seam
(*) clay-rich

detectable amounts, and the interval between the dikes does not. Sodium/aluminum values are essentially constant throughout the profile, except immediately surrounding and within the smaller intrusion where the samples contain twice the normal content. Potassium/aluminum values are high in the 2m interval to the north and immediately adjacent to all other contacts, but to a lesser extent surrounding the smaller dike. All other samples, regardless of position relative to the dikes have essentially identical K/Al values. This pattern of K/Al is reflected by the distribution of phlogopite. Values of Ti/Al are inversely related to K/Al values.

Unnormalized Al concentrations are highest on the north side of the dike complex, but are relatively low between the dikes in less argillaceous samples. The inclusion here again follows the normal pattern. Deviation of the analytical totals from 100% by weight reflect clay contents and clay character of the samples through inferred wt.% H_2O by difference.

Yeso Hills chemistry

The Ca/S values in all bulk rock samples (Table 7) exceeds that ratio required for total consumption of Ca by gypsum - $CaSO_4 \cdot 2H_2O$ - (1.25). Thus, the diffraction data identifying the presence of calcite in addition to gypsum is supported. Sodium, potassium, magnesium, iron, aluminum, and titanium were detected in these samples and although no associative mineralogies were detected in bulk rock diffraction patterns, the silicate fraction indicates these elements contribute to the formation of feldspars, mica, pyrite, and clays.

Chemical trends can be distinguished using the normative comparison to sulfur contents. Iron/sulfur ratios are detected solely

Table 7. Chemical weight ratios (wt.%) of bulk rock fraction, Yeso Hills locality, location LDC.

Sample	S	Si/S	Ti/S	Al/S	Fe/S	Mg/S	Ca/S	Na/S	K/S
S stream cut									
					dike				
47	17.67	0.00	0.0054	0.0042	0.0012	0.0028	1.38	0.0068	0.0011
48	18.07	0.00	0.0010	0.0038	0.00	0.0028	1.33	0.012	0.0006
49	18.12	0.00	0.0003	0.0044	0.00	0.00	1.33	0.00	0.0006
50	18.38	0.00	0.0007	0.0043	0.00	0.0027	1.26	0.010	0.0005
51	17.75	0.00	0.0007	0.0054	0.00	0.0034	1.37	0.018	0.0006
N stream cut									
54	18.21	0.00	0.0007	0.0044	0.00	0.0038	1.30	0.021	0.0016
53	17.79	0.00	0.0013	0.0048	0.0008	0.0028	1.37	0.019	0.0011
					dike				
52	17.81	0.00	0.0007	0.0036	0.00	0.0045	1.38	0.011	0.0011

immediately adjacent to the dikes; Ti/S ratios increase significantly in the gypsiferous sediment close to dike margins.

At dike contacts where mixed-layer illite/saponite is a prominent constituent of the silicate residue, Mg/Al is relatively high (Fig. 19). Both Na/Al and Ca/Al are inversely related to K/Al suggesting an increase in the plagioclase/orthoclase ratio. Diffraction patterns do not record this since the 4.2Å (201) peak orthoclase determination is masked by a prominant quartz peak, that mineral being ubiquitous in this sample suite. In general, Mg/Al ratios reflect clay content of the samples. As indicated in both bulk rock and silicate residue analyses, Ti and Fe concentrations have evidently been supplemented by igneous material in the form of pyrite and ilmenite.

Dike Rock chemistry

The chemistry of dike rock at both the Kerr McGee and Yeso Hills localities (Table 8) resembles that of alkaline olivine basalts (Table 9); however, K_2O values generally exceed maximum values allowed for that definition, CaO is always below the minimum, and Na_2O values are low compared to the values presented. In addition, differences exist between the dikes at each occurrence. Compared to the dike which intrudes the Castile Formation in the Yeso Hills, the intrusion at the Kerr McGee, into the Salado Formation, is lower in Si/Al, Ti/Al, Fe/Al, Ca/Al, and Na/Al, and enriched in Mg/Al and K/Al (Table 10). Compared to analyses reported by Calzia and Hiss (1978), the Kerr McGee analyses of this study agree reasonably well. Dike rock (float) from location LDA most closely resembles the Yeso Hills dike rock, exceptions being higher K/Al and Mg/Al and lower Ca/Al. Chemical analyses of grab samples from the Yeso Hills locally (LDB) indicate various stages of

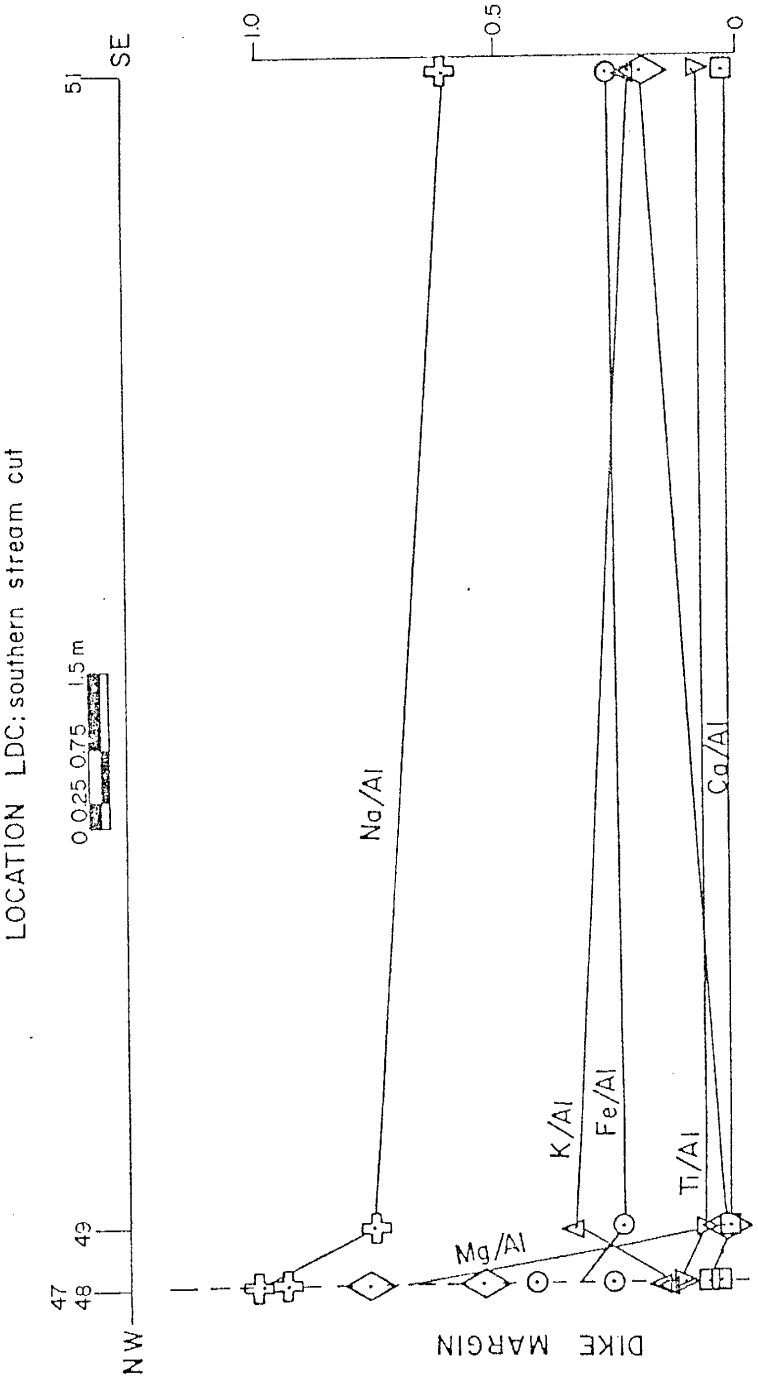

Fig. 19. Distribution of chemical weight ratios of the silicate fraction, Yeso Hills locality, location LDC, southern stream cut.

Table 8. Chemistry of dike rock (wt.%).

Sample	SiO_2	TiO_2	Al_2O_3	Fe_2O_3 (total Fe)	MgO	CaO	Na_2O	K_2O	MnO	total
Kerr McGee sample suite										
23*	50.07	2.29	14.36	11.42	7.22	2.65	1.53	7.99	0.18	97.71
36	49.76	2.23	14.44	11.58	7.59	3.14	1.72	6.93	0.15	97.54
24**	49.10	2.37	13.75	11.89	8.20	3.67	2.20	5.26	0.11	96.55
Yeso Hills sample suite										
southern stream cut - location LDC										
46*	48.16	2.67	13.10	12.46	4.26	6.11	3.67	3.10	0.13	93.66
45D**	48.16	2.44	13.49	11.41	4.50	6.71	3.17	2.89	0.10	92.87
45L†	48.47	2.95	13.34	12.70	4.50	5.00	2.85	2.76	0.08	92.65
location LDB										
18A†	45.82	2.49	13.09	13.86	4.83	5.71	2.50	2.08	0.11	90.49
18B†	50.24	3.00	14.63	10.02	3.19	4.58	2.76	2.16	0.09	90.67
19L†*	63.81	3.52	15.92	1.12	0.35	0.73	3.87	5.29	0.01	94.62
19D†	49.52	2.85	13.64	13.59	3.09	4.34	4.79	1.67	0.08	93.57
location LDA										
17	48.35	2.71	13.43	13.66	6.52	2.64	3.28	4.51	0.12	95.22
Miscellaneous samples										
LD-1	48.10	2.58	12.86	13.11	6.20	4.48	2.99	4.84	0.16	95.32
LD-2	47.69	2.74	12.90	13.26	5.93	4.11	2.84	4.12	0.10	93.69
LD-3	49.43	2.23	13.48	11.63	9.51	3.67	2.21	4.87	0.16	97.19
LD-4	50.45	2.14	13.77	11.24	7.35	2.76	1.15	6.40	0.16	95.42
LD-5	49.02	2.30	13.42	11.60	8.25	3.91	1.95	5.62	0.10	96.17
LD-6	48.82	2.31	12.98	11.38	9.26	4.20	2.25	4.26	0.20	95.66
LD-7	49.55	2.23	13.24	10.76	8.90	4.29	2.16	5.25	0.12	96.50
LD-8	49.04	2.37	13.05	11.47	9.05	4.28	2.37	4.69	0.14	96.46
LD-9	50.00	2.20	13.85	11.36	8.69	3.24	1.70	6.28	0.16	97.48
range††	45.82-50.45	2.14-3.00	12.86-14.63	10.02-13.86	3.09-9.51	2.64-6.71	1.15-4.79	1.67-7.99	0.08-0.20	
mean††	48.93	2.48	13.52	12.02	6.69	4.18	2.53	4.51	0.13	

* margin facies ; ** interior facies ; † weathered ; †† excluding 19L

Table 9. Average chemical compositions of different kinds of flood basalts (in wt.%). Continental tholeiites (144 analyses); oceanic tholeiites (161 analyses); alkaline basalts (199 analyses). From Hyndman (1972, p. 172).

	Continental Tholeiites		Oceanic Tholeiites		Alkaline Olivine Basalt	
	Average	Range	Average	Range	Average	Range
SiO_2	50.7	44.35-54.60	49.3	42.8 -52.56	47.1	41.04-51.4
TiO_2	2.0	0.9 - 3.99	1.8	0.35- 3.69	2.7	0.92- 4.52
Al_2O_3	14.4	12.48-16.32	15.2	7.3 -22.3	15.3	10.11-26.26
Fe_2O_3	3.2	0.95- 7.56	2.4	0.69- 7.90	4.3	0.53-15.85
FeO	9.8	4.18-13.60	8.0	2.86-13.58	8.3	0.48-13.63
MnO	0.2	0.10- 0.3	0.17	0.09- 0.44	0.17	0.06- 0.36
MgO	6.2	3.52-11.16	8.3	4.59-26.0	7.0	2.66-17.87
CaO	9.4	7.45-11.8	10.8	6.69-14.1	9.0	6.81-14.46
Na_2O	2.6	1.8 - 3.47	2.6	0.90- 4.45	3.4	1.35- 4.8
K_2O	1.0	0.19- 1.74	0.24	0.04- 0.70	1.2	0.13- 2.5
P_2O_5		0.09- 0.81	0.21	0.06- 0.56	0.41	0.09- 0.93

Table 10. Chemical weight ratios (wt.%) of dike rock.

Sample	Si/Al	Ti/Al	Fe/Al	Mg/Al	Ca/Al	Na/Al	K/Al	Al
Kerr McGee suite								
23*	3.08	0.18	1.05	0.57	0.25	0.15	0.87	7.60
36	3.04	0.17	1.06	0.60	0.29	0.18	0.75	7.64
23**	3.15	0.20	1.14	0.68	0.36	0.22	0.60	7.28
Yeso Hills suite								
southern stream cut - location LDC								
46*	3.25	0.23	1.26	0.37	0.63	0.39	0.37	6.93
45D**	3.15	0.20	1.12	0.38	0.67	0.33	0.34	7.14
45L†	3.21	0.25	1.26	0.38	0.51	0.30	0.32	7.06
location LDB								
18A†	3.09	0.22	1.40	0.42	0.59	0.27	0.25	6.93
18B†	3.03	0.23	0.91	0.25	0.42	0.26	0.23	7.74
19L†*	3.54	0.25	0.90	0.03	0.06	0.34	0.52	8.43
19D†	3.21	0.24	1.32	0.26	0.43	0.49	0.19	7.22
location LDA								
17	3.18	0.23	1.35	0.55	0.27	0.34	0.53	7.11
Miscellaneous samples								
LD-1	3.30	0.23	1.35	0.55	0.47	0.33	0.59	6.81
LD-2	3.26	0.24	1.36	0.52	0.43	0.31	0.50	6.83
LD-3	3.24	0.19	1.14	0.80	0.37	0.23	0.57	7.13
LD-4	3.23	0.18	1.08	0.61	0.27	0.12	0.73	7.29
LD-5	3.23	0.19	1.14	0.70	0.39	0.20	0.66	7.10
LD-6	3.32	0.20	1.16	0.81	0.44	0.24	0.52	6.87
LD-7	3.30	0.19	1.08	0.77	0.44	0.23	0.62	7.01
LD-8	3.32	0.21	1.16	0.79	0.44	0.25	0.56	6.91
LD-9	3.19	0.18	1.08	0.72	0.32	0.17	0.71	7.33

* margin facies
** interior facies
† weathered

weathering, as evident in hand specimen.

The composition of the dikes changes toward the margins in both instances. At the Kerr McGee mine, the margin is enriched in K/Al and Si/Al, depleted in Mg/Al, Ca/Al, Na/Al, Ti/Al, and Fe/Al (Fig. 20). In the Castile, the margin exhibits higher Fe/Al, Na/Al, Ti/Al, K/Al, and Si/Al and slightly lower Mg/Al and Ca/Al. Numerically, the most significant of these phenomena are those of Mg and K ($\Delta \cong 0.2$) in the Kerr McGee mine and Si, Ca, and Fe ($\Delta \cong 0.1$) in the Yeso Hills.

DISCUSSION

Kerr McGee occurrence

The mineralogical and chemical characteristics of the Kerr McGee sample suite point to several physical and chemical interactions induced by the intrusions.

The unaltered silicate assemblage in evaporite rocks at large distances from the dikes (>7.4m) consists of partially ordered corrensite, dioctahedral illite, talc, chlorite, and pyrite in decreasing order of abundance. This assemblage is modified in an interval 1.5-7.4m from the dikes to a disordered corrensite and slightly greater relative amounts of talc and chlorite compared to the unaltered assemblage. The chemical reaction may follow one such as reaction a) of Table 11. Silicon to aluminum and magnesium to aluminum ratios support their additions to the reactant side of the equation. The tiny amount of excess Al_2O_3 may be incorporated into the lattice structure of another silicate nonstoichiometrically. Remaining minerals show no change in this interval.

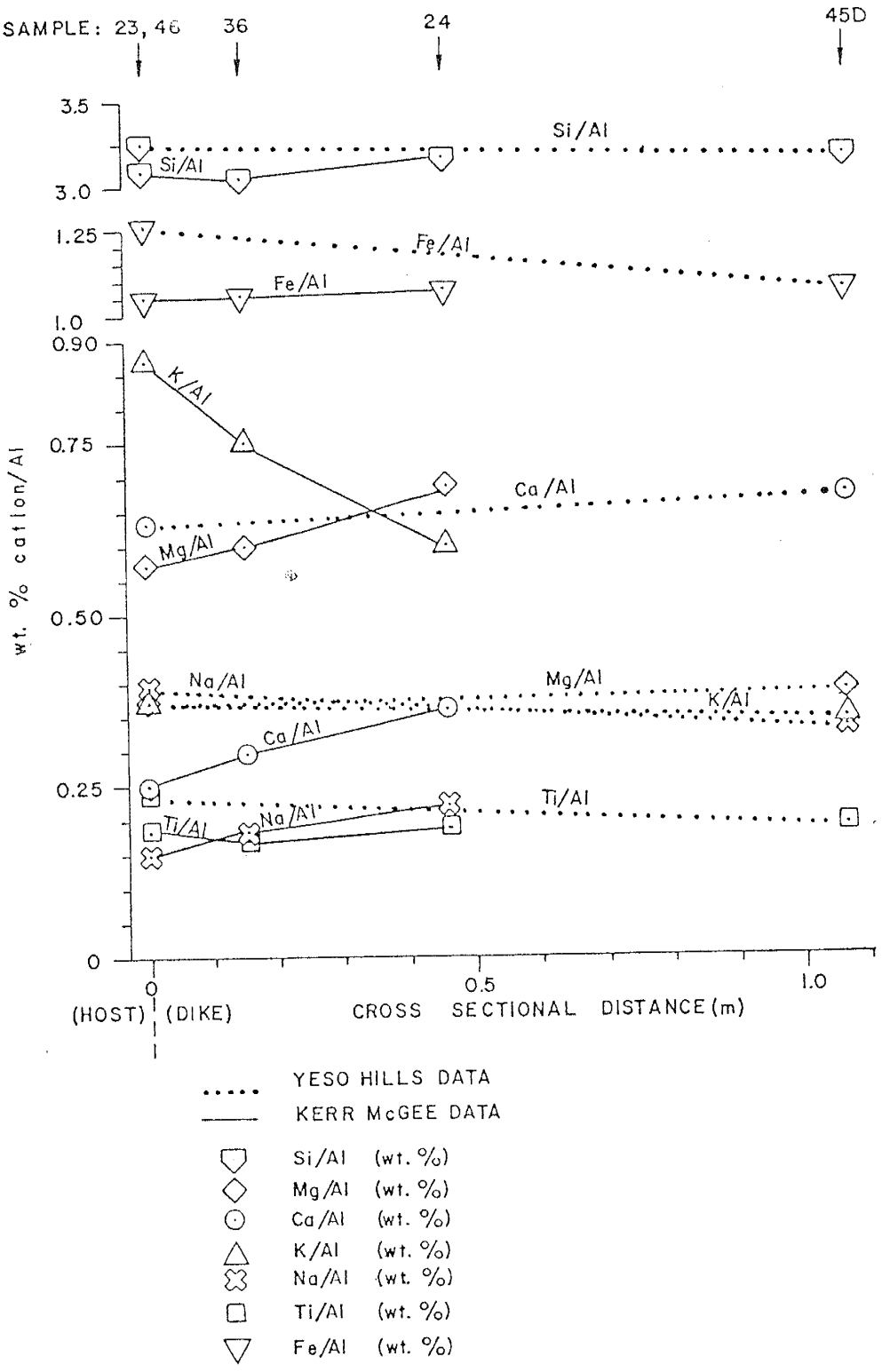

Fig. 20. Distribution of dike rock chemical data.

Table 11. List of reactions attending alteration features.

a) $2(1chl \cdot 1sap) + 9Mg^{2+} + 4SiO_2 + 4.17H_2O \longrightarrow 1(1chl \cdot 1sap) + 2talc + 1chl + 0.33qtz + 0.17Al_2O_3 + 4.59H^+$

b) $KCl + Na^+ \longrightarrow NaCl + K^+$
(sylvite) (halite)

$MgCO_3 + 4CaSO_4 + 2K^+ + 2H_2O \longrightarrow K_2Ca_2Mg(SO_4)_4 \cdot 2H_2O + CO_3^{=} + 2Ca^{2+}$
(magnesite) (anhydrite) (polyhalite)

$CaSO_4 + 2H_2O \longrightarrow CaSO_4 \cdot 2H_2O$
(anhydrite) (gypsum)

c) $2(1chl \cdot 1sap) + 2talc + 1chl + 15SiO_2 + 6H_2O \longrightarrow 2sap + 2(1chl \cdot 3sap) + 1talc + 2Mg^{2+} + 10H^+$

d) $5illite + 13K^+ + 13K^+ + 3clino\text{-}penn\ chl + 31Mg^{2+} + 20.75SiO_2 + 36.5H_2O \longrightarrow 16phlogopite + 17.25H^+$

e) $5illite + 13K^+ + 3clino\text{-}penn\ chl + 4talc + 19Mg^{2+} + 4.75SiO_2 + 20.5H_2O + 6.75H^+ \longrightarrow 16phlogopite$

f) $2.5Kspar + .5Na^+ + .5Ca^{2+} \longrightarrow 1Kspar + 1plag(An50) + 2qtz + 1.5K^+$

(1chl·1sap) - mixed-layer clinochlore chlorite (50%) and saponite (50%) (corrensite)
(1chl·3sap) - mixed-layer clinochlore chlorite (25%) and saponite (75%) (corrensite)
chl - clinochlore chlorite: $(Mg_5Al)(Si_3Al)O_{10}(OH)_8$
sap - saponite: $(R_x \cdot {}^{33}Mg_5)(Si_{3.67}Al_{.33})O_{10}(OH)_2 \cdot nH_2O$
talc: $Mg_3Si_4O_{10}(OH)_2$
illite: $K_{.6}(Mg_{.25}Al_{1.8})(Si_{3.5}Al_{.5})O_{.10}(OH)_2$
clino-penn chl - clinochlore-penninite chlorite: $(Mg_{5.25}Al_{.75})(Si_{3.25}Al_{.75})O_{10}(OH)_8$
phlogopite: $KMg_3(Si_3Al)O_{10}(OH)_2$
Kspar - orthoclase: $KAl\ Si_3O_8$
plag(An50) - plagioclase, anorthite content 50%: $(Na_{.5}Ca_{.5})(Al_{1.5}Si_{2.5})O_8$

In the intervals directly adjacent to dike margins, effects evident by diffraction and fluorescence data can be represented by several equations shown in b) of Table 11. The reactants sylvite, magnesite, sodium (in the form of halite, or from the dike), and possibly some of the anhydrite were provided by the evaporite sequence since these minerals are present in less altered rocks. Anhydrite could also have been contributed by the basalt since the anhydrite beds of the Castile underlie the Salado and likely were assimilated by the dike (see below). The sylvite is present in unaltered rocks, suggesting that its dissolution and the subsequent formation of halite continued into the intermediate zone of alteration, although neither this process nor the consumption of magnesite was completed at the smaller dike. The combined resulting assemblage at the contact follows that indicated by mineralogical and chemical data, with some variability. That variability is that greater sulfate development and a general greater degree of alteration resulted on the north side of the intrusions. The influence of each of the reactions in (b) can easily have changes according to the chemical conditions present; slight variations in these mineralogies exist throughout the alteration profile.

The potash-leaching mechanism at initial high temperatures nearest the dike first involved melting of KCl and NaCl, then development of a solid solution relationship as temperatures decreased, and lastly an unmixing at temperatures which depended on composition (Fig. 21). At greater distances from the dike where melting did not occur but warm NaCl-saturated fluids caused dissolution along with subsequent leaching, the mineral compositions remained unmixed throughout the entire process. These compositions change as K and Br are removed from the system as

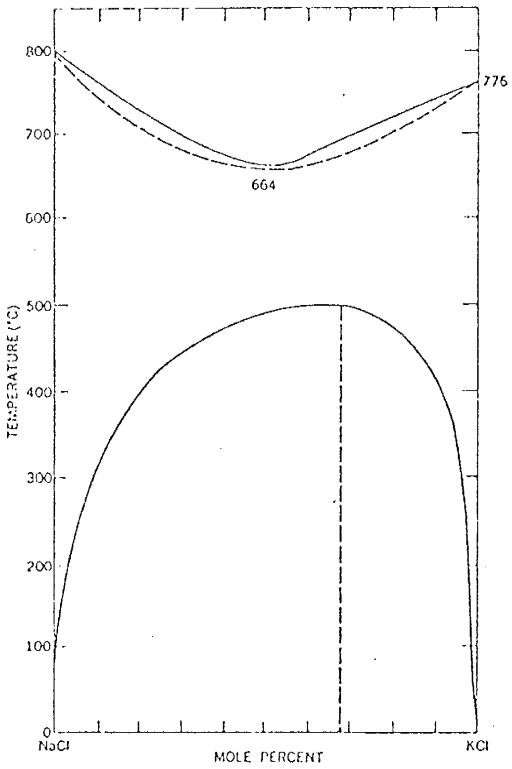

Fig. 21. The binary system NaCl-KCl (from Nguyen - Ba - Chanh, 1964).

KBr or K(Br,Cl) - saturated solutions in amounts dependent on clay content and distance from the dike. The greatest movement of the fluids was toward the dikes along developing clay seams which enabled enrichment of contact evaporites in potassium in the form of phlogopite and polyhalite. Sodium is added to the NaCl-KCl system nearest the dikes. In final stages, NaCl is precipitated and this recrystallized halite remains.

The reactions concerning silicates in the same area utilized the modified assemblage of disordered corrensite and talc, the untouched discrete chlorite, and excess Mg from the margin reaction involving principally chlorides and sulfates. The reaction c) (Table 11) corresponds to the results of this study. The products show that large Mg concentrations were accommodated, at least as much as Al concentrations would allow. The equation also illustrates the inverse relationship between quartz occurrences and mineralogies of the reactant side. An increase in the smectite component of mixed-layers by hydrothermal alteration has been documented in another case by Blatter and others (1973).

The formation of a trioctahedral mica phase, a phlogopite or phlogopitic-clay, at this point may be viewed as an end-point of the alteration sequence. This mineral is the sole phase at the more intensely altered dike contact (north side); it occurs with the discrete smectite and mixed-layer material at all others. The phase is identified as $1M_d$; Yoder and Eugster (1954) found this phase to be that of lowest temperature phlogopite. Its formation consumes excesses from previous reactions and minerals characteristic only of other zones (reaction d), Table 11). One alternative equation which accomplishes

the same feat is shown in reaction e), Table 11. It is also possible that phlogopite could have been formed through the recrystallization of saponite where tetrahedral Si^{4+} is replaced by Al^{3+} and Fe^{3+}, increasing the layer charge from 140 to 210 me/100g. The process in reverse, e.g. the weathering of phlogopite to form saponite, has been introduced by Sridhar and Jackson (1974). However, in this study, since phlogopite and discrete saponite occur in the same interval, any saponite available as a reactant would have to come from the mixed-layer material which is also the necessary source for the formation of discrete and mixed-layer smectites (reaction c), Table 11).

At the northern contact of the smaller intrusion, the sample (35) is stratigraphically lower than those in clay-rich horizons and its silicate assemblage reflects that of unaltered rocks. In addition, it illustrates even greater ordering than normal. Within this dike are two evaporite fractions which independently resemble unaltered and intensely altered assemblages. Possibly one is bordered by the other and a micro-alteration sequence has developed. These and other data indicate the smaller intrusion definitely modified the rock less intensely compared to the larger. Even so, the fact that sample 35 was unchanged suggests that the open-system mobility obviously required for the alteration phases identified in this study was satisfied by the development of clay seams. This is verified by the increase of raw MgO and Al_2O_3 concentrations and thus a relatively higher clay content close to the dikes.

The addition of Mg interlayers to regular interlayer chlorite/smectite, which could be viewed as a general description of the changes in clay character in this investigation, is in response to the

equilibrium between these mixed-layers and a mildly acidic Mg, Na, and K-rich environment (Grim and others, 1960; Glass and others, 1973). In this case, hydrothermal fluids triggered the development, movement, and concentration of this environment which resulted in the alteration profile existing today.

Yeso Hills occurrence

From chemical and mineralogical data, it is evident that contact enrichment of the gypsum by Ti and Fe has been in the form of ilmenite and pyrite, and feldspar modification has followed that of reaction f), Table 11. These non-clay silicate assemblages change only within 0.4m of the dike. The mixed-layer trioctahedral illite/saponite becomes more regular and increases in concentration relative to other minerals within the same interval. Blatter and others (1973) have also recorded this ordering phenomenon adjacent to intrusions. The potassium released by the formation of plagioclase from orthoclase probably contributed to the enrichment of orthoclase relative to plagioclase in the dike margin facies. It is possible that a minor amount of potassium also contributed to the illite to facilitate the increased regularity of the illite-saponite. The simultaneous destruction of some of the saponite component would produce MgO and SiO_2 excesses used in dike margin facies clays and this SiO_2 may also have contributed to orthoclase production in the dike.

The distribution of clay contents in the sediment samples does suggest that the absence of clay at 0.4m from the dike may represent a leach zone which led to the concentration of the clay at the contact. If this leach zone was symmetrical and the sample was at maximum hiatus, the extent of alteration would be perhaps one meter. Neither of

these factors is probably the case. However, since all characteristics indicate that the alteration is not as intense as in the Salado Formation, the extent of alteration is here estimated as being 2-3m into the gypsiferous sediments.

Dike Rock

The textural and spatial relationships of these igneous rocks for the most part match those of typical lamprophyres (Hyndman, 1972, p. 186-192). The small to medium sized dikes are extensively altered, especially their mafic phenocrysts and the few felsic components are anhedral as phenocrysts and otherwise confined to the groundmass. Gross and Heinrich (1966) have reported a few lamprophyres containing felsic constituents of this nature.

Chemically, and to some extent mineralogically, the rocks can be labeled alkaline-rich alkaline olivine basalts (Fig. 22) and they exhibit more severe lamprophyre characteristics towards the borders, as lamprophyres commonly do. These characteristics are evident by chemical analyses of interior and margin facies and are illustrated by the Harker Variation diagram (Fig. 23), which theoretically should show crystallization history from a common parent magma.

At the Kerr McGee occurrence, high K and low Na at margins and the suite as a whole infers that potash available in the ore zone was incorporated by the magma upon its intrusion and sodium from the dike contributed to the reaction releasing that potassium in adjacent non-clay rock salts. X-ray diffraction data on the dikes and plagioclase anorthite contents show that the feldspar compositions reflect these changes. In addition, Ca values vary systematically across the dike, and correspond to the relative proportions of plagioclase vs. alkali

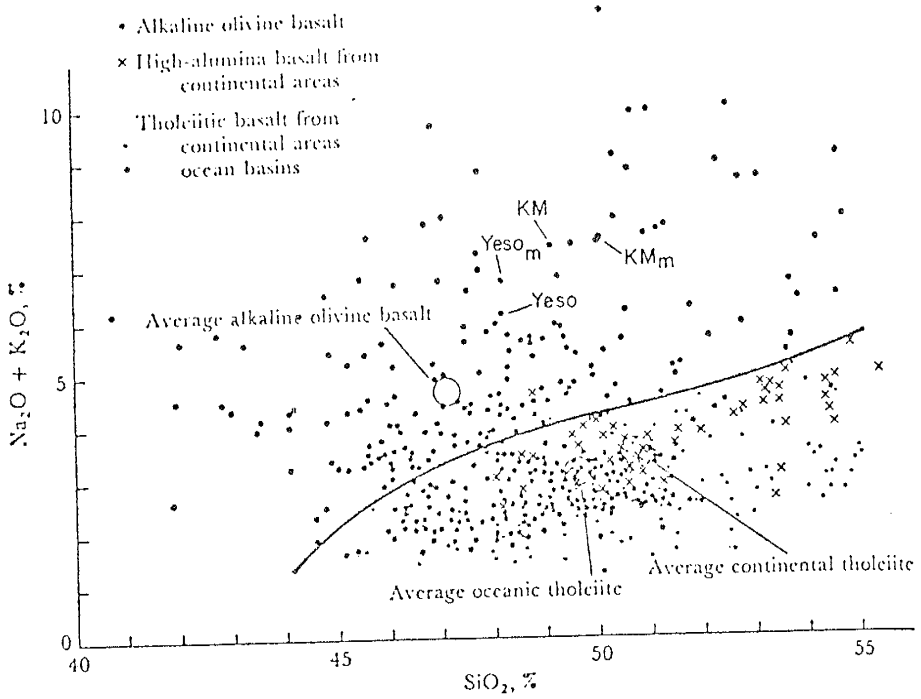

Fig. 22. Alkali-silica variation of basalts. Worldwide occurrences. Analyses from the literature. Plot is of the type used by Tilley (1950) and Kuno (1959). Position of samples of this study are indicated: 1)Kerr McGee dike rock margin facies as KM_m, 2)Kerr McGee dike rock interior facies as KM, 3)Yeso Hills dike rock margin facies as $Yeso_m$, and 4)Yeso Hills dike rock interior facies as Yeso. (Modified from Hyndman, 1972, p.172).

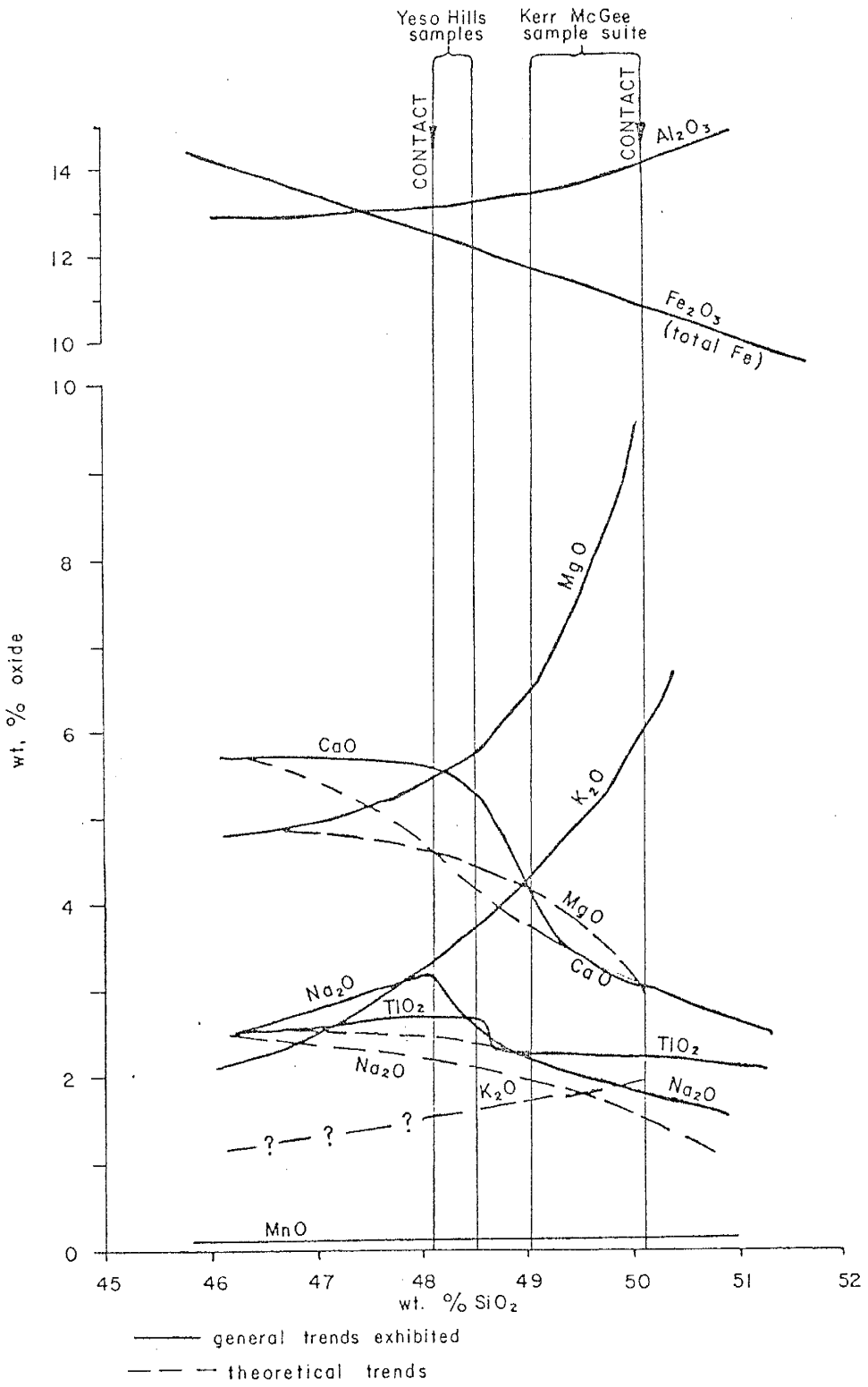

Fig. 23. Harker Variation Diagram from data in Table 8; curves generated from analyses of dike rock collected in this study and of dike rock contributed by Elliot Geophysical Co., Tucson, Ariz. from the same and/or similar localities. Yeso Hills sample region excludes weathered rock analyses. Plot type from Harker (1909).

feldspar (assumed to be orthoclase) from interior to margin.

Calcium from the gypsum of the Castile Formation and sodium from halite beds contained within that formation have been assimilated by the dike in the Yeso Hills. The potash anomaly in dike margins, although lower than in the Kerr McGee, is present here also, and feldspars show similar distribution patterns. The exception is that plagioclase persists even at dike margins, along with the potassium feldspar; a higher percentage of the former at margins accounts for higher sodium contents.

In both instances the formation of orthoclase, presumably relatively late in the crystallization sequence, was triggered by contact effects and resulted in subhedral crystallization of that mineral in the rock. These same contact effects, in their diversity, must have caused the difference in clay character toward dike margins at the two localities. At the Kerr McGee, the margin shows an absence of chlorite compared to a chlorite + chlorite/smectite mixed-layer assemblage towards the interior. Yeso Hills dike shows the latter assemblage at its margins and a smectite as the sole phase towards the interior. Magnesium has been removed from these igneous-derived clays, more extensively at the Kerr McGee, and possibly contributes to the Mg-rich clay of the host horizons.

The marginal enrichment within the dikes in Ti/Al and Fe/Al in the Yeso Hills is evidently a result of the higher percentage of ilmenite ($FeTiO_3$) in the groundmass of the chilled margins. The sediments immediately adjacent to the dike have been contaminated in this manner also. However, at the Kerr McGee, the opposite phenomenon is seen - the contact area is depleted in these elements, possibly as a

result of their migration during alteration processes.

Several hypotheses have been presented in the literature concerning the formation of lamprophyres (see Hyndman, 1972, p. 186-192), including differentiation (Joplin, 1966) or crystallization ± resorption (Luth, 1967; Velde, 1967) of alkaline olivine basaltic magma. It is apparent from this study's chemical analyses and even thin section observations where vugs contain recrystallized host material, a form of residual assimilation, that the dike rocks have been severely contaminated by alkalies from wall rocks. The major alkali contribution is K_2O from the potash deposits in the Kerr McGee mine; that of the Yeso Hills is Na_2O derived from salt beds contacted during injection of the magma. When these major deviations, those for alkaline earths, and the weathered nature of the Yeso Hills rocks are accommodated, theoretical curves emerge and the dikes appear to have originated from the same material.

The temperature of magma intrusion, a fluid state since chilled margins developed, may have been between 800°C and 600°C. This is lower than normal for a basaltic magma but the salt beds served to depress the melting point. The salts in the Kerr McGee mine apparently became molten and recrystallized to form a thin halo adjacent to the dike, disrupting strata. This molten state facilitated development of interfingering and brecciated salt and dike material at dike margins. Since the gypsum of the Castile Formation did not become fluid, no brecciation or interfingering occurred in the Yeso Hills area.

SUMMARY AND CONCLUSIONS

In the Salado Formation at the Kerr McGee Potash Facility, a

normal silicate assemblage of partially ordered corrensite, dioctahedral illite, talc, chlorite and pyrite was modified between 1.5m and 7.4m from the dike. Here a disordered corrensite and larger relative abundances of talc and chlorite replaced partially ordered corrensite. Sylvite was dissolved, potash leached, and halite crystallized. This process was continued and expanded to facilitate the dissolution of magnesite and formation of halite and Ca and K, Mg sulfates at 1.5-0m from the dikes. In addition, the silicate assemblage resulting at 1.5-7.4m is altered to saponite and irregular smectitic mixed-layer, less talc, and phlogopite. The latter is the sole phase at more intensely altered points.

These silicate reactions involved the additions of chlorite and/or talc (or Mg and SiO_2) and are a response to a mildly acidic Mg, Na, and K-rich environment induced by the hydrothermal action of the intrusions on soluble fractions of the host rocks. The alteration affects are most intense on the north side of the larger dike, probably due to an apophysis of the intrusion below the drift floor; they are less prominent and do not reach a comparable level of equilibrium at the smaller dike. Similarly, thin clay seams have developed in response to these intensities, and may have provided and/or supplemented the mechanism for open-system mobility, necessarily in the direction of the dikes, required for the development of the alteration sequence at the Kerr McGee mine.

All characteristics indicate that hydrothermal alteration of the gypsum of the Castile Formation extended perhaps 2 or 3m from dike contacts. The prominent alteration, present at the contact, is in the form of ordering and concentrating trioctahedral illite/saponite and

forming plagioclase and free quartz from orthoclase.

The intrusions themselves responded to wall rock compositions through assimilation at margins resulting in an increased orthoclase/plagioclase (andesine) ratio and late stage vug formation containing evaporite material. At both localities, a definite two-way interaction between dike and sediments has been recorded. The two dike complexes studied appear to be genetically related when contact assimilation effects are removed. It is presumed they intruded the Ochoan sediments at a temperature of 600°C - 800°C causing melting of the salts of the Salado Formation but not the gypsum of the Castile Formation.

The dike lies only 11.3km NW of the proposed radioactive waste disposal site and presumably the Salado Formation at the Kerr McGee is representative of salts of the Salado that will host this waste. The heat produced by radioactive decay in the debris will be dry heat, and if defined as low-level, the temperature will be around 300°C, which is at most one half the temperature of intrusion of the basaltic lamprophyre at the Kerr McGee. The alteration characteristics at this dike are those which involved warm fluids. But where a very thin envelope of melted and subsequently recrystallized white halite surrounds the dike, the effect is primarily thermal, except that fluids served to depress the melting point of the salts and leach the potash. Even so, this depression could not have reached a level which is of concern in the waste disposal question. Thus, it appears that no major alteration would result from 300°C of dry heat alone in these evaporites.

ACKNOWLEDGMENTS

I wish to thank Dr. Marc Bodine, Jr. for his invaluable advisement

and guidance on this project, and Sandia Laboratories for their monetary support which made the research feasible. Thanks must also go to the New Mexico Bureau of Mines and Mineral Resources for the use of X-ray equipment, to Joseph Taggart for troubleshooting these machines and aiding in evaluating the chemical analyses. My thesis committee, including Dr. Marc Bodine, Jr., Dr. John MacMillan, and Dr. James Robertson, all contributed constructive corrections to the final manuscript; Patricia Valentine meticulously typed the text.

REFERENCES CITED

Adams, J. E., Cheney, M. G., DeFord, R. K., Dickey, R. I., Dunbar, C. O., Hills, J. M., King, R. E., Lloyd, E. R., Miller, A. K., and Needham, C. E., 1939, Standard Permian section of North America: Am. Assoc. Petroleum Geologists Bull., v. 23, no. 11, p. 1673-1681.

Adams, S. S., 1969, Bromine in the Salado Formation: N. Mex. Bur. Mines & Mineral Resources, Bull. 93, 122p.

Blatter, C. L., Robertson, H. E., and Thompson, G. R., 1973, Regularly interstratified chlorite-dioctahedral smectite in dike-intruded shales, Montana: Clays & Clay Minerals, v. 21, no. 4, p. 207-212.

Bodine, M. W., Jr., and Fernalld, T. H., 1973, EDTA dissolution of gypsum, anhydrite, and Ca-Mg carbonates: Jour. Sed. Petrology, v. 43, p. 1152-1156.

Brandvold, L. A., 1974, Atomic absorption methods for analysis of some elements in ores and concentrates: N. Mex. Bur. Mines & Mineral Resources, Circ. 142, 22p.

Calzia, J. P., and Hiss, W. L., 1978, Igneous rocks in northern Delaware Basin, New Mexico and Texas: N. Mex. Bur. Mines & Mineral Resources, Circ. 159, p. 39-45.

Darton, N. H., 1928, "Red beds" and associated formations in New Mexico with an outline of the geology of the state: U. S. Geol. Survey Bull. 794, 372p.

Fournier, R. O., 1961, Regular interlayered chlorite-vermiculite in evaporite of the Salado Formation, New Mexico: U. S. Geol. Survey Prof. Paper 424-D, p. 323-327.

Glass, H. D., Frye, J. C., and Leonard, A. B., 1973, Clay minerals in east-central New Mexico: N. Mex. Bur. Mines & Mineral Resources, Circ. 139, 14p.

Grim, R. E., Droste, J. B., and Bradley, W. F., 1960, A mixed-layer clay mineral associated with an evaporite: Clays & Clay Minerals, v. 8, p. 228-236.

Gross, E. B., and Heinrich, E. W., 1966, Petrology and mineralogy of the Mount Rosa area, El Paso and Teller Counties, Colorado - Part 3, Lamprophyres and mineral deposits: Am. Mineralogist, v. 51, p. 1433-1442.

Harker, Alfred, 1909, The natural history of igneous rocks: New York, Macmillan, 384p.

Hyndman, D. W., 1972, Petrology of igneous and metamorphic rocks: New York, McGraw-Hill, 533p.

Jones, C. L., 1954, The occurrence and distribution of potassium minerals in southeastern New Mexico in Guidebook of Southeastern New Mexico: Stipp, T. F., ed., N. Mex. Geol. Soc. Fifth Field Conf., p. 107-112.

_____1972, Permian basin potash deposits, southwestern United States in Geology of Saline Deposits: Unesco, Earth Sci. Ser., no. 7, p. 191-201.

_____1973, Salt deposits of Los Medanos area, Eddy and Lea Counties, New Mexico, with sections on ground water hydrology by M. E. Cooley and surficial geology by C. O. Bachman: U. S. Geol. Survey open file report 4339-7, 67p.

_____and Madsen, B. M., 1959, Observations on igneous intrusions in late Permian evaporites, southeastern New Mexico: Geol. Soc. America Abs., v. 70, p. 1625-1626.

_____and Madsen, B. M., 1968, Evaporite geology, fifth ore zone, Carlsbad district, southeastern New Mexico: U. S. Geol. Survey Bull., v. 1252-B, 21p.

Joplin, G. A., 1966, On lamprophyres: Royal Soc. New South Wales, Jour. Proc., v. 99, p. 37-43.

Kelley, V. C., 1971, Geology of the Pecos country, southeastern New Mexico: N. Mex. Bur. Mines & Mineral Resources, Mem. 24, 75p.

King, P. B., 1942, Permian of west Texas and southeastern New Mexico: Am. Assoc. Petroleum Geologists Bull., v. 26, p. 535-763.

Kuno, H., 1959, Origin of Cenozoic petrographic provinces of Japan and surrounding areas: Bull. Volcanologique, ser. 11, v. 20, p. 37-76.

Lang, W. B., 1947, Occurrence of Comanche rocks in Black River valley, New Mexico: Am. Assoc. Petroleum Geologists Bull., v. 31, p. 1472-1478.

Linn, K. O., and Adams, S. S., 1966, Barren halite zones in potash deposits, Carlsbad, New Mexico in Second Symposium on Salt: Rau, J. L., ed., N. Ohio Geol. Soc., v. 1, p. 59-69.

Lippmann, F., 1956, Clay minerals of the Röt member of the Triassic near Göttingen, Germany: Jour. Sed. Petrology, v. 26, p. 125-139.

Luth, W. C., 1967, $KAlSiO_4$-Mg_2SiO_4-SiO_4-H_2O - Part 1: Inferred phase relations and petrologic applications: Jour. Petrology, v. 8, p. 372-416.

Marr, H. E., III, 1976, XRF4 - Computer programing for X-ray analysis: U. S. Bur. Mines, Info. Circ. 8712, 32p.

Maxwell, J. A., 1968, Rock and mineral analysis, Chemical analysis, v. 27: New York, Interscience Publishers, 584p.

Nguyen-Ba-Chanh, 1964, Équilibres des systémes binaires d'halogénures de sodium et potassium a l'état solide: Jour. Chimie Physique, v. 61, no. 10, p. 1428-1433.

Pratt, W. E., 1954, Evidences of igneous activity in the northwestern part of the Delaware Basin in Guidebook of Southeastern New Mexico: Stipp, T. F., ed., N. Mex. Geol. Soc. Fifth Field Conf., p. 143-147.

Schaller, Waldemar, and Henderson, Edward, 1932, Mineralogy of drill cores from the potash field of New Mexico and Texas: U. S. Geol. Survey Bull., v. 833, 124p.

Sokolov, P. N., Matuskin, R. G., and Pustyl'nikov, A. M., 1975, Interaction between dolerites and saliferous deposits of the Siberian Platform: Geologiya i Geofizika, v. 16, no. 8, p. 78-86.

Sridhar, K., and Jackson, M. L., 1974, Layer charge decrease by tetrahedral cation removal and silicon incorporation during natural weathering of phlogopite to saponite: Soil Sci. Soc. Am. Proc., v. 38, p. 847-851.

Tilley, C. E., 1950, Some aspects of magmatic evolution (presidential address): Geol. Soc. London Quart. Jour., v. 106 pt. 1, no. 421, p. 37-61.

Urry, W. E., 1936, Post-Keweenawan time scale, including two charts in National Research Council Rept. Comm. on Measurement of Geologic Time: 1935-1936, exh. 2, p. 35-40.

Velde, D., 1967, Sur un lamprophyre hyperalcalin potassique; la minette de Sisco (ile de Corse): Soc. Franc. Minéral. Crist. Bull., v. 90, no. 2, p. 214-223.

Yoder, H. S., Jr., and Eugster, H. P., 1954, Phlogopite synthesis and stability range: Geochem. et Cosmochim. Acta, v. 6, p. 157-185.

APPENDICES

LIST OF APPENDICES

APPENDIX I

Marine Assemblages in Marine Evaporite Rocks

The silicates in evaporites have been investigated extensively in the German Zechstein. Here, muscovite (illite) and chlorite, both principal constituents in the strata, and mica and quartz ubiquitous, are frequently accompanied by talc, koenenite, corrensite, and montmorillonite; combinations vary with the stratigraphy (Füchtbauer and Goldschmidt, 1959; Kühn, 1968).

The clay seams, or tongesteines, exhibit dominant illite and chlorite with corrensite and koenenite present also. Talc is a major constituent of sulfatgesteines, or anhydritic layers, accompanied by significant amounts of illite and chlorite. Also reported are lesser amounts of corrensite, mixed-layers, montmorillonite, and koenenite. Carbonate-rich strata contain, again, dominantly illite and chlorite. In rock salt beds and potash beds the relative clay content is significantly lower than in the horizons described above, and the character of the clay assemblages much more diverse. Generally illite and chlorite prevail, however, and koenenite becomes more predominant, especially in ore zones. In addition, corrensite, talc, boracite, montmorillonite, and even kaolinite have been recorded in various beds. (Füchtbauer and Goldschmidt, 1959; Dreizler, 1962; Kühn, 1968; Pundeer, 1969).

Accessory to evaporitic chlorides and sulfates, non-clay minerals of the assemblages include quartz, feldspars, dolomite, magnesite, calcite, siderite, celestite, hematite, and pyrite. In anhydrite layers, feldspars, dolomite and magnesite are present in significant quantities; quartz is present only in the >2μ fraction. Karbonatgesteines are

(understandably) enriched in the accessory minerals dolomite, calcite and siderite, and also pyrite, but not magnesite. Hematite is relatively abundant in tongesteines. (Füchtbauer and Goldschmidt, 1959; Dreizler, 1962; Pundeer, 1969).

Retsof salts of New York State resemble those of the Zechstein with regard to silicate assemblages in that illite (recrystallized) and chlorite (authigenic) are dominant minerals in the silicate fraction (Bodine and Standaert, 1977).

In the salts of the Permian Salado Formation of New Mexico, corrensite or its randomly ordered mixed-layer analog is the most abundant clay mineral of an assemblage which includes illite, chlorite, mixed-layer muscovite/vermiculite or muscovite/montmorillonite, and talc (Bailey, 1949; Grim and others, 1960; Fournier, 1961; Glass and others, 1973). Potash ore zones within the Salado are reported to contain, along with clays, principally halite, with polyhalite, anhydrite, gypsum, quartz, opal, magnesite, calcite, dolomite, celestite, sylvite, carnallite, kainite, kieserite, langbeinite, leonite, luenburgite, bloedite, epsomite, glauberite, hematite, and pyrite, generally between clay seams (Schaller and Henderson, 1932; Grim and others, 1960).

Currently a study of a drill core which cuts these evaporite sequences fifty feet into the Castile Formation is being conducted by Bodine, MacMillan, and Laskin at New Mexico Institute of Mining and Technology. They have found the silicates quartz, illite, and corrensite ± chlorite ± talc to be the common assemblage in the stratigraphic intervals examined in the Salado Formation. The mixed-layer talc/saponite generally occurs near and in polyhalite occurrences. All clay seams examined exhibited the assemblage illite + quartz + corrensite.

In addition to talc/saponite and corrensite, minor amounts of another mixed-layer clay, irregular illite/saponite was occasionally detected; every sample contained discrete saponite and/or saponite as a component of these mixed-layer clays. Magnesite commonly accompanied these assemblages, usually as an accessory mineral. Talc and serpentine are rare in occurrence; the distribution of the latter is on or below the Salado/Castile formational contact, and the distribution of the former is sporadic. Within the Castile the average assemblage appears to be dominant serpentine with saponite and chlorite, sometimes in mixed-layer form.

APPENDIX II

Geology of Ochoan Evaporites

Geologic History

In Ochoan time the presence of the Guadalupian Capitan Front and an oceanward bar formed the Delaware Basin (Adams, 1944; King, 1947). The bar theory allows hypothetical restriction of ocean water circulating into the basin and subsequent concentration of the brines through evaporation. The brines concentrated to the point of salt saturation and resulted in the precipitation and deposition of evaporite sequences.

The vertical distribution of evaporites was first theoretically determined by Usiglio (1849); his and studies of others determined that, assuming equilibrium, first carbonates, then sulfates, halite, and finally potassium and magnesium bittern salts precipitate from concentrated oceanic brines with progressive evaporation. This distribution has been applied to model basins by various authors (Jacka and Franco, 1974; Scruton, 1953). The models and comparisons to present-day evaporites have attempted to resolve the problems of lateral variation of evaporites, repetition of sequences, and extreme thicknesses of the deposits generated from too shallow depths of sea water.

It has been proposed that dynamic polythermal system(s), e.g. heat induced convection currents (Borchert, 1933, 1934, 1935, 1940, 1959; and others) and/or basin configuration (Schmalz, 1969; Sloss, 1969; Scruton, 1953) influences lateral variation in the deposits. The repetition of evaporite sequences has been explained by periodic influxes of sea water causing dilution of the brine and thus, undersaturation and halting of precipitation of some compounds and, replenishment and saturation of

others of lower solubility. This phenomenon could have been caused by several conditions which approximate a simple influx of sea water, such as break down of the restricting bar, slowing and/or halting of basin rate of subsidence, slight increase in sea level, and change of movement of salinity gradients by currents (King, 1947; Schmalz, 1969; Sloss, 1969).

Compensation of the great thicknesses of evaporite deposits are not so easily accomplished. It is unrealistic to assume the large amount of sea water required to generate the deposits could have been contained in the basin at one time or even been influxed and evaporated in the determined time period of Ochoan deposition. Even assuming a very deep basin existed, the deposits would have filled it before the 1220m thick sequence was completed. Schmalz (1969) has proposed a deep water basin model for evaporite deposition; in contrast, Sloss (1969) feels that layered solutions and subsidence rates play major roles in the deposition of evaporites.

In the Permian Basin, the most accepted model for deposition is that of a relatively deep progressive subsidence-caused basin which experienced periodic influxes resulting in some repetition of evaporite sequences. The oldest formation of Ochoan time is the Castile Formation, principally laminated anhydrite and calcite with two major beds of halite (Fig. II-1). The sequence of anhydrite overlying halite infers an influx of sea water. Anderson and others (1972) believe the laminations in the anhydrite to be a record of seasonal changes, e.g. climatic temperature controlled precipitation. The Salado Formation overlies the Castile and contains principally halite, a few anhydrite beds, and zones rich in potassium and magnesium bittern salts.

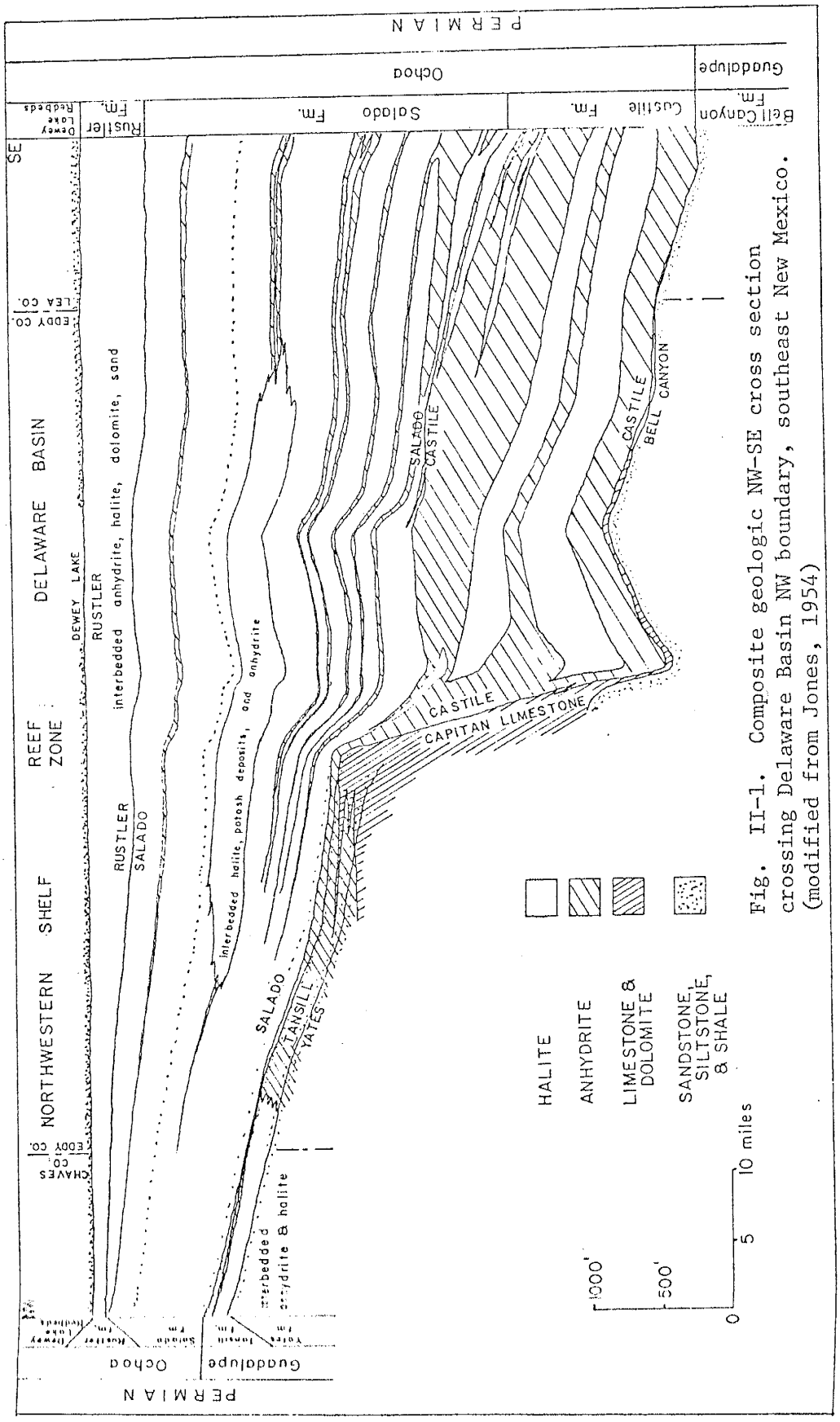

Fig. II-1. Composite geologic NW-SE cross section crossing Delaware Basin NW boundary, southeast New Mexico. (modified from Jones, 1954)

Theoretically the anhydrite layers represent a significant influx period, especially where present higher in the sequence; zones of bittern salt enrichment represent near completion of evaporation and attendant shallowing of the basin.

Overlying the Salado, the Rustler Formation, composed of limestone and anhydrite beds, represents a series of fresh water additions to the basin which never become quite saline enough to contribute major chloride compositions. Marking an end to the Ochoan, the Dewey Lake Redbeds followed a receding shoreline southward and formed a thin veneer over the evaporites.

Mineral Diagenesis

Metasomatism has evidently been a most active mechanism in developing the mineralogical and spatial distribution of the evaporites we see today from theoretical distributions. Recrystallization, pseudomorphous replacements, and clay developments characterize the alteration of the deposits. Stewart (1963) lists influences on the alteration of the original evaporites. Penecomtemporaneous conditions include: 1) mineral - brine reaction, 2) early formed mineral - residual liquid reaction, 3) mineral - early interstitial liquid reaction, 4) sea or terrestrial water influx, and 5) temperature variations. Post consolidation influences have been most far-reaching and extensive in their effects and include: 1) burial (geothermal metamorphism), 2) percolating ground water, and 3) igneous activity (thermal metamorphism). Affects of burial are believed to be a significant contribution to the final form of the sequences. For example, massive thicknesses of precipitated gypsum are converted to anhydrite with burial. However, ground water has had far-reaching effects through erosion and solutioning

mechanism. Circulation of these waters, facilitated by post-Permian tilting and faulting, enabled anhydrite beds to change back to gypsum, and bittern salts to undergo extensive and complex alterations. (Stewart, 1963; Hills, 1968).

Schaller and Henderson (1932) recorded many replacement textures in Permian Basin drill cores of the Salado Formation, including: 1) anhydrite replaced by halite or leonite or magnesite or polyhalite or polyhalite plus halite or coarser grained anhydrite or gypsum, 2) anhydrite or halite or polyhalite replaced by carnallite, 3) glauberite replaced by polyhalite or halite or polyhalite plus halite, 4) halite replaced by polyhalite, 5) langbeinite replaced by kainite, 6) kieserite replaced by leonite or polyhalite, 7) sylvite replaced by langbeinite or polyhalite, 8) leonite replaced by polyhalite. It can be seen that the metasomatism of the salts is highly intensive and involves the majority of the minerals present.

It is believed that mixed-layer clays, including corrensite, and talc have formed authigenically during diagenesis or mild "metamorphism" (burial) of evaporites. It is agreed that corrensite formed from montmorillonite, possibly mixed with chlorite, interacting with a mildly acidic Mg, Na, and K-rich environment. This environment is different from the weakly alkaline conditions of the oceanic brine from which the evaporites precipitated (Bailey, 1949; Becher, 1964/65; Grim and others, 1960; Kühn, 1968; Lippmann and Savascin, 1969; Pundeer, 1969; Bodine and others, 1973; Glass and others, 1973; Kopp and Fallis, 1974).

These authors feel that in most cases, chlorite may also have formed authigenically or, epigenetically under semisaline conditions. One suggested authigenic method (Kühn, 1968) involves the combination

$$MgCl + H^{+} \rightarrow HCl + Mg^{2+}$$

then application of the hydrochloric acid to the decomposition of micas. The procedure forms quartz and illite in addition to chlorite. It has been conceded that illite or biotite can be produced in salt clay, but generally understood that their major origin in evaporites is as clastic detritus (Kühn, 1968; Glass and others, 1973; and others). Many feel that the regeneration of this illite is a major diagenetic change (Adams, 1969; Pundeer, 1969; and others); Pundeer (1969) believes that this and other diagenetic changes are the result of increased salinity of pore solutions.

Quartz, in some cases detrital, contributes to the authigenic formation of evaporite clay minerals (Kühn, 1968); Bodine and others (1973) site dissolution of amorphous silica for talc crystallization. But at least some of the quartz and feldspars present have also been formed following deposition (Lippmann and Savascin, 1969; Pundeer, 1969); and accompanying pH decrease (Bodine and others, 1973).

This pH decrease may account for the stability of kaolinite in some occurrences. The formation of montmorillonite requires a pH more alkaline than original oceanic brine. It is probable that neither kaolinite nor montmorillonite formed with the evaporites, but rather, are detrital or volcanic in origin (montmorillonite) and/or local pH conditions during diagenesis were changed by brine metamorphism or infiltrating solutions (Kühn, 1968). A modified pH provides for conditions favorable to formation of corrensite also.

The data indicates that major changes in silicate fractions included in the salts are accommodated during burial and ground water action in addition to the obvious affect on soluble salts. It is

$$MgCl + H^{+} \rightarrow HCl + Mg^{2+}$$

then application of the hydrochloric acid to the decomposition of micas. The procedure forms quartz and illite in addition to chlorite. It has been conceded that illite or biotite can be produced in salt clay, but generally understood that their major origin in evaporites is as clastic detritus (Kühn, 1968; Glass and others, 1973; and others). Many feel that the regeneration of this illite is a major diagenetic change (Adams, 1969; Pundeer, 1969; and others); Pundeer (1969) believes that this and other diagenetic changes are the result of increased salinity of pore solutions.

Quartz, in some cases detrital, contributes to the authigenic formation of evaporite clay minerals (Kühn, 1968); Bodine and others (1973) site dissolution of amorphous silica for talc crystallization. But at least some of the quartz and feldspars present have also been formed following deposition (Lippmann and Savascin, 1969; Pundeer, 1969); and accompanying pH decrease (Bodine and others, 1973).

This pH decrease may account for the stability of kaolinite in some occurrences. The formation of montmorillonite requires a pH more alkaline than original oceanic brine. It is probable that neither kaolinite nor montmorillonite formed with the evaporites, but rather, are detrital or volcanic in origin (montmorillonite) and/or local pH conditions during diagenesis were changed by brine metamorphism or infiltrating solutions (Kühn, 1968). A modified pH provides for conditions favorable to formation of corrensite also.

The data indicates that major changes in silicate fractions included in the salts are accommodated during burial and ground water action in addition to the obvious affect on soluble salts. It is

apparent that these influences are extremely variable, and no single mechanism can explain the genesis of any given mineral.

APPENDIX III

Analytical Procedures

Raw Data and Statistics

The fluorescence data on bulk rock salts (Table III-2) was evaluated using the least squares fit method on the indicated salt mixture standards. In seven of nine cases, the fit of the standard data points to the curve was $\geq$ 0.99, and in all cases, $\geq$ 0.93 (Table III-3). The relative percent error of the standard values compared to those derived from the curve were lowest for major elements; as might be expected, the numbers are high for minor constituents by nature of the calculation. The equation

$$\frac{\left|\text{wt.\% known concentration} - \text{wt.\% calculated (from curve) concentration}\right|}{\text{wt.\% known concentration}} \times 100$$

was applied. Aluminum values were so low that an attempt to record comprehensible data of standards of comparable compositions failed. Excluding Al_2O_3, the totals of the analyses approached 100% ± 3% by weight for relatively pure salts, and were significantly lower in clay-rich samples, indicating Al_2O_3 and water is present in the samples.

The curve fits for the bulk gypsum samples (Tables III-4 and III-5) using calcium sulfate and salt mixture standards in six of nine cases were $\geq$ 0.99 and in all cases $\geq$ 0.95. As for the rock salt, relative % error was only high for elements of low concentration.

The gypsum-derived silicates (Table III-6) were done by acid decomposition and atomic absorption, accompanied by the appropriate calculations to report the data in weight percent. Sample 53 was run with

Table III-1. XRF settings.

Element/Rock	KV/MA	tube	crystal	analyzer	counter	high voltage	coll.	vacuum (<200 microns)	gain (coarse X fine)	E	ΔE	discriminator upper	discriminator lower	discriminator thres.	discriminator zero	discriminator amp	-TC (sec) @ 3% stad deviation	gas
SiO_2/clay	50/35	Cr14	KAP	MCA	FPC	2100	F	✓	1.x1.			6.14	2.40	9.0	7.76	1.0	0.3	P-75
/clay	40/20	Cr14	gyp	MCA	FPC	1400	F	✓	1.x1.			4.7	2.1	9.0	8.6	1.0	> 0.5	P-10
/gyp,salt	50/35	Cr14	KAP	SCA	FPC	2100	C	✓	8x4	1.2	1.87						> 5.0	P-75
/dike																		
Al_2O_3/clay	50/35	Cr14	KAP	MCA	FPC	2100	F	✓	1.x1.			5.34	1.88	9.0	7.76	1.0	≥ 1.0	P-75
/salt	50/35	Cr14	KAP	SCA	FPC	2100	C	✓	8x4(4x8?)	0.94	1.73						>10.0	P-75
/gyp	50/35	Cr14	KAP	SCA	FPC	2100	F,C	✓	8x4(4x8?)	0.94	1.73						>10.0	P-75
/dike																		
TiO_2/dike	40/20	Cr14	qtz	SCA	SCIN	850	F	x	½x1.0	0.16	1.05						1.0	
/clay	40/20	Cr14	qtz	SCA	SCIN	850	F	x	½x1.0	0.16	1.05						< 5.0	
/gyp	40/20	Cr14	qtz	SCA	SCIN	850	F	x	8x5	0.16	1.05						>10.0	
/salt																		
Fe_2O_3/dike	40/20	Cr14	qtz	SCA	SCIN	850	F	x	½x1.0	0.28	1.28						0.5	
/clay	40/20	Cr14	qtz	SCA	SCIN	850	F	x	½x1.0	0.26	1.26						1.0	
/gyp	40/20	Cr14	qtz	SCA	SCIN	850	F	x	8x5	0.28	1.28						>10.0	
/salt	40/20	Cr14	LIF200	MCA	SCIN	850	F	x	8x5			1.7	0.15	9.0	7.76	1.0	avg 0.2	
MgO/dike	50/35	Cr14	KAP	MCA	FPC	2050	C	✓	8x5			4.41	1.32	9.0	7.76	1.0	< 5.0	P-75
/clay	50/35	Cr14	KAP	SCA	FPC	2050	backed off C	✓	8x5	0.48	1.32						1.0	P-75
/gyp,salt	50/35	Cr14	KAP	SCA	FPC	2100	C	✓	4x8	0.66	1.54						10.0	P-75
K_2O/clay	40/20	Cr14	qtz	SCA	FPC	1300	F	✓	1.x1.	0.45	0.28						< 0.1	P-10
/gyp	21/8	Cr14	LIF200	SCA	FPC	1350	F	✓	8x5	0.96	1.01						>10.0	P-10
/salt	30/15	Cr14	qtz	SCA	FPC	1350	F	✓	8x5	0.96	1.01						1.0-0.05	P-10
/dike																		
Na_2O/clay	50/35	Cr14	gyp	SCA	FPC	2100	C	✓	1.x1.	0.40	0.73						>10.0	P-75
/gyp	50/35	Cr14	KAP	SCA	FPC	2100	C	✓	8x4(4x8?)	0.46	1.31						5.0	P-75
/salt	50/35	Cr14	gyp	SCA	FPC	2100	C	✓	4x8	0.40	0.73						0.5	P-75
/salt	50/35	Cr14	KAP	MCA	FPC	2100	C	✓	8x4			3.03	0.86	9.0	7.76	1.0	5.0	P-75
/dike																		
CaO/dike	25/10	Cr14	qtz	SCA	FPC	1250	F	✓	8x5	1.25	1.12						>10.0	P-10
/clays	40/20	Cr14	LIF200	MCA	FPC	1350	F	✓	8x5			4.4	2.1	9.0	7.76	1.0	10.0	P-10
/gyp	21/8	Cr14	qtz	SCA	FPC	1350	F	✓	8x3.5	1.05	1.15						< 0.1	P-10
/salt	35/15	Cr14	LIF200	SCA	FPC	1350	F	✓	8x5	1.05	1.15						0.2-4.0	P-10
MnO/salt	40/20	Mo	qtz	MCA	SCIN	850	F	x	8x4			2.8	1.35	9.0	7.76	1.0	>10.0	
/dike	40/20	Mo	qtz	SCA	SCIN	850	F	x	½x1.0	0.33	1.17						10.0	
/clay	40/20	Mo	qtz	SCA	SCIN	850	F	x	½x1.0	0.33	1.17						>10.0	
/gyp	40/20	Mo	qtz	SCA	SCIN	850	F	x	8x5	0.675	0.725						>10.0	
SO_4/salts,gyp	50/35 or lower	Cr14	KAP	MCA	FPC	2100	C	✓	4x4			3.4	1.43	9.0	7.76	1.0	0.2-4.0	P-75
Cl/salt	25/10 or lower	Cr14	KAP	MCA	FPC	2100	C	✓	4x4			3.68 3.92	1.62 1.79	9.0	7.76	1.0	0.2	P-75
Br/salt	50/35	Cr14	LIF200	MCA	SCIN	850	F	x	4x7			1.34	1.18	9.0	7.76	1.0	5.0-8.0	

Table III-2. Bulk rock salt analyses, Kerr McGee (wt %).

Sample	SiO_2	Fe_2O_3 (total Fe)	Mg	Ca	Na	K	SO_4	Cl	ppm Br	total
JT-3(*)	no data	0.25	1.19	no data	7.94	no data	21.70	no data	28	—
20	0.50	0.01	0.17	0.76	37.92	0.78	1.26	61.06	46	102.46
22	3.63	0.58	1.43	D/T	5.22	12.10	D/T	10.34	14	—
21	0.50	0.22	0.12	0.49	35.80	0.89	0.94	57.55	150	96.51
21S	0.10	0.07	0.08	0.65	38.11	0.70	1.00	62.12	58	102.83
30*	3.70	0.34	1.23	3.01	23.06	4.73	6.20	42.87	132	85.14
23P	0.00	0.25	1.05	D/T	4.65	11.67	D/T	4.21	56	—
23S	0.26	0.08	0.35	6.75	23.93	4.70	13.18	36.85	47	86.10
27*	8.28	0.39	1.89	4.18	10.64	6.41	8.15	35.90	174	75.84
					dike					
28W	0.56	0.03	0.15	0.24	37.42	0.64	0.00	63.05	65	102.39
29	10.98	0.40	2.52	0.16	24.27	3.76	0.00	49.49	248	91.58
JT-1	3.96	0.19	1.99	0.39	29.44	5.15	0.33	54.37	203	95.82
31*	6.31	0.44	2.08	1.11	18.84	5.18	2.14	45.74	226	81.84
32	1.49	0.12	0.33	0.02	35.17	1.07	0.00	62.19	109	100.39
33*	7.00	0.57	1.39	1.37	23.86	3.20	2.75	45.95	214	86.09
33S	0.62	0.04	0.11	0.75	36.97	0.38	0.36	62.26	52	101.49
35	2.42	0.25	0.48	0.52	33.14	1.72	0.65	58.06	108	97.24
					dike					
34	0.50	0.02	0.08	0.82	36.75	0.29	0.17	62.48	50	101.11
34D	13.27	1.27	2.58	0.05	14.91	2.66	0.00	41.35	334	76.09
					dike					
37WDC	1.74	0.25	0.39	2.20	31.11	4.13	4.37	55.74	110	99.93
37MDC	4.52	0.20	1.00	1.08	29.95	2.83	1.98	55.46	114	97.02
38(*)	2.89	0.46	0.41	0.05	37.26	0.67	0.00	59.83	108	101.57
39(*)	9.85	0.46	1.57	0.08	29.46	1.50	0.00	52.38	168	95.30
40	6.97	0.55	1.85	0.33	27.78	2.23	0.27	52.15	213	92.13
41	7.38	0.41	1.77	0.64	20.03	6.46	1.80	47.52	284	86.01
JT-5	4.56	0.23	1.53	1.13	25.30	6.17	2.31	51.18	160	92.41
CL-77-7U	0.64	0.18	0.17	0.36	19.26	15.85	0.38	62.49	122	99.33
CL-77-7L(*)	9.70	0.83	2.89	0.001	10.40	10.24	0.00	43.02	510	77.08
CL-77-8	5.82	0.36	1.65	0.16	22.09	6.57	0.00	51.66	144	88.31

* clay seam ; (*) clay-rich ; D/T = dead time on counter

Table III-3. Statistics from linear regression for bulk rock salt analyses, Kerr McGee.

Analyzed	Regression constants (intercept)	(slope)	Coefficient of determination (fit)	Standards (data points)	Respective relative % error on data pts.
SiO_2	- 0.117964	0.773944	0.999934	DTS-1 (U.S.G.S.) salt stnd/NaCl: 100/0,75/25, 25/75,90/10,zero	0, 26, 10, 11,9,zero
Fe_2O_3 (as total Fe)	- 0.014710	0.139581	0.962837	salt stnd/NaCl: 100/0, 75/25,40/60,25/75,5/95, 10/90,90/10,50/50,zero	0, 0,20,33,73, 8,9,0,zero
Mg	- 0.011195	0.294334	0.989839	salt stnd/NaCl: 100/0, 90/10,75/25,50/50, 40/60,10/90,5/95,zero	0, 7,0,13, 9,22,0,zero
Ca	- 0.031239	0.253064	0.930895	salt stnd/NaCl: 100/0, 90/10,75/25,40/60, 50/50,25/75,10/90,5/95, zero	2, 14,86,29, 7,71,0,65, zero
Na	+ 0.614688	28.925617	0.998682	TS: 1,6,5,4, MB-76-5EDTA, CS-7,zero	2,8,1,3, 13, 10,zero
				For #37MDC: salt stnd/ NaCl: 100/0,75/25, 50/50,5/95; TS-4,zero	2,11, 17,9,2,zero
K	+ 0.082036	2.712388	0.996758	salt stnd/Nacl: 10/90, 50/50,5/95,40/60,zero	3, 3,6,5,zero
SO_4	- 0.911270	7.382240	0.990113	TS:30,4,29,27,35	2, (zero), 15,1,3
Cl	+ 0.477162	64.107206	0.992246	TS:30,29,27,35,21,zero	6,1,4,1,1,zero
Br	-11.671848	147.450354	0.993449	ppm Br: 545+,467+, 389+,311+(labeled 224+) 234+,156+(labeled 113+) 78+(labeled 56+), 2.9(ultrapure NaCl), 32(reagent NaCl)	1,6, 0,6, 1,1, 23, 1, 44

Table III-4. Bulk gypsum analyses, Yeso Hills (wt %).

Sample	SiO_2	TiO_2	Al_2O_3	Fe_2O_3 (total Fe)	Mg	Ca	Na	K	SO_4	total
S stream cut										
47	0.00	0.16	0.14	0.03	0.05	24.47	0.12	0.02	52.94	77.93
48	0.00	0.03	0.13	0.00	0.05	24.02	0.21	0.01	54.15	78.60
49	0.00	0.01	0.15	0.00	0.00	24.11	0.00	0.01	54.30	78.58
50	0.00	0.02	0.15	0.00	0.05	23.21	0.19	0.01	55.08	78.71
51	0.00	0.02	0.18	0.00	0.06	24.34	0.32	0.01	53.17	78.10
N stream cut										
52	0.00	0.02	0.12	0.00	0.08	24.54	0.19	0.02	53.35	78.32
53	0.00	0.04	0.16	0.02	0.05	24.32	0.34	0.02	53.30	78.25
dike										
54	0.00	0.02	0.15	0.00	0.07	23.62	0.39	0.03	54.56	78.84

Table III-5. Statistics from linear regression for bulk gypsum analyses, Yeso Hills

	SiO_2	TiO_2	Al_2O_3	Fe_2O_3 (total Fe)	Mg	Ca	Na	K	SO_4
Regression constants:									
1) intercept	-0.002817	-0.003253	+0.005163	-0.037936	-0.006437	+4.443625	+0.176794	-0.004320	+14.442213
2) slope	0.102817	0.043925	0.164311	0.064044	0.068352	18.896695	2.499786	2.884307	41.670114
Coefficient of determination (fit):	1.000000	0.983402	0.974684	0.955313	0.995580	0.999420	0.996104	0.999993	0.986210*
Data points (standards):	salt stnd / $CaSO_4 \cdot 2H_2O$	salt stnd / $CaSO_4 \cdot 2H_2O$	salt stnd / $CaSO_4 \cdot 2H_2O$	salt stnd / $CaSO_4 \cdot 2H_2O$	salt stnd / $CaSO_4 \cdot 2H_2O$	salt stnd / $CaSO_4 \cdot 2H_2O$	salt stnd / $CaSO_4 \cdot 2H_2O$	salt stnd / $CaSO_4 \cdot 2H_2O$	100% $CaSO_4 \cdot 2H_2O$
	0/100	0/100	40/60	0/100	0/100	0/100	0/100	0/100	TS:
	10/90	10/90	50/50	10/90	20/80	20/80	20/80	10/90	26
		20/80	70/30	20/80	40/60	40/60	40/60		25
		40/60	90/10	40/60	50/50		zero		
		50/50	100/0						
		70/30	zero						
		100/0							
		zero							
Relative % error on data points, respectively:	NA(zero)	NA(zero)	8	NA(zero)	NA(zero)	0.3	NA(zero)	NA(zero)	0.6
	0	25	4	0	0	1.0	7.4	0	1.2
		0	10	30	5.3	0.5	1.6		0.7
		13	8	0	0		zero		
		0	7						
			5						

*better fit achieved but relative error increased

Table III-6. Analysis of gypsum-derived silicates (wt %), Yeso Hills.

Sample	SiO_2	TiO_2	Al_2O_3	Fe_2O_3 (total Fe)	MgO	CaO	Na_2O	K_2O	total
S stream cut				dike					
47		1.15	10.75	2.19	5.07	0.43	7.65	1.07	28.31
48		1.50	12.08	3.92	8.31	0.66	8.21	1.16	35.84
49		0.99	13.96	2.61	0.52	0.27	7.64	3.14	29.13
51		1.03	12.71	2.61	2.23	0.32	5.54	1.82	26.26
N stream cut									
53	61.52	0.64	6.62	2.65	14.86	0.002	5.34	0.70	92.33
				dike					

Analyses for samples 47, 48, 49, and 51 were obtained by AA; sample 53 was obtained by XRF + matrix correction.

Table III-7. Chemical weight ratios of gypsum-derived silicates, Yeso Hills.

Sample	Si/Al	Ti/Al	Fe/Al	Mg/Al	Ca/Al	Na/Al	K/Al	Al
S stream cut								
dike								
47		0.12	0.27	0.54	0.05	1.00	0.16	5.69
48		0.14	0.43	0.78	0.07	0.95	0.15	6.39
49		0.08	0.25	0.04	0.03	0.77	0.35	7.39
51		0.09	0.27	0.20	0.03	0.61	0.22	6.73
N stream cut								
53	8.22	0.11	0.53	2.56	0.0004	1.13	0.17	3.50
dike								

Table III-8. Chemical weight ratios of rock salt-derived silicates, Kerr McGee.

Sample	Si/Al	Ti/Al	Fe/Al	Mg/Al	Ca/Al	Na/Al	K/Al	Al
JT-3(*)	2.98	0.04	0.26	2.38	0.013	0.08	1.03	7.09
22	2.99	0.04	0.48	2.37	0.018	0.09	1.08	6.98
21	3.02	0.05	0.14	2.21	0.008	0.19	0.83	7.15
30*	2.95	0.05	0.18	2.28	0.009	0.13	0.91	7.21
			dike					
29*	3.36	0.04	0.08	2.56	0.00	0.14	1.04	6.43
32	4.07	0.07	0.27	3.23	0.00	0.17	0.21	5.12
33*	3.80	0.08	0.36	2.46	0.00	0.11	0.26	5.99
35	4.86	0.05	0.24	3.39	0.00	0.28	0.71	4.36
			dike					
34D	3.36	0.07	0.67	2.48	0.013	0.16	0.20	6.31
			dike					
37MXD(T)	4.08	0.06	0.31	3.32	0.00	0.30	0.77	5.30
37MDC(E)	4.02	0.05	0.42	3.07	0.0005	0.20	0.96	5.44
38	3.62	0.08	0.51	2.46	0.003	0.14	0.24	6.12
39	3.66	0.09	0.36	2.60	0.00	0.11	0.20	5.89
40	3.32	0.07	0.53	2.47	0.008	0.13	0.21	6.39
41	3.44	0.08	0.42	2.48	0.002	0.13	0.22	6.33
JT-5	3.94	0.09	0.81	2.77	0.004	0.14	0.22	5.47
CL-77-7L(*)	3.21	0.08	0.38	2.33	0.002	0.09	0.19	6.70
CL-77-8	3.88	0.08	0.46	2.89	0.00	0.13	0.19	5.51

* clay seam
(*) clay-rich
T total (dike + evaporite) clay
E evaporite clay

silicates from the Kerr McGee sample suite since the amount of residue did allow fluorescence preparation.

Chemical data on samples of the dike rock (Table III-9) was analyzed using least squares fit on U.S.G.S. igneous standards, and in all cases the coefficient of determination exceeded 0.99. Relative % errors on the standards was generally excessive for ultramafic standards of low elemental concentrations. The totals of the analyses allow for water and also evaporite constituents, not analyzed.

Manipulation of all the above data was limited to testing fit and relative % error with and without zero as a standard point, and eliminating standards only when they lie outside the range of unknowns (causing the curve to change) and/or when all data indicated bad concentration values (especially mixture standards).

An attempt was made to apply the matrix correction program "SELF" (personal communication, Jacques Renault, 1978) based on Holland and Brindle's (1966) Mercury autocode routine to the raw dike rock data. The program calculates absorption coefficients for each standard from the compositions and raw data of all the standards (Table III-10). Then the absorption coefficients for an unknown are calculated and recalculated (using data on the unknown) from the standard similar to the unknowns chosen by the operator (Table III-11). In all cases, U.S.G.S. standard BCR-1 was chosen here as a starting point in the reiteration. The results (Table III-12) were found to be unsatisfactory as the reiteration also considered total weight percent as a function of final matrix correction. It is interesting to note that the program emphasized alkaline earth trends in the rocks (Fig. III-1).

In the above analyses standards with a similar matrix to unknowns

Table III-9. Statistics from Linear Regression for dike rocks.

Regression constants:	SiO_2	TiO_2	Al_2O_3	Fe_2O_3 (total Fe)	MgO	CaO	Na_2O	K_2O	MnO
1) intercept	+16.522554	+0.064033	- 0.892125	- 0.530534	+0.164330	+0.062434	-0.094767	-0.151500	-2.016823×10^{-3}
2) slope	38.609539	2.135443	14.381456	13.749931	2.861875	4.903417	3.339201	1.953171	0.168732
3) fit (coefficient of determination):	0.996016	0.997752	0.993848	0.993944	0.989639	0.999506	0.997046	0.998179	0.996111
Data Points: (standards) (USGS)	W-1 GSP-1 AGV-1 BCR-1 G-2 PCC-1 Los Pinos (NMBMMR)	BCR-1 AGV-1 G-2 GSP-1 W1	W-1 GSP-1 AGV-1 BCR-1 G-2 PCC-1 Los Pinos (NMBMMR)	BCR-1 AGV-1 G-2 GSP-1 W-1	W-1 AGV-1 BCR-1 zero	AGV-1 BCR-1 G-2 GSP-1 zero	BCR-1 W-1 GSP-1 PCC-1 G-2 zero	W-1 GSP-1 AGV-1 BCR-1 G-2 PCC-1	W-1 AGV-1 BCR-1 GSP-1 G-2 DTS-1 zero
Respective relative % error on data points	1% 1% 1% 1% 2% 0.3% 1%	0% 3% 2% 1% 4%	4% 0.2% 8% 1% 0.3% 14% 3%	1% 9% 2% 7% 1%	2.5% 7% 12.5% zero	1% 0.02% 3% 3% zero	0.9% 7.4% 1.4% 733% 1.2% zero	7% 1% 3% 6% 1% 34%	0% 13.4% 0% 0% 6% 91% zero

Table III-10

Mass absorption coefficients:

	Si	Ti	Al	Fe	Mg	Ca	Na	K	X(Mn)
SiO_2	644	174	1009	65	1642	303	2791	441	81
TiO_2	1271	88	1972	240	3177	155	5343	1451	301
Al_2O_3	2407	159	893	59	1454	231	2471	398	74
Fe_2O_3	2173	156	3358	59	5380	272	8994	2432	74
MgO	2166	142	3395	53	1242	252	2112	364	66
CaO	1052	589	1634	221	2631	129	4425	1371	277
Na_2O	1971	129	3069	47	5035	229	1543	321	60
K_2O	931	591	1444	220	2324	1033	3902	1393	278
MnO	1947	140	3010	53	4326	243	8072	34	66

Absorption coefficients of standards

	1	2	3	4	5
SiO_2	1265	1053	1153	1229	1039
TiO_2	214	198	195	199	194
Al_2O_3	1542	1207	1304	1526	1182
Fe_2O_3	82	75	75	79	73
MgO	2214	1919	2051	2321	1889
CaO	279	332	300	289	325
Na_2O	3590	3054	3172	3691	2918
K_2O	767	590	635	794	543
MnO	103	94	94	99	92

Back calculated concentrations for standards, excluding zero:

	SiO_2	TiO_2	Al_2O_3	Fe_2O_3	MgO	CaO	Na_2O	K_2O	MnO	
1 (W-1)	52.64	1.04	15.00	11.09	6.62	10.96	2.15	0.64	0.17	known
	51.19	1.08	17.19	11.41	6.81	10.82	2.34	0.36	0.17	back calc'd
2 (GSP-1)	67.38	0.66	15.25	4.33	0.96	2.02	2.80	5.53	0.04	
	68.70	0.64	14.17	4.04	1.02	1.95	2.36	5.67	0.04	
3 (AGV-1)	59.00	1.04	17.25	6.76	1.53	4.90	4.26	2.89	0.10	
	59.93	1.05	15.77	7.06	1.30	5.12	4.02	3.03	0.10	
4 (BCR-1)	54.50	2.20	13.61	13.40	3.46	6.92	3.27	1.70	0.18	
	55.67	2.18	15.39	13.06	3.02	7.03	3.98	2.16	0.18	
5 (G-2)	69.11	0.50	15.40	2.65	0.76	1.94	4.07	4.51	0.03	
	67.14	0.48	14.00	2.66	1.19	1.81	3.84	4.06	0.04	

Equations for standards excluding zero, where C = mass absorption coefficient times intensity:

$[SiO_2] = (C - (512.759))/12.8704$
$[TiO_2] = (C - (-4.99872))/93.6259$
$[Al_2O_3] = (C - (-591.681))/137.568$
$[Fe_2O_3] = (C - (.705139))/6.00511$
$[MgO] = (C - (96.6161))/737.562$
$[CaO] = (C - (22.7426))/54.1694$
$[Na_2O] = (C - (1026.33))/669.164$
$[K_2O] = (C - (236.472))/258.073$
$[MnO] = (C - (-.617188))/602.4$

Table III-10 (continued).

Back calculated concentration for standards including zero:

	SiO_2	TiO_2	Al_2O_3	Fe_2O_3	MgO	CaO	Na_2O	K_2O	MnO	
1 (W-1)	52.64	1.04	15.00	11.09	6.62	10.96	2.15	0.64	0.17	known
	55.00	1.08	17.84	11.40	6.79	10.74	2.64	0.71	0.17	back calc'd
2 (GSP-1)	67.38	0.66	15.25	4.33	0.96	2.02	2.80	5.53	0.04	
	65.79	0.63	13.71	4.08	1.05	2.08	2.66	5.51	0.04	
3 (AGV-1)	59.00	1.04	17.25	6.76	1.53	4.90	4.26	2.89	0.10	
	60.39	1.04	15.90	7.07	1.33	5.18	3.88	3.12	0.10	
4 (BCR-1)	54.50	2.20	13.61	13.40	3.46	6.92	3.27	1.70	0.18	
	57.76	2.20	15.39	13.04	3.03	7.04	3.84	2.34	0.18	
5 (G-2)	69.11	0.50	15.40	2.65	0.76	1.94	4.07	4.51	0.03	
	64.83	0.47	13.48	2.70	1.22	1.94	3.74	4.05	0.04	
zero	0.00	0.00	0.00	0.00	0.00	0.00	0.00	0.00	0.00	
	-1.12	0.03	0.20	-0.06	-0.09	-0.24	-0.21	-0.44	0.00	

Equations for standards including zero, where C = mass absorption coefficient times intensity:

$$[SiO_2] = (C - (23.4225))/20.8777$$
$$[TiO_2] = (C - (-2.69878))/92.0081$$
$$[Al_2O_3] = (C - (-19.588))/100.437$$
$$[Fe_2O_3] = (C - (.367085))/6.03972$$
$$[MgO] = (C - (64.3176))/744.852$$
$$[CaO] = (C - (13.2029))/55.4595$$
$$[Na_2O] = (C - (188.489))/910.898$$
$$[K_2O] = (C - (126.556))/285.775$$
$$[MnO] = (C - (-.347652))/600.488$$

Table III-11. Calculated absorption coefficients from matrix correction program "SELF" for dike rocks.

Sample	SiO_2	TiO_2	Al_2O_3	Fe_2O_3 (total Fe)	MgO	CaO	Na_2O	K_2O	MnO
Kerr McGee sample suite									
23	1301	228	1575	90	2245	374	3708	843	113
36	1313	223	1585	88	2243	359	3686	830	110
24	1332	213	1615	85	2256	337	3655	811	106
Yeso Hills suite									
location LDC									
46	1301	208	1582	84	2367	309	3678	809	105
45D	1294	211	1555	84	2310	306	3626	792	105
45L	1302	201	1571	82	2335	308	3694	806	102
location LDB									
18A	1326	202	1598	81	2359	300	3763	824	101
18B	1248	197	1462	80	2229	302	3537	745	100
19L	1056	192	1178	79	1914	334	2952	557	99
19D	1295	191	1557	77	2383	296	3627	774	96
location LDA									
17	1355	202	1645	81	2363	330	3704	818	102
miscellaneous samples									
LD-1	1312	210	1617	84	2336	330	3692	819	105
LD-2	1319	205	1617	82	2342	323	3710	819	103
LD-3	1304	205	1592	81	2192	327	3539	763	102
LD-4	1266	213	1533	84	2182	347	3600	787	105
LD-5	1293	213	1580	84	2219	336	3600	790	106
LD-6	1303	205	1597	81	2201	321	3547	763	102
LD-7	1287	211	1576	84	2190	330	3539	769	105
LD-8	1301	208	1597	82	2213	325	3560	772	103
LD-9	1287	212	1566	84	2188	342	3571	780	105

Table III-12. Analyses of dike rock matrix corrected by "SELF"

Sample	SiO_2	TiO_2	Al_2O_3	Fe_2O_3 (total Fe)	MgO	CaO	Na_2O	K_2O	MnO	total
Kerr McGee suite										
23*	48.01	2.59	16.44	12.93	7.37	3.22	1.21	12.70	0.20	104.67
36	47.98	2.46	16.59	12.80	7.76	3.75	1.46	10.75	0.16	103.71
24**	47.51	2.50	16.26	12.60	8.46	4.16	2.22	7.78	0.12	101.61
Yeso Hills suite										
southern stream cut (location LDC)										
46*	49.92	2.80	15.51	13.01	4.46	6.63	4.35	4.26	0.13	101.07
45D**	49.65	2.57	15.67	12.01	4.61	7.26	3.69	3.87	0.10	99.44
45L†	50.49	2.98	15.67	12.96	4.66	5.34	3.37	3.76	0.09	99.33
location LDB										
18A†	47.06	2.52	15.66	13.93	5.08	5.98	3.00	2.86	0.11	96.21
18B†	51.07	2.98	15.90	10.11	3.08	4.77	3.11	2.64	0.09	93.75
19L†*	60.69	3.36	14.31	1.47	0.04	0.42	3.70	5.10	0.01	89.10
19D†	51.88	2.73	15.85	13.00	3.18	4.42	5.61	2.08	0.07	98.83
location LDA										
17	46.94	2.72	16.20	13.82	6.99	2.79	4.06	6.65	0.12	100.29
miscellaneous samples										
LD-1	50.28	2.73	15.59	13.74	6.53	5.12	3.54	6.88	0.16	104.56
LD-2	49.88	2.82	15.63	13.64	6.25	4.57	3.37	5.82	0.11	102.09
LD-3	52.11	2.29	16.03	11.83	9.53	4.10	2.47	6.42	0.16	104.95
LD-4	52.15	2.28	15.75	11.86	7.27	3.21	1.26	8.78	0.17	102.75
LD-5	51.03	2.45	15.84	12.24	8.33	4.51	2.21	7.73	0.11	104.45
LD-6	51.11	2.38	15.52	11.59	9.31	4.64	2.53	5.59	0.20	102.86
LD-7	51.63	2.36	15.61	11.31	8.89	4.89	2.42	6.99	0.13	104.24
LD-8	51.36	2.46	15.60	11.85	9.14	4.79	2.68	6.25	0.14	104.28
LD-9	52.32	2.34	16.17	11.95	8.67	3.76	1.90	8.55	0.17	105.82

* margin facies
** interior facies
† weathered

NOTE: samples 17, 19L, 23, 24, and 36 excluded zero in their curves

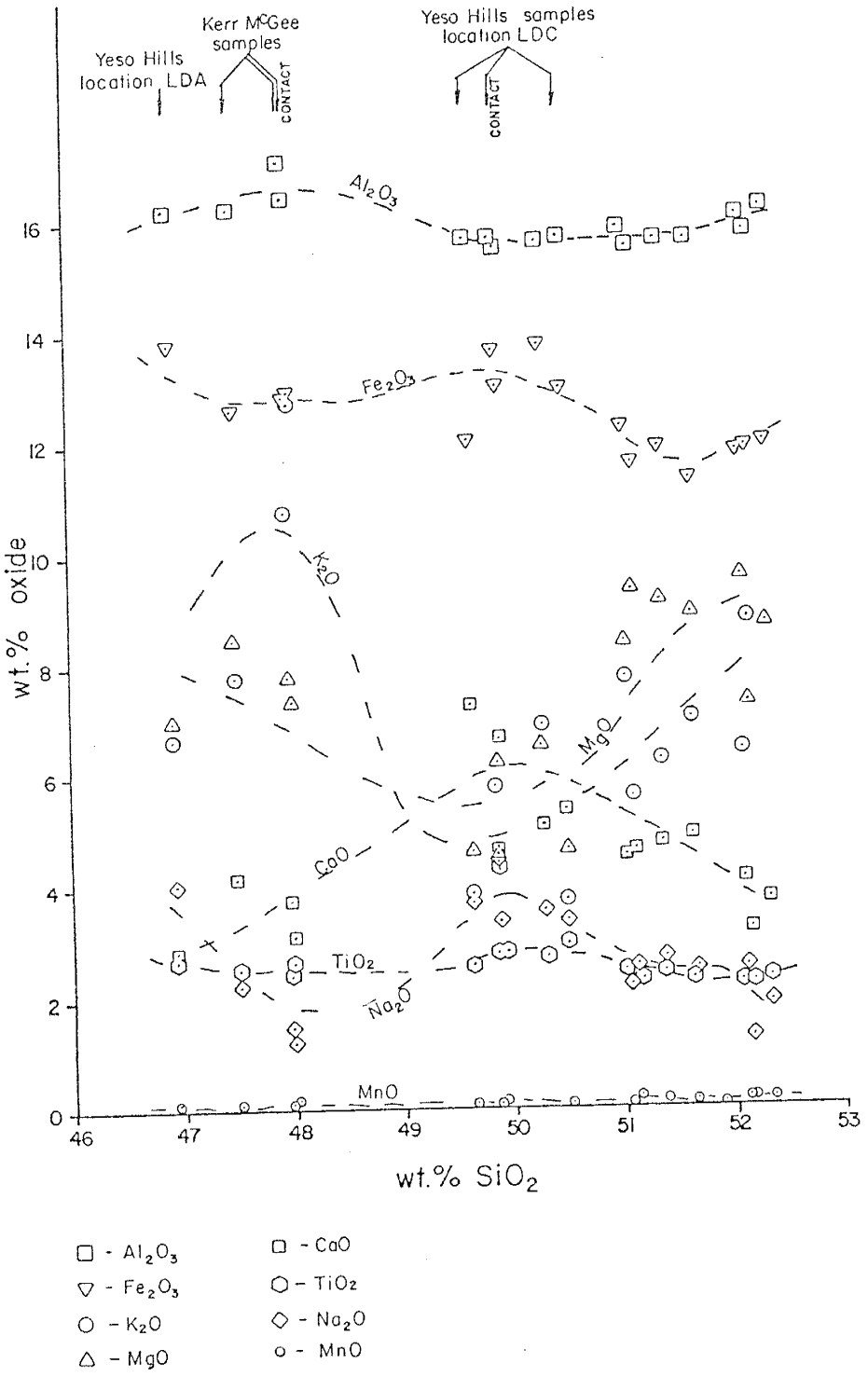

Fig. III-1. Dike rock analyses from matrix correction program "SELF". Plot is that of Harker (1909).

were used; this condition was available for silicate residues but proved unsatisfactory. The improvement of clay fraction chemical analyses through the application of the interelemental matrix correction program "XRF8" originally designed by Marr III (1976) and extensively modified by Joseph Taggart (personal communication, 1978) is significant (Table III-13). The totals reflect water (clay) content and vary reasonably with respect to 100% by weight. For all elements, the fit is improved from as low as 0.96 to $\geq$ 0.99 and in six of eight cases to $\geq$ 0.999. The sample and population standard deviations decrease, and the sample RMS (root mean square) and curve RMS increase with absorption coefficient considerations compared to linear regression calculations.

The calculation method included in the program for the sample standard deviation statistic, the measure of dispersion around the mean, is as follows:

$$\sqrt{\frac{\sum_{i}^{n} T^2 - \frac{\sum_{i}^{n} T^2}{n}}{n}} = S$$

where T is the change in concentration between the known standard value and the value calculated from the curve, and n is the number of standards. The population standard deviation is found by

$$S \cdot \sqrt{\frac{n-1}{n}} = S'$$

The sample standard deviation will approach that of the population as n is increased.

Table III-13A. SiO_2 data

SAMPLE	BOOK CONC	CALC CONC	
1 W1	52.640	52.306	STD
2 GSP1	67.380	67.881	STD
3 AGV1	59.000	60.210	STD
4 BCR1	54.500	54.269	STD
5 G2	69.110	68.242	STD
6 PCC1	41.900	42.843	STD
7 DTS1	40.500	39.680	STD
8 MAG1	50.870	50.347	STD
9 QL01	65.150	65.158	STD
10 MB5	46.820	47.152	STD
11 MB4	47.190	46.749	STD
12 MB3	45.560	45.750	STD
13 CS7	42.280	42.313	
14 CS37	59.310	62.509	
15 JT5		46.154	
16 JT3		45.241	
17 MB21		46.143	
18 MB30		45.455	
19 MB22		44.657	
20 MB29		46.210	
21 MB32		44.628	
22 MB33		48.675	
23 MB35		45.370	
24 MB34D		45.405	
25 MBMXD		46.247	
26 MBMDC		46.785	
27 MB38		47.483	
28 MB39		46.144	
29 MB40		45.420	
30 MB41		46.532	
31 CL7L		45.993	
32 CL8		45.829	
33 MB3F		46.269	
34 MB3MP		46.416	
35 MB53		61.518	

COMPONENT	COEFFICIENT	CONTRIBUTION
BKGD	-1.13	0.479
SI02	4496.79E-05	1.000
TI02	3850.99E-05	0.016
AL203	-9123.77E-05	0.051
FE203	-1709.46E-05	0.008
MGO	7264.20E-05	0.019
CAO	2084.01E-06	0.013
NA20	-1.00	0.850
K20	9078.64E-06	0.007

GOODNESS OF FIT	= .99987
SAMPLE STD DEV	= .633243
POPULATION STD DEV	= 2.27642
SAMPLE RMS	= .252285
CURVE RMS	= .242388

Statistics from linear regression:

COMPONENT	COEFFICIENT	CONTRIBUTION
BKGD	-0.81	0.398
SI02	3858.93E-05	1.000

GOODNESS OF FIT	= .999436
SAMPLE STD DEV	= 1.3197
POPULATION STD DEV	= 4.74416
SAMPLE RMS	= .1459
CURVE RMS	= .140177

Table III-13B. TiO_2 data

SAMPLE	BOOK CONC	CALC CONC	
1 W1	1.070	1.075	STD
2 GSP1	0.660	0.645	STD
3 AGV1	1.040	1.032	STD
4 BCR1	2.200	2.200	STD
5 G2	0.500	0.440	STD
6 PCC1	0.015	0.002	STD
7 DTS1	0.013	-0.012	STD
8 MAG1	0.750	0.741	STD
9 QL01	0.630	0.686	STD
10 MB5	0.620	0.730	STD
11 MB4	0.560	0.602	STD
12 MB3	0.500	0.499	STD
13 CS7	0.940	0.857	
14 CS37	0.660	1.049	
15 JT5		0.849	
16 JT3		0.433	
17 MB21		0.549	
18 MB30		0.597	
19 MB22		0.474	
20 MB29		0.412	
21 MB32		0.568	
22 MB33		0.796	
23 MB35		0.392	
24 MB34D		0.731	
25 MBMXD		0.509	
26 MBMDC		0.444	
27 MB36		0.770	
28 MB39		0.877	
29 MB40		0.751	
30 MB41		0.858	
31 CL7L		0.920	
32 CL8		0.754	
33 MB3F		0.113	
34 MB3MP		0.599	
35 MB53		0.640	

COMPONENT	COEFFICIENT	CONTRIBUTION
BKGD	0.67	0.698
TI02	1.32	1.000
SI02	-0.32	0.400
AL203	-0.22	0.307
FE203	-9282.97E-05	0.108
MGO	-0.11	0.070
CAO	1967.98E-07	0.003
NA20	-0.96	2.005
K20	7021.20E-05	0.131

GOODNESS OF FIT	= .997283
SAMPLE STD DEV	= .0488594
POPULATION STD DEV	= .175643
SAMPLE RMS	= .252313
CURVE RMS	= .242414

Statistics from linear regression:

COMPONENT	COEFFICIENT	CONTRIBUTION
BKGD	9053.36E-05	0.101
TI02	1.22	1.000

GOODNESS OF FIT	= .983911
SAMPLE STD DEV	= .118895
POPULATION STD DEV	= .427413
SAMPLE RMS	= .146187
CURVE RMS	= .140452

Table III-13C. Al_2O_3 data

SAMPLE	BOOK CONC	CALC CONC	
1 W1	15.000	15.070	STD
2 GSP1	15.250	15.460	STD
3 AGV1	17.250	16.682	STD
4 BCR1	13.610	13.613	STD
5 G2	15.400	14.568	STD
6 PCC1	0.740	0.343	STD
7 DTS1	0.240	0.622	STD
8 MAG1	16.770	16.701	STD
9 QL01	16.120	17.373	STD
10 MB5	11.200	10.849	STD
11 MB4	10.680	11.011	STD
12 MB3	12.590	12.436	STD
13 CS7	14.870	14.994	
14 CS37	9.740	12.721	
15 JT5		10.336	
16 JT3		13.401	
17 MB21		13.508	
18 MB30		13.630	
19 MB22		13.160	
20 MB29		12.137	
21 MB32		9.677	
22 MB33		11.313	
23 MB35		8.237	
24 MB34D		11.928	
25 MBMXD		10.016	
26 MBMDC		10.271	
27 MB38		11.571	
28 MB39		11.132	
29 MB40		12.079	
30 MB41		11.964	
31 CL7L		12.655	
32 CL8		10.420	
33 MB3F		11.324	
34 MB3MP		11.419	
35 MB53		6.616	

COMPONENT	COEFFICIENT	CONTRIBUTION
BKGD	0.64	0.761
AL203	6822.62E-05	1.000
SI02	2438.49E-05	0.035
TI02	-0.11	0.129
FE203	2340.95E-05	0.031
MGO	-0.35	0.261
CAO	2973.77E-06	0.053
NA20	-0.96	2.299
K20	-6014.66E-06	0.013

GOODNESS OF FIT	= .998626
SAMPLE STD DEV	= .517522
POPULATION STD DEV	= 1.86042
SAMPLE RMS	= .255434
CURVE RMS	= .245413

Statistics from linear regression:

COMPONENT	COEFFICIENT	CONTRIBUTION
BKGD	-2143.24E-05	0.016
AL203	0.11	1.000

GOODNESS OF FIT	= .983824
SAMPLE STD DEV	= 1.77542
POPULATION STD DEV	= 6.38239
SAMPLE RMS	= .200055
CURVE RMS	= .192207

Table III-13D. Fe_2O_3 data

SAMPLE	BOOK CONC	CALC CONC
1 W1	11.090	11.046 STD
2 GSP1	4.330	4.411 STD
3 AGV1	6.760	7.067 STD
4 BCR1	13.400	13.285 STD
5 G2	2.650	2.183 STD
6 PCC1	8.350	8.443 STD
7 DTS1	8.640	8.498 STD
8 MAG1	7.090	7.091 STD
9 QL01	4.420	4.581 STD
10 MB5	3.960	4.279 STD
11 MB4	1.750	1.947 STD
12 MB3	1.040	1.003 STD
13 CS7	2.830	2.477
14 CS37	4.240	3.808
15 JT5		6.373
16 JT3		2.665
17 MB21		1.479
18 MB30		1.835
19 MB22		4.840
20 MB29		0.698
21 MB32		1.949
22 MB33		3.111
23 MB35		1.488
24 MB34D		6.027
25 MBMXD		2.344
26 MBMDC		3.249
27 MB38		4.453
28 MB39		3.070
29 MB40		4.813
30 MB41		3.767
31 CL7L		3.630
32 CL8		3.638
33 MB3F		0.261
34 MB3MP		0.940
35 MB53		2.653

COMPONENT	COEFFICIENT	CONTRIBUTION
BKGD	0.88	0.970
FE203	0.15	1.000
SI02	-0.19	0.251
TI02	-8948.78E-05	0.097
AL203	-0.24	0.341
MGO	-3799.48E-05	0.026
CAO	-2817.57E-06	0.046
NA20.	-0.95	2.082
K20	-4921.38E-05	0.097

GOODNESS OF FIT	= .998936
SAMPLE STD DEV	= .233678
POPULATION STD DEV	= .840043
SAMPLE RMS	= .256066
CURVE RMS	= .24602

Statistics from linear regression:

COMPONENT	COEFFICIENT	CONTRIBUTIO.
BKGD	0.21	0.234
FE203	0.15	1.000

GOODNESS OF FIT	= .96181
SAMPLE STD DEV	= 1.40018
POPULATION STD DEV	= 5.03345
SAMPLE RMS	= .227206
CURVE RMS	= .218293

Table III-13E. MgO data

SAMPLE	BOOK CONC	CALC CONC	
1 W1	6.620	6.375	STD
2 GSP1	0.960	0.433	STD
3 AGV1	1.530	2.072	STD
4 BCR1	3.460	3.518	STD
5 G2	0.760	1.193	STD
6 PCC1	43.180	42.750	STD
7 DTS1	49.800	50.437	STD
8 MAG1	2.830	2.422	STD
9 QL01	0.940	1.091	STD
10 MB5	24.660	25.214	STD
11 MB4	27.610	24.981	STD
12 MB3	26.750	28.016	STD
13 C57	22.860	23.479	
14 CS37	11.830	10.591	
15 JT5		25.161	
16 JT3		27.944	
17 MB21		26.235	
18 MB30		27.254	
19 MB22		27.455	
20 MB29		27.285	
21 MB32		27.409	
22 MB33		24.389	
23 MB35		24.504	
24 MB34D		25.939	
25 MBMXD		29.170	
26 MBMDC		27.730	
27 MB38		24.975	
28 MB39		25.399	
29 MB40		26.187	
30 MB41		25.976	
31 CL7L		25.856	
32 CL8		26.380	
33 MB3F		28.486	
34 MB3MP		27.208	
35 MB53		14.859	

COMPONENT	COEFFICIENT	CONTRIBUTION
BKGD	-1932.00E-06	0.003
MGO	3885.52E-05	1.000
SIO2	1713.63E-05	0.033
TIO2	7869.43E-06	0.012
AL2O3	2273.08E-05	0.047
FE2O3	-9836.36E-06	0.017
CAO	-1252.52E-06	0.029
NA2O	-1.02	3.231
K2O	5995.41E-06	0.017

GOODNESS OF FIT	= .998464
SAMPLE STD DEV	= .948066
POPULATION STD DEV	= 3.40817
SAMPLE RMS	= .266248
CURVE RMS	= .255803

Statistics from linear regression:

COMPONENT	COEFFICIENT	CONTRIBUTION
BKGD	-1903.15E-05	0.029
MGO	3968.92E-05	1.000

GOODNESS OF FIT	= .997274
SAMPLE STD DEV	= 1.26318
POPULATION STD DEV	= 4.54098
SAMPLE RMS	= .247112
CURVE RMS	= .237417

Table III-13F. CaO data

SAMPLE	BOOK CONC	CALC CONC	
1 W1	10.960	10.933	STD
2 GSP1	2.020	2.072	STD
3 AGV1	4.900	5.117	STD
4 BCR1	6.920	6.881	STD
5 G2	1.940	1.950	STD
6 PCC1	0.510	0.545	STD
7 DTS1	0.150	0.131	STD
8 MAG1	1.410	1.386	STD
9 QL01	3.170	2.979	STD
10 MB5	0.010	-0.006	STD
11 MB4	0.000	-0.056	STD
12 MB3	0.000	0.009	STD
13 CS7	0.050	0.096	
14 CS37	0.750	0.936	
15 JT5		0.028	
16 JT3		0.126	
17 MB21		0.078	
18 MB30		0.086	
19 MB22		0.182	
20 MB29		-0.008	
21 MB32		-0.114	
22 MB33		-0.037	
23 MB35		-0.186	
24 MB34D		0.115	
25 MBMXD		-0.023	
26 MBMDC		0.003	
27 MB38		0.028	
28 MB39		-0.071	
29 MB40		0.066	
30 MB41		0.016	
31 CL7L		0.019	
32 CL8		-0.023	
33 MB3F		-0.009	
34 MB3MP		-0.038	
35 MB53		0.002	

COMPONENT	COEFFICIENT	CONTRIBUTION
BKGD	9.55	0.619
CAO	6.26	1.000
SIO2	-0.73	0.058
TIO2	0.10	0.006
AL2O3	-4.29	0.366
FE2O3	-1.46	0.106
MGO	-2.90	0.118
NA2O	-0.97	0.125
K2O	-0.18	0.021

GOODNESS OF FIT	= .999546
SAMPLE STD DEV	= .0896449
POPULATION STD DEV	= .322262
SAMPLE RMS	= .247392
CURVE RMS	= .237687

Statistics from linear regression:

COMPONENT	COEFFICIENT	CONTRIBUTION
BKGD	-8392.62E-05	0.006
CAO	6.05	1.000

GOODNESS OF FIT	= .999129
SAMPLE STD DEV	= .124075
POPULATION STD DEV	= .446035
SAMPLE RMS	= .247296
CURVE RMS	= .237594

Table III-13G. Na_2O data

SAMPLE	BOOK CONC	CALC CONC	
1 W1	2.150	2.128	STD
2 GSP1	2.800	2.690	STD
3 AGV1	4.260	4.207	STD
4 BCR1	3.270	3.308	STD
5 G2	4.070	4.129	STD
6 PCC1	0.006	0.138	STD
7 DTS1	0.007	-0.086	STD
8 MAG1	3.430	3.417	STD
9 QL01	4.070	4.174	STD
10 MB5	1.190	1.132	STD
11 MB4	1.850	1.720	STD
12 MB3	0.920	1.004	STD
13 CS7	1.150	1.213	
14 CS37	6.270	1.806	
15 JT5		1.018	
16 JT3		0.804	
17 MB21		1.841	
18 MB30		1.244	
19 MB22		0.866	
20 MB29		1.219	
21 MB32		1.138	
22 MB33		0.858	
23 MB35		1.625	
24 MB34D		1.403	
25 MBMXD		2.131	
26 MBMDC		1.446	
27 MB38		1.131	
28 MB39		0.866	
29 MB40		1.153	
30 MB41		1.087	
31 CL7L		0.833	
32 CL8		0.939	
33 MB3F		0.910	
34 MB3MP		1.274	
35 MB53		5.343	

COMPONENT	COEFFICIENT	CONTRIBUTION
BKGD	-2.12	1.074
NA2O	0.88	1.000
SIO2	1.32	0.818
TIO2	0.19	0.096
AL2O3	0.13	0.084
FE2O3	-0.35	0.202
MGO	0.96	0.305
CAO	-0.99	7.423
K2O	-0.12	0.109

GOODNESS OF FIT	= .999047
SAMPLE STD DEV	= .0860483
POPULATION STD DEV	= .309332
SAMPLE RMS	= .247481
CURVE RMS	= .237772

Statistics from linear regression:

COMPONENT	COEFFICIENT	CONTRIBUTION
BKGD	-2698.442-05	0.013
NA2O	0.90	1.000

GOODNESS OF FIT	= .984401
SAMPLE STD DEV	= .348083
POPULATION STD DEV	= 1.25131
SAMPLE RMS	= .104419
CURVE RMS	= .100323

Table III-13H. K_2O data

SAMPLE	BOOK CONC	CALC CONC
1 W1	0.640	0.658 STD
2 GSP1	5.530	5.503 STD
3 AGV1	2.890	2.881 STD
4 BCR1	1.700	1.679 STD
5 G2	4.510	4.442 STD
6 PCC1	0.004	-0.019 STD
7 DTS1	0.001	-0.021 STD
8 MAG1	3.570	3.583 STD
9 QL01	3.490	3.557 STD
10 MB5	1.370	1.518 STD
11 MB4	4.400	4.460 STD
12 MB3	8.040	8.045 STD
13 CS7	2.000	1.859
14 CS37	1.380	1.668
15 JT5		1.448
16 JT3		8.851
17 MB21		7.139
18 MB30		7.889
19 MB22		9.056
20 MB29		8.030
21 MB32		1.317
22 MB33		1.885
23 MB35		3.747
24 MB34D		1.499
25 MBMXD		4.902
26 MBMDC		6.310
27 MB38		1.738
28 MB39		1.386
29 MB40		1.603
30 MB41		1.660
31 CL7L		1.558
32 CL8		1.286
33 MB3F		8.322
34 MB3MP		7.129
35 MB53		0.696

COMPONENT	COEFFICIENT	CONTRIBUTION
BKGD	0.34	0.199
K2O	0.58	1.000
SIO2	-0.17	0.119
TIO2	5209.91E-05	0.030
AL2O3	-3605.72E-05	0.028
FE2O3	-8773.88E-05	0.058
MGO	-2411.58E-06	0.001
CAO	-1.00	8.735
NA2O	2433.39E-05	0.029

GOODNESS OF FIT	= .999677
SAMPLE STD DEV	= .0690909
POPULATION STD DEV	= .248373
SAMPLE RMS	= .247538
CURVE RMS	= .237827

Statistics from linear regression:

COMPONENT	COEFFICIENT	CONTRIBUTION
BKGD	7233.89E-05	0.042
K2O	0.59	1.000

GOODNESS OF FIT	= .999107
SAMPLE STD DEV	= .11492
POPULATION STD DEV	= .413121
SAMPLE RMS	= .104793
CURVE RMS	= .100681

The root mean square formula for the standard samples is

$$\sqrt{\frac{\sum_{i}^{n}\left(\frac{\text{calc'd conc.} - \text{known conc.}}{n}\right)^2}{n-1}}$$

and that for the standard curve is

$$\sqrt{\frac{\sum_{i}^{n}\left(\frac{\text{calc'd conc.} - \text{known conc.}}{n}\right)^2}{n}}$$

Since the fits of the curves are definitely improved with matrix corrections, reasoning implies that error calculations of standard values would decrease. Standard deviation measurements improve as expected; RMS errors do not. The opposing trends of these error measurements are especially confusing when one considers that they all record, in different statistical methods, the difference between curve-calculated and known concentrations of the standards, and thus, the accuracy of the curve. The inconsistency of RMS error trends, although small compared to those of standard deviation and fit, may be a function of the equation; the equations generally used (Renault, personal communication, 1977) are:

$$\sqrt{\frac{\sum_{i}^{n}\left(c_i - m_i\right)^2}{n}} = \text{absolute RMS error}$$

and

$$\sqrt{\frac{\sum_{i}^{n}\left(\frac{c_i - m_i}{m_i}\right)^2}{n}} = \text{relative RMS error}$$

where c_i is the curve calculated concentration, and m_i the known concentration of the i^{th} element, and n is the number of standards. Obviously these formulas do not match those used by the computer program.

APPENDIX IV

Polyhalite Dike of the International Minerals Corporation Mine

Diffraction Data

A thin polyhalite vein in the International Minerals Corporation potash mine was sampled by Dr. Marc Bodine, Jr. The author determined by diffraction the mineralogical content of the zones within and adjacent to the dike over a 17cm span outward into the host evaporites. The samples cover a 5m interval along the strike of the dike. The interior portion of the dike exhibits a 1-1.5cm halite rich vein bordered by a 1.5-3cm zone of predominant halite with significant polyhalite. Following this zone is a discontinuous interval containing halite and only trace polyhalite. This irregular and somewhat banded portion varies from 0 to 2.5cm in width, and in only one of four samples is it well developed. Water leached salt residues of the host evaporite contain widely varying relative intensities of quartz and magnesite, as much as intermediate intensities of feldspar, and trace of illite. In one instance, gypsum and polyhalite were also detected, in another, pyrite - all having relatively high intensities. Five centimeters from the apparent margin of the vein the salt appears to be cleaner; however, virtually no mineralogical differences were found.

Chemical Data

The chemical analyses of whole rock samples surrounding the polyhalite (Table IV-1) reveal very high SO_4 contents, higher than the highest recorded from Kerr McGee samples. Surfur to chlorine ratios (Table IV-2) at > 1.5-3.0cm from the vein exceed all Kerr McGee samples

Table IV-1. Bulk rock salt chemical analyses of polyhalite dike, International Minerals Corporation (wt %)

	SiO_2	Fe_2O_3 (total Fe)	Mg	Ca	Na	K	SO_4	Cl	Br (ppm)	total
					dike					
14B	0.02	0.22	0.36	5.46	25.84	3.84	10.90	42.71	24	89.35
13B	0.32	0.19	0.42	5.58	23.96	4.00	10.98	41.72	28	87.17
12B	0.24	0.55	0.52	4.77	23.42	4.04	10.48	42.69	48	86.71
4B	0.00	0.21	0.33	5.57	25.32	3.88	11.00	42.03	25	88.34
4E	0.39	0.10	0.11	1.38	35.29	1.08	2.48	58.49	40	99.32

Regression constants, fit & data points + % relative error as for Kerr McGee bulk rock salts.

Table IV-2. Chemical weight ratios of bulk rock salts from polyhalite dike, International Minerals Corporation.

	Si/Cl	Fe/Cl	Mg/Cl	Ca/Cl	Na/Cl	K/Cl	S/Cl
				dike			
14B	0.0002	0.0036	0.0084	0.128	0.6050	0.0899	0.0852
13B	0.0036	0.0032	0.010	0.134	0.5743	0.0959	0.0878
12B	0.0026	0.0090	0.012	0.112	0.5486	0.0946	0.0819
4B	0.00	0.0035	0.0079	0.133	0.6024	0.0923	0.0874
4E	0.0031	0.0012	0.0019	0.0236	0.6034	0.0185	0.0142

excepting those which are sulfate-rich on the north side. The Si/Cl ratios are lower than or comparable to the lower range of values in the Kerr McGee potash mine where salt has been intensely altered adjacent to the lamprophyre dikes. Sodium/ chlorine values are also comparable to those in the same zone in the Kerr McGee. Relative to chlorine, Ca contents 1.5-3.0cm from the vein resemble the highest found in the Kerr McGee mine, those in virtually pure polyhalite samples. Magnesium at this distance from the vein compares to Kerr McGee salts at dike contacts; outside this interval the Mg concentration parallels intensely leached salts of the Kerr McGee, and Ca that of sulfate-absent samples. Potassium/chlorine values approximate Kerr McGee clay seam values; at greater than 1.5-3.0cm the value approximates the moderately altered rocks at Kerr McGee. Iron values exhibit a similar pattern - intense alteration followed by altered, relatively pure salt. Bromine levels are very low, approximating (outside) or lower than (within the 1.5-3.0cm interval) the altered clay - poor salts of the Kerr McGee sample suite. This is due to the predominance of sulfate minerals in the assemblage. Analytical totals suggest that minor clay is present within a distance of 1.5-3.0cm and is enveloped by non-argillaceous material.

Discussion and Summary

The chemical analyses reflect the presence of significant polyhalite, in addition to halite, in the interval bordering the vein. In fact, these chemical trends suggest development of an alteration zone combining the characteristics in the Kerr McGee, specifically, those of extensive sulfate development, exemplified by breccia-containing material, and contact clay seam formation. Outside of this interval, in places up to 2.5cm wide, a semi-continuous interval of virtually

pure halite possibly stained by minor amounts of sulfides and/or hydrocarbons envelops the border zone, and indeed is very nearly identical to bleached salts present at dike margins in the Kerr McGee occurrence.

APPENDIX V

Data From Other Sources

Fluid Inclusion Work on Salts

The investigation of fluid inclusions in salts adjacent to the intrusions in the Kerr McGee mine was conducted on samples at 1-2cm, 0.2m, and 2.5m from the larger dike contact by Edwin Roedder (personal communication, 1978). Roedder found that most of the inclusions were normal, two-phase with small bubbles, and from these determined the following information:

sample	temperature of homogenization (°C) min.	max.	number of inclusions run
1-2cm	71	116	7
0.2m	60	110	6
2.5m	85	88	9

Joseph Taggart (personal communication, 1978) discovered fluid inclusions adjacent to the dike were maximum at 150°C.

Freezing runs on two of the samples, at 1-2cm and 2.5m, revealed that temperature of first melting was well below that of a pure $NaCl-H_2O$ system (-28°C and -31.0°C, respectively). Dissolution of the last phase, presumed to be a hydrate other than $NaCl \cdot 2H_2O$, occurred at +11 - +18°C and +4 - +7.2°C, respectively. The sample at 1-2cm from the dike exhibited one inclusion entirely different in character; it apparently contained a mixture of gases, including CO_2.

Crushing tests revealed that the two-phase inclusions and those with the sole phase being a gas all contain a total or partial vacuum bubble or are under a vacuum. This infers that the inclusions trapped

steam bubbles ± gas and brines. Conversely, a few single phase inclusions (likely CO_2 gas) are under greater than atmospheric pressure, estimated to be from 30 or 40 to 100 times normal atmosphere.

Roedder concedes that there are problems in interpretation where steam originating and dense gas pressure inclusions occur in the same sample. Furthermore, calculations involving the latter and assuming 380 bars confining pressure yield obvious erroneous trapping temperatures for the dense gas inclusions.

In addition to these inconsistencies, the determined temperatures of homogenization does not agree with field evidence that salts immediately adjacent to the dike were molten during the time of intrusion. Unmistakenly, the total types and stages of influencing processes are unidentifiable from present knowledge, excepting that at some stage, steam was trapped and at another, fluid inclusions indicating high temperature of formation may have been modified to the present relatively low temperature of homogenization. The freezing/melting tests support the geologic evidence of existence of a non-pure NaCl system.

Dike Information

Calzia and Hiss (1978) have analyzed igneous rocks from the Kerr McGee dike system; the chemical analyses are reported in Table V-1. They conducted petrographic studies on the two localities of this study and on a core of the dike located between the sites; their findings generally coincide with those of this investigation. In addition to these investigations, they have compiled a list of occurrences of the dike (Table V-2), and report K-Ar and He-method age dating of the dikes at the Kerr McGee mine as 32.2 ± 1.0 million years.

Jones and Madsen (1959) described the dike and its alteration

Table V-1. Kerr McGee dike rock analyses (wt.%) from Calzia and Hiss (1978).

	G-018	G-021	G-024
SiO_2	44.90	46.00	46.10
Al_2O_3	14.20	13.20	14.50
Fe_2O_3	2.80	3.60	3.10
FeO	7.30	7.30	7.50
MgO	6.00	6.00	5.10
CaO	3.90	3.40	2.40
Na_2O	3.80	2.00	2.50
K_2O	4.80	6.30	8.00
H_2O^+	2.87	2.74	3.14
H_2O^-	1.22	1.83	0.92
TiO_2	2.40	2.80	2.30
P_2O_5	1.20	1.30	1.20
MnO	0.14	0.19	0.12
CO_2	0.20	0.10	0.10
SO_3	1.25	0.42	0.27
Cl	1.15	0.38	1.10
F	0.16	0.16	0.17
S	0.55	0.30	0.20
Total	93.84	98.02	98.72

G-018 main dike, northern margin
G-021 main dike
G-024 subdike

Table V-2. Listing of dike occurrences, Delaware Basin (from Calzia and Hiss, 1978).

	Location[2]	Name Elevation (ft)	Igneous rock intercepts (depth in ft)	Original description of igneous rock	Age of country rock (series and formation name, if known)	Reference
			Test Wells			
1.	12/18S/32E 1980 FSL, 2302 FEL	Humble State BO #3 3995	8170–8430	Basalt fragments	Permian (Leonardian)	Garner Wilde (1976, personal commun.)
2.?[1]	22/18S/34E 2310 FSL, 1980 FEL	Forest Oil Co. Continental State #1 4009	7210–8640			Elliott (1976) No igneous rocks G. P. Walker (1977, written commun.)
3.	12/20S/32E NW 1/4	IMC ConcDale #95	2239			Elliott (1976)
4.	14/20S/32E 2905 FSL, 365 FWL	Noranda HB #10 3520	1700–1804	Black basalt	Permian (Ochoan Salado Formation	Frank Condon (1977, personal commun.)
5.	21/21S/32E 1980 FS & EL	Texas Moore #1 3505	2115–2160	Basalt	Permian (Ochoan)	Flawn (1956, p. 64)
6.	16/21S/30E 1980 FSL, 660 FWL	Perry R. Bass Big Eddy #44 3324 KB	11,230–11,270 12,470–12,550 12,700–12,900 13,170–13,330	Granite-diorite do do Not described	Permian (Wolfcampian) Pennsylvanian (Morrowan) do do	W. J. Parsons (1977, written commun.)
7.?[1]	30/21S/30E 660 FSL, 3300 FEL	Stanolind Duncan #1 3320	470–2710 (8 intercepts)			Elliott (1976) No igneous rocks, G. P. Walker (1977, written commun.)
8.	9/22S/29E 660 FSL, 660 FEL	H & W Drilling Co. Danford #1 3247	2208–2230	Basalt sill	Permian (Ochoan Castile Formation)	P. T. Hayes (1976, written commun.)

Table V-2. Continued

	Location[2]	Name Elevation (ft)	Igneous rock intercepts (depth in ft)	Original description of igneous rock	Age of country rock (series and formation name, if known)	Reference
			Test Wells			
9.	25/22S/28E 1980 FS & EL	Perry R. Bass Big Eddy #43 3168	940-1150 1990-2080	Black, basic igneous material	Permian (Ochoan Salado or Castile Formations)	W. J. Parsons (1977, written commun.)
10.	28/25S/24E 660 FS & EL	CITCO Government #1M 3766	7498-7521	Diorite (includes green hornblende, brown biotite, abundant pyrite)	Mississippian (lower Chesterian or upper Meramecian)	G. P. Walker (1977, written commun.
11.	34/25S/24E 2310 FS & EL	Black River Corp. Cities Fed. #2 3705	7242-7245 7248-7266 7271-7280	Sills (probably basaltic rock as suggested by wireline correlation)	do	Do.
12.	11/26S/24E 1980 FNL, 2080 FEL	J. M. Huber #1 Superior USA 3752	7492-7495 7535-7540 7554-7556 7591-7600	Very fine grained to coarse-grained diorite sills	do	Do.
13.	12/26S/24E 1980 FNL, 660 FEL	Superior Oil Corp. #1 Government "134" 3866	7780-7804	Sills (probably basaltic rock as suggested by wireline correlation)	do	Do.
14.	14/26S/24E 1980 FNL, 2043 FEL	J. M. Huber #1 Western USA 3827	8021-8023 8027-8032 8028-8072	Fine- to medium-grained diorite sills	do	Do.
15.	22/26S/25E 1650 FN & WL	Hydrocarbon Exploration Inc. Marathon Fed. #1 3635	10,162-10,182	Sill	do	Do.
16.	28/26S/25E 2080 FNL, 1980 FWL	Coquina Oil Corp. Black River Fed. #1 3704	9889-9910	Diorite sill, trace of biotite	do	Do.

Table V-2. Continued

	Location[2]	Name Elevation (ft)	Igneous rock intercepts (depth in feet)	Original description of igneous rock	Age of country rock (series and formation name, if known)	Reference
			Test Wells			
17.	6/Blk 61/T1S 1980 FSL, 660 FEL	Natural Gas Exploration Corp. Pokorny #1 3875 (approx.)	9600-9625 9631-9650	Sill of granular, pyritic igneous rock	Pennsylvanian (lower Morrowan sandstone, shale and limestone)	Do.
			10,358-10,375	Sill of igneous rock with glauconite and pyrite	Mississippian (lower Chesterian or upper Meramecian)	
18.	18/Blk 61/T1S 660 FSL, 1980 FEL	Continental Oil Corp. Pokorny #1 3800 (approx.)	9790-9807 9810-9815 9819-9831	Sills of andesite with trace of glass	Pennsylvanian (Morrowan shale	Do.
19.	31/Blk 61/T1S 660 FSL, 1980 FEL	Texaco Culberson Fee #1M 3600 (approx.)	9896-9900 10,076-10,081 10,105-10,113 10,160-10,390	Andesite Fine-grained diorite do Fine- to medium-grained diorite, biotite increases near base	Mississippian or Pennsylvanian (Chesterian or lower Morrowan shale)	Do.
20.	46/Blk 63/T1S 660 FNL, 1980 FEL	Socony Mobil State Cowden B#1 4006 DF	7330-7350 7400-7452 7640-7665	Sills of quartz diorite	Mississippian (Chesterian shale)	H. J. Homquest (1977, personal commun.)
				Sills at 7330-7336 and 7418-7430 classified as trachyte	Mississippian or Pennsylvanian (upper Chesterian or lower Morrowan shale)	G. P. Walker (1977, written commun.)
21.	12/Blk 63/T2S 1980 FSL, 660 FEL	Magnolia Mobil Homer Cowden #1 3917	8738-8770 8810-9122	Sill	Mississippian or Pennsylvanian (upper Chesterian or lower Morrowan shale)	G. P. Walker (1977, written commun.
				Sill between 8760-8770 classified as biotite syenodiorite	Pennsylvanian	Flawn (1956, p. 148)
				Sill at 8730-9140 classified leuco syenodiorite		Pratt (1954, p. 147)

Table V-2. Continued

	Location[2]	Name Elevation (ft)	Igneous rock intercepts (depth in feet)	Original description of igneous rock	Age of country rock (series and formation name, if known)	Reference
22.	18/Blk 63/T2S 1980 FN & EL	Socony Mobil State Barret #1 4269 DF	7335-7355	Monzonite sill	Mississippian (Chesterian shale)	H. J. Homquest (1977, personal commun.)
				Sill at 7349-7353 classified syenodiorite or diorite	Mississippian or Pennsylvanian (upper Chesterian or lower Morrowan shale)	G. P. Walker (1977, written commun.)
23.	33/Blk 62/T2S 1980 FS & EL	TXL Culberson Fee #1B-T 4000 (approx.)	10,145-10,150	Not described	do	Do.
				Mines		
24.	31/20S/32E	Kerr-McGee 3560 (approx.)	1530	Two basalt dikes; N44-46°E, nearly vertical	Permian (Ochoan Salado Formation)	This report
25.	6/21S/31E	Kerr-McGee 3601 (approx.)	1400	Trachyte dike, 8 ft wide, nearly vertical	do	Wm. Henderson (1977, personal commun.)
26.	36/21S/29E	IMC 3320 (approx.)	790	Basalt or lamprophyre dike, 1 ft wide	do	Hiss (1975)
27.	2/22S/29E	IMC 3335 (approx.)	875 (Polyhalite at 738 ft)	Dikes of basalt and alkalic intrusive rocks 0.3 ft wide that grade upward and laterally to polyhalite	Permian (Ochoan Castile and Salado Formations)	Jones and Madsen (1959)

[1]Question mark indicates conflicting reports regarding the occurrence of igneous rock at that location.

[2]Test wells located in New Mexico are listed as section/township/range with reference to New Mexico Principal Meridan and Base Line. The remaining test wells are listed as section/block/township with reference to Texas and Pacific Railroad Survey in Culberson County, Tex. All mines are in New Mexico. Abbreviations: FN (or S, E, or W)L = distance, in feet, from north (or south, east, or west) line of the section; KB = kelly bushing; DF = derrick floor.

effects in the International Minerals Corporation. The dike is typically less than one foot thick and exhibits intersecting vertical and sub-horizontal fissures with halite and polyhalite and accessory pyrite and hydrocarbon present. The polyhalite and accessory minerals are considered to be epigenetic. Solutions are believed to be responsible for the leaching of hematitic sylvite, for the information of blue halite, and of kainite and bloedite from langbenite 12.7cm (5") from the dike. Rock salt has been bleached and recrystallized 1.3 to 3.8cm (1/2 to 1 1/2 inches) from the contact. The alkaline basaltic dike upward and laterally changes abruptly to a polyhalite vein containing minor dolomite and pyrite with a small amount of crystalline hydrocarbon.

In a supplement to the above description, Jones (1973) sites halite, siderite, calcite, and natrolite as filling the widely reported 2mm scattered amygdules contained within the dike rock. From a detailed statistical study of the vesicles from the Kerr McGee, Joseph Taggart (personal communication, 1978) reports the presence of the following minerals: anhydrite, barite, biotite, siderite, pyrite, blue halite, potassium feldspar pseudomorphous after plagioclase, and possibly an Fe, Mg-silicate.

APPENDIX VI

Recommended Further Study

1. It is herein recommended that a more detailed investigation on the clay seams vs. associated salts be made in order to verify the role of these seams in the alteration processes at the Kerr McGee mine.

2. It is suggested that statistical data be collected on fluid inclusions adjacent to the dike at the Kerr McGee to supplement past work (Roedder) for better estimates of intrusion temperatures and/or post-intrusion processes.

3. A detailed study on dike included evaporite pods may resolve inconsistencies revealed in this study.

4. A comparison of the quantity and composition of different size fractions of the silicate residues at both localities may indicate reaction avenues.

5. In the Yeso Hills, the alteration sequence could be better defined with a larger number of more closely spaced samples. This will be feasible only if exposures warrant, e.g. if the pervasive slumping in the area preventing definition of relation to the intrusions can be overcome by statistical sampling methods.

6. Typical silicate assemblages of the Castile Formation can only be defined by analyzing drill core throughout the basin. This would verify whether the pervasive quartz and feldspars in the Castile exposure of the Yeso Hills is a function of proximity to basin boundaries, thus suggesting a clastic origin for these minerals.

7. The submittal of the lamprophyre for analyses as a standard is proposed here.

8. The variation of Br contents in different fractions of the evaporites

is suggested here as a project that could contribute to understanding the physical process involved in the alteration profile.

APPENDIX VII

Additional References

Adams, J. E., 1944, Upper Permian Ochoa series of Delaware Basin, west Texas and southeastern New Mexico: Am. Assoc. Petroleum Geologists Bull., v. 28, no. 11, p. 1956-1625.

Anderson, R. Y., Dean, W. E., Jr., Kirkland, D. W., and Snider, H. I., 1972, Permian Castile varved evaporite sequence, west Texas and New Mexico: Geol. Soc. America Bull., v. 83, p. 59-86.

Bailey, R. K., 1949, Talc in the salines of the potash field near Carlsbad, Eddy County, New Mexico: Am. Mineralogist, v. 34, p. 757-759.

Becher, A., 1964/65, Eine Tonmineralfolge vom Beckeneand zum Beckininneren im Bunstsandstein Nordost-Bayems: Beitr. Mineral. Petrol., v. 11, p. 586-613.

Bodine, M. W., Jr., Fernalld, T. H., and Standaert, R. R., 1973, The talc-quartz association in marine evaporite rocks: Am. Geophys. Union Trans. Abs., v. 54, p. 487.

_____and Standaert, R. R., 1977, Chlorite and illite compositions from Upper Silurian rock salts, Retsof, New York: Clays and Clay Minerals, v. 25, p. 57-71.

Borchert, Hermann, 1933, Die Vertaubungen der Salzlagerstätten und ihre Ursachen; pt. 1 - Physikalisch-chemische Grundlagen: Kali, v. 27, p. 97-100.

_____1934, 1935, Die Vertaubungen der Salzlagerstätten und ihre Urasachen; pt. 2 - Das dynamisch-polytherme System der Salze der ozeanen Salzablagerungen: Kali, 1934, v. 28, p. 290-296, 301-305; 1935, v. 29, p. 1-5.

_____1940, Die Salzalagerstätten des deutschen Zechsteins: Archiv für lagerstättenforschung, no. 67, 196p.

_____1959, Ozeane Salzlagerstätten: Berlin, Gebrüder Borntraeger.

Dreizler, Ingo, 1962, Mineralogische Untersuchungen an zwei Gipsvorkommen der Werraseric (Zechstein); Beitr. Mineral. Petrol., v. 8, p. 323-338.

Flawn, P. T., 1956, Basement rocks of Texas and southeast New Mexico: University of Texas Bureau of Economic Geology, Bull. 5605, 261p.

Füchtbauer, Hans, and Goldschmidt, Hertha, 1959, Die Tonminerale der Zechsteinformation: Beitr. Mineral. Petrol., v. 6, p. 320-345.

Hills, J. M., 1968, Permian Basin field area west Texas and southeastern New Mexico in Saline Deposits: Matiox, R. B., ed., Geol. Soc. America Spec. Paper 88, p. 17-27.

Hiss, W. L., 1975, Stratigraphy and ground-water hydrology of the Capitan aquifer, southeastern New Mexico and western Texas: University of Colorado, Boulder, Ph.D. thesis, 396p.

Holland, J. G., and Brindle, D. W., 1966, A self-consistent mass absorption correction for silicate analysis by x-ray fluorescence: Spectrochim. Acta, v. 22, no. 12, p. 2083-2093.

Jacka, A. D., and Franco, L. A., 1974, Deposition and diagenesis of Permian evaporites and associated carbonates and clastics on shelf areas of the Permian Basin in Fourth Symposium on Salts: Coogen, A. H., ed., Northern Ohio Geol. Soc., v. 1, p. 67-89.

King, P. B., 1942, Permian of west Texas and southeastern New Mexico: Am. Assoc. Petroleum Geologists Bull., v. 26, p. 535-763.

King, R. H., 1947, Sedimentation in the Permian Castile sea: Am. Assoc. Petroleum Geologists Bull., v. 31, no. 3, p. 470-477.

Kopp, O. C., and Fallis, S. M., 1974, Corrensite in the Wellington Formation, Lyons, Kansas: Am. Mineralogist, v. 59, p. 623-624.

Kühn, Robert, 1968, Geochemistry of the German potash deposits in Saline Deposits: Matiox, R. B., ed., Geol. Soc. America Spec. Paper 88, p. 427-504.

Lippmann, F., and Savascin, M. Y., 1969, Mineralogische Untersuchungen an Lösungsrückständen eines württembergischen Keupergipsvorkommens, Tschermaks: Miner. u. Petrogr. Mitt., v. 13, p. 165-190.

Pundeer, G. S., 1969, Mineralogy, genesis and diagenesis of a brecciated shaley clay from the Zechstein evaporite series of Germany: Contr. Mineralogy and Petrology, v. 23, p. 65-85.

Schmalz, R. F., 1969, Deep water evaporite deposition: A genetic model: Am. Assoc. Petroleum Geologists Bull., v. 53, no. 4, p. 798-823.

Scruton, P. C., 1953, Deposition of evaporites: Am. Assoc. Petroleum Geologists Bull., v. 37, p. 2498-2512.

Sloss, L. L., 1969, Evaporite deposition from layered solutions: Am. Assoc. Petroleum Geologists Bull., v. 53, no. 4, p. 776-789.

Stewart, F. H., 1963, Data of geochemistry; chapter Y, Marine evaporites: U. S. Geol. Survey Prof. Paper 440-Y, 52p.

Usiglio, J., 1849, Annales Chim. Phys., ser. 3, v. 27, p. 92, 172.

This thesis is accepted on behalf of the faculty of the Institute by the following committee:

Date May 4, 1979